Using immunofluorescence techniques to Identify T cells in the foreskin tissue after medical male circumcision

By

Shorok Sebaa

SBXSHO001

A dissertation presented in fulfillment of the requirement for the degree of

MSc (Med) in Clinical Sciences and Immunology

Division of Immunology

Department of Pathology

Faculty of Health Science

University of Cape Town

February 2022

DECLARATION

I, **Shorok Sebaa**, hereby declare that the work on which this dissertation/thesis is based is my original work (except where acknowledgements indicate otherwise) and that neither the whole work nor any part of it has been, is being, or is to be submitted for another degree in this or any other university.

I empower the university to reproduce for the purpose of research either the whole or any portion of the contents in any manner whatsoever.

Signature: Signed by candidate

Date: 14/02/2022

Table of Contents

Preface

I wish to extend my gratitude and appreciation to my supervisor, Professor Clive Gray for offering me the opportunity to work on this research project, for his time, mentorship and guidance; I have learned so much from him and gained so much confidence in my abilities as a scientist. I wish to offer my deepest thanks to my co-supervisor, Dr. Nyaradzo Chigorimbo-Tsikiwa for her support, wholehearted supervision, encouragement and for being a role model. I wish to thank my mentor Dr. Kyle O' Hagan who trained and supported me and had a great impact on the quality of my work and wellbeing.

To Professor Tomas Hope, Dr. Ann Marie Carias and Dr. Ramon Lorenzo-Redondo of Feinberg School of Medicine at Northwestern University for their great assistance with image analysis and counting of cells.

I wish to acknowledge the support from Dr. Sonwabile Dzanibe who has been a huge support in data analysis and a wonderful friend who I am proud to have by my side. I also wish to acknowledge the support of Dr. Nadia Ikumi in imaging analysis and guiding me in finding the most optimal image analysis software. I wish to thank my team members who became friends and sisters over the years: Bokani Nleya, Christen Da Costa, Lerato Rametse and Nobomi Dontsa. I wish to thank the study coordinator Michael Mndini who has done exceptional work that enabled the conduction of the study. I wish to thank the lab manager Berenice Alinde for her training and ensuring the lab was always a safe environment for students and staff to conduct their research.

I dedicate this dissertation to my parents, who dedicated their lives to me fulfilling all my potentials. I am beyond grateful to the values they instilled in me that led me to perceive knowledge as the most honorable gift. I would like to thank my three incredible brothers: Mohamed, Islam and Abdulrahman for their continuous support through love, humor and kindness. There is so much peace in knowing that I am always supported by them. I wish to thank my sister-in-law Amira Haridy and my beautiful niece and nephew: Ayla and Omran for the deep love, laughter and friendship. I want to also thank my cat for being my best companion, support system and for giving me such pure love.

To my friend Millicent Omondi who provided input in data analysis and supported my journey deeply. To my office mates Mikhail Smith, Saori Iwase and Tatenda Murangi. To

Dhuraiyah Abdullatief and Faldeelah Fisher for being so loving and efficient in all student matters.

I wish to thank my friend Amany Adel who has been consistent through all stages of my adult life and contributed so much to my wellbeing and understanding of life. To my cousin Alaa Naguib whose support and unconditional love kept me floating through the most difficult times.

I would like to wholeheartedly thank Mandela Rhodes foundation for their unwavering support throughout my master's degree and inspiring me in so many ways as a young African scholar to become the best version of myself. I would have not been here today without their effort. I specially thank Shaun Johnson who we lost in 2020 after he touched so many lives, including mine, deeply as one of the kindest souls who inspired people through kindness.

I wish to thank my friends Passant almaghrabi, Aya Tammam, Jeanine Botha, Nada Abdelaziz, Mona Allaam, Othniel Jean Konan, Willard Mapulanga, Isabel Khumalo, John Iradukunda, Theresa Ayerigah, Akiko Suzuki, Carine Rugorirwera, Emilia Appiah, Heather Dixon, Kirra Evans, Nathan Odiase, Tafadzwa Kwaramba and Nyotu Gitau for their persistent support and care through the past few years; I am forever grateful.

I wish to thank the National Institutes of Health, R01 DK108434 grant for funding the study and enabling this work.

I Finally wish to highlight the circumstances in which this dissertation was written during the COVID-19 pandemic. The pandemic and the following lockdown have drastically affected the lab accessibility and access to samples in the following months. Hence, it has led to not finishing the last experiments leading to completion of this dissertation.

"Science is not only a disciple of reason but, also, one of romance and passion."

Stephen Hawking

List of publications and presentations

1- Gray CM, O'Hagan KL, Lorenzo-Redondo R, Olivier AJ, Amu S, Chigorimbo-Murefu N, Harryparsad R, Sebaa S, et al. **Impact of chemokine C–C ligand 27, foreskin anatomy and sexually transmitted infections on HIV-1 target cell availability in adolescent South African males.** Mucosal Immunol. 2019;13(1):118–27.

2- Sebaa S, O'Hagan KL, Chigorimbo-Tsikiwa N, Amu S, Lorenzo-Redondo R, Carias A M, Chiodi F, Cianci G C, Hope T, Gray CM. **Impact of CCL27 on HIV-1 target-cell abundance in the foreskin epithelium**. Conference on retroviruses and opportunistic infections, March 8-11, 2020, Boston, Massachusetts. Poster presentation.

LIST OF ABBREVIATIONS

CCL27	C-C Chemokine Ligand 27
CCR5	C-C Chemokine Receptor Type 5
CD	Cluster Of Differentiation
CT	*Chlamydia trachomatis*
CXCR4	C-X-C Chemokine Receptor Type 4
DCs	Dendritic Cells
FOV	Field of view
FS	Foreskin tissue
GP	Glycoprotein
HIV	Human Immunodeficiency Virus
HPV	Human Papilloma Virus
HSV-2	Herpes Simplex Type 2
IDL	Interactive Data Language
IL-8	Interleukin-8
IF	Immunofluorescence
IFNγ	Interferon Gamma
LCs	Langerhans Cells
MG	*Mycoplasma genitalium*
MMC	Medical Male Circumcision
MSM	Men who have sex with men
MIG	Monokine Induced By γ-Interferon
NIH	National Institutes of Health
NG	*Neisseria gonorrhea*
NK	Natural Killer Cells
PEP	Post Exposure Prophylaxis
PrEP	Pre-Exposure Prophylaxis
RORγt	Retinoic Acid Receptor-Related Orphan Receptor Gamma-T
RT	Reverse Transcriptase
SIV	Simian Immunodeficiency Virus
STIs	Sexually Transmitted Infections

Th1	T Helper 1 Cells
Th17	T Helper 17 Cells
Th2	T Helper 2 cells
Th22	T Helper 22 Cells
Tfh	Follicular Helper T Cells
Th9	T Helper 9 Cells
Tregs	T Regulatory Cells
TLR	Toll-Like Receptors
TLR2	Toll-Like Receptor 2
TRAIL	Tumor Necrosis Factor Related Apoptosis-Inducing Ligand
TNFα	Tumor Necrosis Factor α
TV	*Trichomonas vaginalis*
UM	Urethral Meatus
VL	Viral Load
VMMC	Voluntary Medical Male Circumcision
WHO	World Health Organization

List of figures

List of tables

Abstract

Background: Medical Male Circumcision (MMC) plays an important role in reducing the risk of acquiring sexually transmitted infections (STIs) such as Human papilloma virus (HPV), Herpes simplex type 2 (HSV-2) and HIV-1. The foreskin tissue (FS) is a site abundant in Langerhans cells (LCs), macrophages and T helper cells that express CD4 and CCR5 that are target markers for HIV-1 binding and viral infection. The foreskin tissue may also contribute chemokines and cytokines including those that promote inflammation such as IL-17, IL-1β, IL-8, MCP-1 and MIG. The inner foreskin has been shown to contain higher levels of CD4+CCR5+ cells and thus more susceptible to HIV infection compared to the outer foreskin. It was demonstrated that the majority of chemokines measured were highly expressed in the inner foreskin compared to the outer foreskin including CCL27 which was approximately 7-fold higher in the inner foreskin compared to the outer foreskin, in congruent with the higher density of CD4+CCR5+ observed in the epithelium of the inner foreskin. In this study, we hypothesized that CCL27 upregulation in the inner foreskin triggers the recruitment of CD4+ T cells to the epithelium of the foreskin tissue. This could subsequently lead to increased susceptibility to infections in the inner foreskin tissue. The aims of this dissertation were: 1) to measure the impact of CCL27 on the recruitment of CD4+ T cells to the epithelium of the foreskin tissue using immunofluorescence imaging. 2) to compare manual counting and semi-automated method for counting dually positive cells. 3) to use multiparameter flow cytometry to characterize the cells recruited under the influence of CCL27.

Methodology: Inner foreskin tissue (n=11) and outer foreskin tissue (n=4) explants were treated with either TNFα or CCL27 and evaluated using immunofluorescence imaging to quantify the levels of CD3 and CD4 expressing cells. Dually positive CD3+CD4+ cells were counted manually using softworx software on the Deltavision microscope and with semi-automated counting using PIPSQUEAK on ImageJ. TNFα and CCL27 treated inner and outer FS cells were immunophenotyped using polychromatic flow cytometry to measure and compare the densities of Th17 and Th22 cells under the influence of the chemokines.

Results: Exogenous exposure of inner foreskin tissue explants to TNFα showed a significant increase in the median density of CD3+CD4+ T cells in the epithelium of the inner foreskin

(p=0.035) from 78.90 cells/mm^2 (IQR: 33.02-127.50) in the unstimulated inner foreskin explants to 134.80 cells/mm^2 (IQR: 109.30-206.60). Similarly, the addition of exogenous CCL27 resulted in the median density of CD3+CD4+ T cells in the epithelium of the inner foreskin to increase from the unstimulated inner foreskin (value above) to 164.80 cells/mm^2 (IQR: 140.30-184.90, p=0.008). No significant difference was observed in the median density of CD3+CD4+ T cells in the outer foreskin tissue explants after exposure to TNFα and CCL27 (36.50 cells/mm^2, IQR: 18.29-96.65 in the unstimulated tissues compared to 65.12 cells/mm^2, IQR: 7.30-202.80 in the TNFα stimulated tissues; p>0.999 and 24 cells/mm^2, IQR: 11.35-149.40 for the CCL27 stimulated tissues; p=0.686). The median density of CD3+CD4+ T cells in the epithelium of unstimulated inner foreskin tissue showed a trend of an increase from the unstimulated outer foreskin tissue but was not statistically different (127.50 cells/mm^2, IQR: 89.22-219.50 in the inner foreskin compared to 36.52 cells/mm^2, IQR:18.29-96.65 in the outer foreskin explants; p=0.057). When comparing the cell counting methods: manual counting vs semi-automated counting, we observed that the manual counting method estimated higher numbers of dually positive cells compared to the semi-automated method in samples measuring <100 cells/mm^2 meanwhile the semi-automated counting method estimated higher cell numbers in samples measuring >200 cells/mm^2. Despite these differences, there was strong correlation (R=0.782, p<0.0001) in cell numbers counted in the inner foreskin between the two methods. We next employed flow cytometry to phenotype CD4+ T cell subsets in FS-derived cells and observed no significant differences in the frequencies of Th17 and Th22 cells migrating from TNFα and CCL27 treated inner and outer foreskin whole tissues compared to controls. The median frequency of Th17 cells in the inner foreskin whole tissue in the unstimulated explants was 27.75% (IQR: 8.19-45.90%) vs 24.45% (IQR: 8.67-38.38%, p=0.625) in TNF treated explants and 27.90% (IQR:7.96-46.10%, p>0.999) in CCL27 treated explants. The median frequency of Th22 cells in the inner foreskin in the unstimulated tissue explants was 8.80% (IQR: 1.68-12.60%) vs 5.30% (IQR: 0.96-7.67%, p=0.250) in TNFα treated explants and 4.90% (IQR:0.75-7.39%, P=0.125) in CCL27 treated explants. Meanwhile, the median frequency of Th17 cells in the outer foreskin in the unstimulated tissue explants was 21.60% (IQR: 15.40-37.33%) vs 28.20% (IQR: 14.60-39.40%, P=0.750) in TNFα treated explants and 22.90% (IQR:22.90-29.50%, p>0.999) in CCL27 treated explants. The median frequency of Th22 cells in the outer foreskin in the unstimulated tissues was 4.67% (IQR: 2.30-12.90%) vs 5.37% (IQR: 5.34-7.58%, P=0.750) in TNFα treated

tissues and 4.45% (IQR:3.64-5.98%, p>0.999) in CCL27 treated tissues. Furthermore, FS cells isolated using Dispase had significantly lower median frequencies of cells expressing CCR6 (18.35%, IQR:1.33-28.30%) compared to whole tissue controls (41.90%, IQR: 22.46-67%, p=0.031). This impacted the characterization of CD4+ T cell subsets in FS cells and limited our ability to adequately phenotype and measure the impact of TNFα and CCL27 on FS-derived cells using flow cytometry.

Conclusion: This study demonstrates that exogenous exposure of FS to TNFα and CCL27 increased the density of CD3+CD4+ T cells in the epithelium of the inner but not the outer foreskin tissue. It was noteworthy that the density of CD3+CD4+ in the epithelium of the inner foreskin was higher than the outer in the unstimulated tissues, suggesting that the proinflammatory environment in the inner FS potentially leads to higher density of T cells in the inner FS even without exogenous stimulation. These results suggest a possible mechanism for recruiting HIV target cells in the inner foreskin tissue associated with higher levels of CCL27 that recruits HIV-1 target T cells during inflammatory responses. A limitation to this conclusion is the small sample size in the outer foreskin. The study also shows potential bias depending on the method used to quantify dually positive cells, whereby semi-automated counting underestimated the densities of CD3+CD4+ T cells compared to manual counting and therefore careful consideration is required when selecting the quantification method. Furthermore, there were no significant difference in the frequencies of Th17 and Th22 cells after exposure to TNFα and CCL27 using flow cytometry. The effects of Dispase on cell surface marker expression and the low cell yield across the experiments impacted the characterization of Th17 and Th22 using flow cytometry and thus limiting capacity to determine how CCL27 influences these T cell subsets.

Chapter 1: literature review

Table of Contents

1.1 Overview of male circumcision

Male circumcision is the process of removing some or all the foreskin tissue surrounding the glans penis. It is one of the oldest and most common practices across the world (1,2). Male circumcision is performed for many reasons including religious, cultural, cosmetic or health reasons (3). Historically, male circumcision was practiced as early as 2300 BC (4). It is performed as a traditional practice among many groups in Africa, Asia and Aboriginal Australia and religiously among Muslims and Jews (2,5). However, circumcision of male infants and boys became a more common practice correlated with health benefits including better hygiene and protection against sexually transmitted infections (STIs) specifically Human Immunodeficiency Virus (HIV) infection (6,7). The role of the medical male circumcision, involving the removal of more than 95% of the foreskin, in the protection against HIV and STIs has been suggested to be due to various reasons including the high density of HIV-1 target cells including T cells and Langerhans cells in the foreskin tissue (8,9). These cells inhabit the foreskin tissue and are considered important role players in the HIV infection (10–14). In this dissertation, two immunofluorescence techniques were used to characterize T cells in the foreskin tissue: Immunofluorescence imaging and flow cytometry. Immunofluorescence imaging was a useful tool for viewing spatial distribution of cells in the foreskin tissue and recruitment of cells in the epithelium of the foreskin tissue. Meanwhile, multiparameter flow cytometry was a method to measure total frequencies of cells and fluorescence intensity of different markers in the tissue. In this dissertation, T cells were characterised in the foreskin tissue under the influence of Tumor Necrosis Factor α (TNFα) and C-C Chemokine Ligand 27 (CCL27) using these two methods.

1.2 The male reproductive system

The male reproductive system is composed of the penis, the testes, the accessory glands and the genital ducts (15,16). The accessory glands are made up of the prostate, bulbourethral glands and the seminal vesicles while the duct system consists of the efferent ducts, epididymis, vas deferens and rete testes (15,17). The primary organs in the male reproductive system are the testes. The testes are an immune privileged site and consist of the interstitium and the seminiferous tubules (15,16). They respond to hormonal

stimulation; Leydig cells are responsible for androgen production while Sertoli cells facilitate spermatogenesis (15,16).

1.2.1 The penis and the foreskin tissue

The penis is the male external organ and its central canal, the urethra, forms a common conduit for urine and semen (18). The uncircumcised penis consists of the penile shaft, glans, meatus, the frenulum and the inner and outer foreskin tissues (Figure 1.1). The foreskin naturally covers the penis in all primates; specifically, it covers the coronal sulcus, glans and the meatus of a non-erect penis (15,19). The foreskin consists of connective tissue containing collagen-producing dermal fibroblasts and covered by a keratinized stratified squamous epithelium (15). The outer foreskin is attached to the penile shaft and is always exposed to the environment, unlike the inner foreskin that is attached to the penis at the coronal sulcus and is only exposed during erection (20). The inner foreskin is usually lighter in color compared to the outer foreskin tissue (9). The sub-preputial space is the space occurring between the inner foreskin and the glans and it is an anaerobic environment (19). Circumcision eliminates that space and exposes the glans to the external environment in both erect and flaccid states (19).

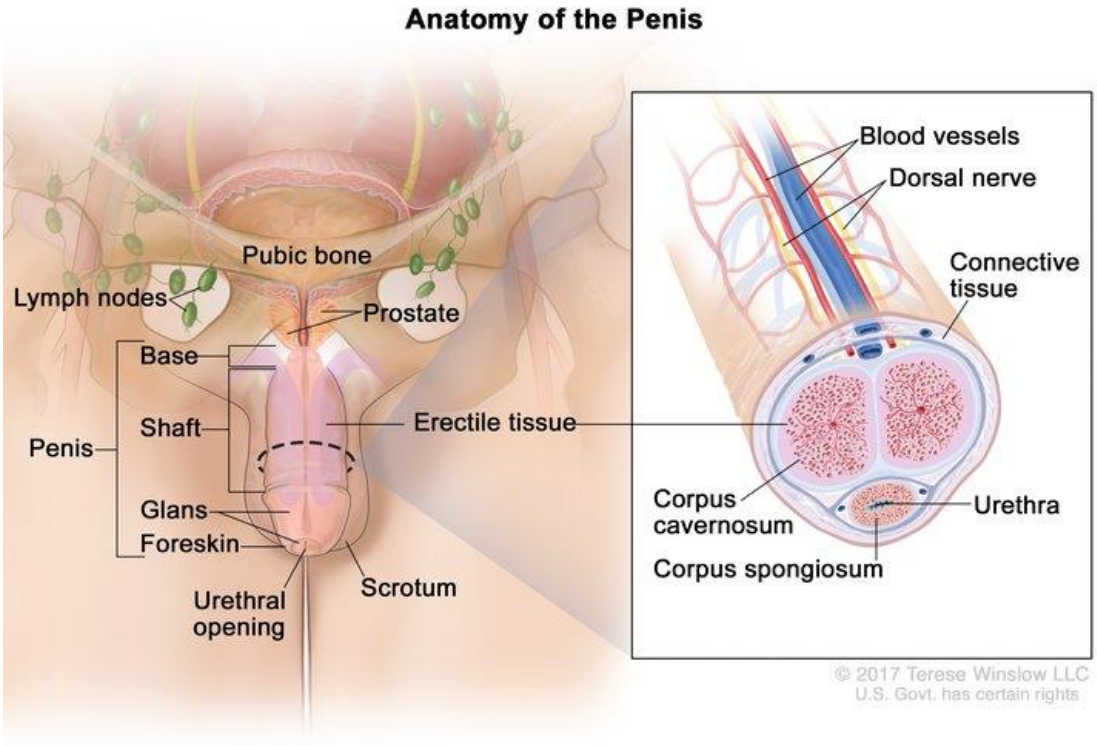

Figure 1.1: Anatomy of the penis showing the foreskin tissue, urethra and glans (21).

The foreskin is rich in Langerhans cells, macrophages and T-cells which express cluster of differentiation 4 (CD4), CCR5 and other receptors and co-receptors that are considered essential for HIV-1 attachment and entry (8,9). Furthermore, the foreskin tissue has been observed to be a major site for HIV entry in men (22–24). The selective entry of HIV via the inner foreskin was first suggested by Patterson et al. by showing cell-free HIV-1 particles infecting Langerhans cells of inner foreskin while no uptake was noticed in outer foreskin, suggesting that the inner foreskin was preferentially infected by HIV (24). This was also observed by Ganor et al. using inner and outer foreskin tissue explants exposed to HIV infected cells and showing the inner foreskin was preferentially infected compared to the outer foreskin (25). It was observed that the size of foreskin also significantly affected HIV incidence rates mainly because a larger surface area was correlated with more HIV target cells in the foreskin tissue (26).

1.2.2 Foreskin tissue and dysbiosis in male genital tract

Microbiome dysbiosis of an intact foreskin was observed to increase the skin's vulnerability and compromise the barrier integrity allowing HIV penetration (27–29). An intact foreskin is a rich environment for anaerobic bacteria to thrive as opposed to a circumcised penis where the microbiome shifts towards an aerobic environment (30). Furthermore, uncircumcised males who were more susceptible to HIV had higher percentages of penile anaerobic bacteria including *Prevotella, Dialister, Finegoldia and Peptostreptococcus* (30). These penile anaerobes were seen to correlate with higher production of proinflammatory chemokines that are involved in HIV target cells recruitment to the foreskin tissue. For example, Interleukin-8 (IL-8) increased with the increase of anaerobes in the foreskin (30). Anaerobic dysbiosis within intact foreskin was found to be one of the reasons why uncircumcised individuals had higher proinflammatory cytokine levels in the male genital tract and hence a more inflammatory environment that might promote HIV acquisition (31). Anaerobe abundance was directly correlated with HIV seroconversion: HIV seroconversion rates increased by 28% to 40% for each 10 fold increase in anaerobic abundance (30). Ten anaerobic genera were seen to decrease significantly after circumcision and they comprised 60% of total penile bacterial load in uncircumcised men (32). One year after Medical Male Circumcision, total bacterial load and microbial biodiversity decreased along with a

significant reduction in proportion of anaerobic microbiota. Aerobic bacteria were also seen to increase post circumcision, albeit not significantly (32).

1.3 Medical male circumcision

Medical male circumcision (MMC) is the removal of all the foreskin tissue and fully exposing the glans penis by a trained health care professional. MMC has been endorsed by World Health Organization (WHO) and UNAIDS as a method to reduce HIV acquisition (33,34). MMC as a strategy to reduce HIV acquisition was rolled out after data from three randomized control trials in Kenya, Uganda and South Africa indicated that MMC provided 52-64% protection from HIV infection (35–37).

As a result, circumcision programs have been rolled out since 2008 in many African countries in order to actively decrease new HIV infections (38). In sub-Saharan Africa, it was estimated that 26.8 million men and boys had undergone MMC in 15 countries from 2008-2019 (39). From 2008 to 2020, South Africa has performed a total number of approximately 4.46 million MMCs (39). It was estimated using mathematical modeling that MMC programs averted around 340 thousand new HIV infections in sub-Saharan Africa by 2019 (39). Despite evidence of the efficacy of circumcision in the reduction of HIV infection in men, MMC is not effective in reducing female HIV acquisition from their HIV infected male partners (40).

Figure 1.2 illustrates the different techniques for performing MMC; the forceps guided method is the simplest with the use of a pair of forceps to guide the procedure, the dorsal slit technique and the sleeve resection method which is the best cosmetically and needs most skill (41).

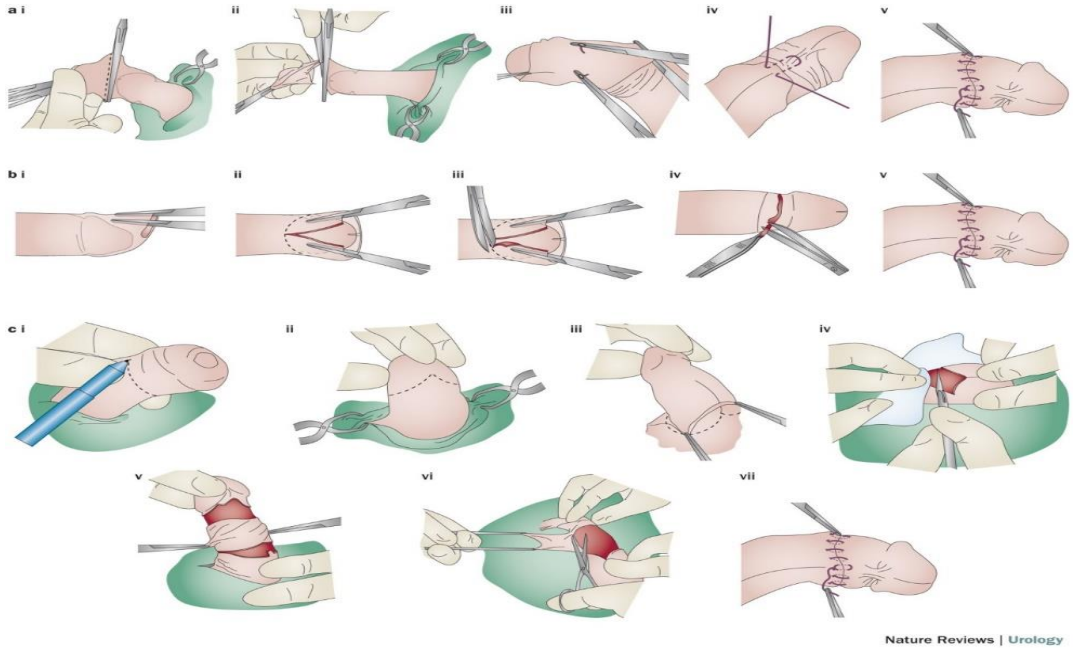

Figure 1.2: Surgical methods used in MMCs. a) Forceps guided method b) Dorsal-slit method c) Sleeve resection method (41).

1.3.1 Traditional circumcision

Ritual male circumcision is a practice prominent across many cultures including Sub-Saharan Africa, Aboriginal Australia and Southeast Asia (2,42,43). In South Africa, the Xhosa ethnic group practice ritual circumcision as a rite for boys to transition into manhood (44). However, medically unsupervised practices have been reported to cause hospital admittance, death and genital amputation in some cases (45,46). The South African government is supervising traditional circumcision to reduce complications and ensure sterilization of instruments used in the practice (47). Furthermore, traditional circumcision can involve removal of only a part of the foreskin tissue and not the complete removal which decreases efficacy of protection against STIs (48,49). Training of surgeons is ongoing and registration with the South African department of health to ensure compliance to infection control procedures and decrease complications (48,49).

1.3.2 MMC and sexually transmitted infections

One of the mechanisms hypothesized for the role MMC plays in the reduction in HIV acquisition is the reduction of the risk of acquiring different STIs (50–52). MMC was observed to reduce the risk of acquiring Human Papilloma Virus (HPV) and Herpes simplex type 2 (HSV-2) (51–53). Furthermore, among women who had circumcised male partners,

decreased risk of STIs was reported including HPV, *Trichomonas vaginalis* and Bacterial vaginosis (54,55). Moreover, female partners of circumcised males were reported to have a lower risk of cervical cancer (56). It was reported in one clinical trial that MMC decreased the risk of acquiring *Trichomonas vaginalis* (TV), *Chlamydia trachomatis* (CT) but not *Neisseria gonorrhea* (NG) (57,58). However, a separate trial observed no protection against the same STIs (59). *Mycoplasma genitalium* (MG) infection was reported to be decreased among circumcised men compared to uncircumcised men (59). However, MMC did not have an effect on the prevalence of MG infection in female partners of circumcised men (60). One study showed no correlation between MMC and acquisition of syphilis while another observed a significant reduction in syphilis infection in HIV infected men while there was a non-significant reduction in HIV negative men (51,61).

1.4 Human Immunodeficiency virus

Human Immunodeficiency virus is a global burden. It was identified as the causative agent for Acquired immune deficiency syndrome (AIDS) in 1983 (62) and officially named HIV in 1986 (63). Nearly 37.60 million people worldwide were living with HIV in 2020 with 1.50 million new cases in 2020 (64). Since the beginning of the epidemic, HIV/AIDS related illnesses have been the cause for 34.70 million deaths (64).

It was estimated that 61% of HIV new cases are in Sub-Saharan Africa as illustrated in Figure 1.3 (65). In South Africa, it was estimated that 7.70 million people live with HIV in 2018 (65). This is more than 20% of the global HIV burden and accounts for a third of all new HIV infections in southern Africa (66).

UNAIDS has set a 90-90-90 plan which aimed that by 2020 (67):

1. 90% of people living with HIV will know their HIV status.
2. 90% of people diagnosed with HIV will receive antiretroviral therapy.
3. 90% of people receiving antiretroviral therapy will have viral suppression.

It was proposed that the achievement of these targets by 2020 will allow the world to end the AIDS epidemic by 2030 (67). In December 2020, 84% of people living with HIV globally knew their HIV status, and 73% were on antiretroviral therapy and 66% were virally suppressed (64).

In Eastern and southern Africa, it is reported that new HIV infections have decreased by 38% and AIDS related deaths by 49% in 2019 (68). 72% of people living in sub-Saharan Africa were on treatment and 65% had suppressed viral loads (68). The sub-Saharan Africa region is closing in on the 90–90–90 testing and treatment targets (68). UNAIDS has since revised these targets to 95-95-95 goals for 2021-2026 aiming that by 2026, 95% of people living with HIV will have known their status, 95% of diagnosed HIV patients will receive antiretroviral therapy and 95% of the people undergoing treatment will be virally suppressed (69).

Many strategies have been rolled out in the efforts to improve preventative measures against HIV including voluntary HIV testing, encouraging the use of condoms, providing Antiretroviral treatment regimens, Pre exposure prophylaxis (PrEP), post exposure prophylaxis (PEP) and Voluntary medical male Circumcision (VMMC) (69,70).

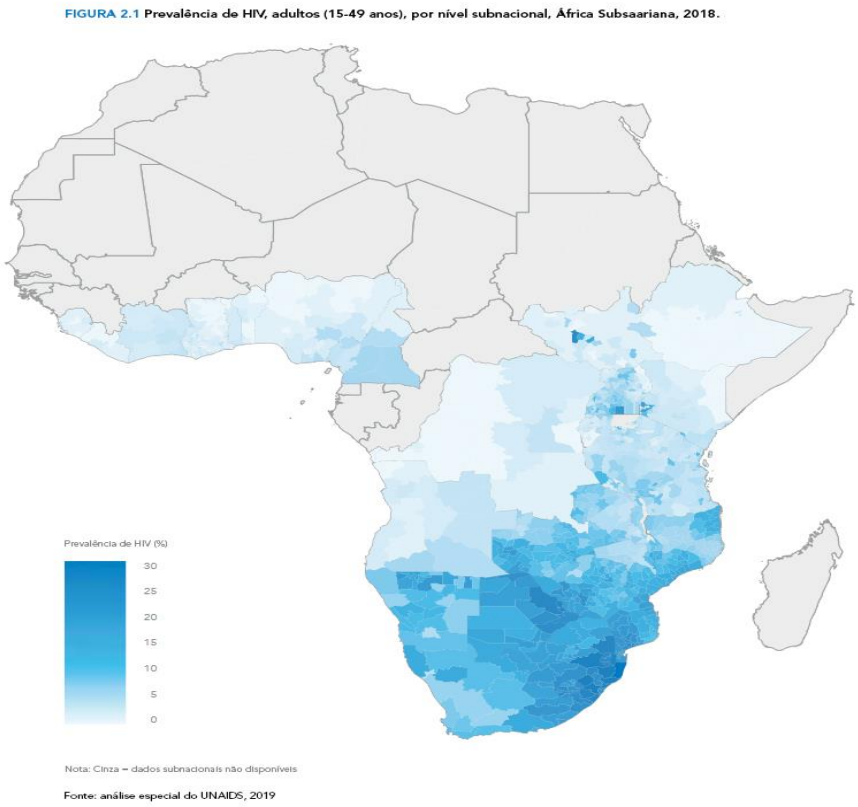

Figure 1.3: Prevalence of HIV in adults aged 15-49 in the African continent (65).

1.4.1 HIV transmission across individuals

It was estimated that heterosexual transmission was the cause for around 70% of HIV-1 infections worldwide (71). An estimation of HIV transmission per each sexual contact

showed a variation in the risk around the world. Female-to-male transmission was estimated to be 0.04% per sexual act while male-to-female was exactly double with a 0.08% in high income countries (72). In low-income countries, female-to-male transmission was 0.38% per act and male-to-female transmission was 0.3%. Women are at risk of HIV acquisition through both penile-vaginal and penile-anal routes (73). The estimates for men who have sex with men (MSM) per sexual contact were higher with a percentage of 1.70% per act (72).

The stage of HIV infection of the sexual partner also affected transmission risk; acute and late HIV stages were correlated with an elevation in HIV transmission per sexual act than the asymptomatic stage of men not undergoing treatment, 9.20 times and 7.30 times, respectively (72). Additionally, the presence or history of genital ulcers in either partner increased transmission per act 5.30 times. Finally, the study showed that for female to male transmission, transmission per sexual act was twice higher in non-circumcised males compared to circumcised males (72). Viral load (VL) has also been seen to have an undeniable effect of increasing the risk of HIV acquisition. It has been observed that for every 10-fold increase in VL in the transmitting partner, there was a 2.50-fold increase in transmission (74,75).

1.4.2 HIV infection at the cellular level

HIV infection of a cell involves complex interactions between the host cell and the virion (76). It starts by the binding of the surface glycoprotein gp120 on the virus to the CD4 receptor on the target cell (Figure 1.4). An HIV target cell is a cell that is susceptible to HIV infection due to expression of the marker CD4 and the co receptors C-C chemokine receptor type 5 (CCR5) or C-X-C chemokine receptor type 4 (CXCR4) such as Macrophages, T helper cells, dendritic cells and astrocytes (77–80). Virions binding to CCR5 are known as R5 tropic while virions binding to CXCR4 are known as X4 tropic HIV. Dual tropism is ability of virus to bind through either CCR5 or CXCR4 (81–83). CCR3 has also been identified as a co receptor for HIV infection to microglia (84). A conformational change takes place in both CD4 and gp120 molecules to facilitate the binding to the co-receptors: CCR5 or CXCR4 on the cell surface (77,78). This allows more conformational changes in gp120 and gp41 (85). Gp41 forms a channel that fuses the cell membrane to the viral envelope (85).

After the fusion of the membranes, the viral capsid translocates into the cytoplasm and the capsid contents are released. The capsid is taken up by an endosome and the change in the

pH causes the liberation of the capsid contents into the cytoplasm (86). Reverse transcriptase (RT) is then activated, and HIV RNA is transcribed into DNA while the RNA is degraded by RNase H. This is followed by converting the DNA single strand of the virion into a double stranded DNA by the DNA-dependent DNA polymerase activity of RT (87). Integrase then inserts the proviral genome into the host cell genome. By that step, HIV infection to the cell is complete (87).

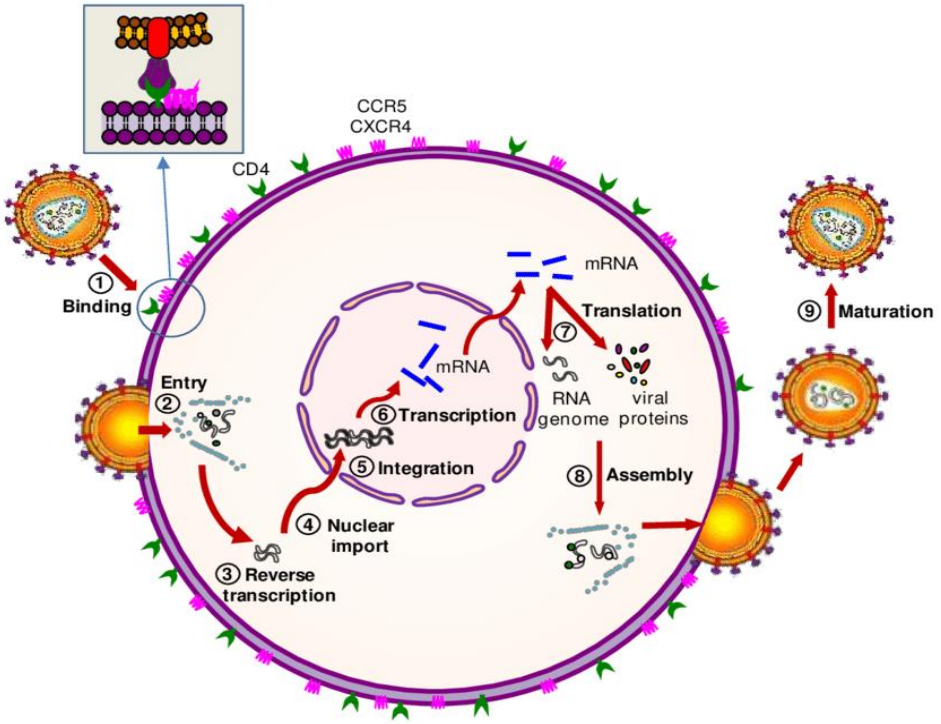

Figure 1.4: Steps of HIV-1 replication cycle from binding and entry to formation of new virions (88).

1.4.3 Foreskin tissue and HIV infection

There are several hypotheses that explain why the foreskin (and inner foreskin specifically) is a major role-player in HIV acquisition. It was suggested that an intact foreskin provides a bigger surface area for HIV to interact with target cells in the male genital tract at infection (26,89). Kigozi et al. clinical trial reported that the average foreskin surface area was significantly higher in men who became HIV infected compared to those men remaining uninfected (26). It was also observed that removing the prepuce decreases the number of HIV target cells available to interact with HIV (50,90). Furthermore, the inner foreskin has been shown to have a relatively thinner keratin layer (stratum corneum) compared to the outer foreskin and the penile shaft (24,91–93). A thick keratin layer would imply more barrier integrity and prohibit HIV penetration into the cells. Based on that theory,

circumcision would remove a surface more vulnerable to HIV infection by the removal of the inner foreskin. However, a few studies observed the difference in the keratin thickness between the inner and outer foreskin was non-significant, in contradiction to those findings (27,94).

1.4.4 Impact of inflammation on HIV Susceptibility

The foreskin tissue is a site abundant in HIV target cells such as Langerhans cells and CD4+ T cells which appear to be enriched in the inner foreskin tissue compared to the outer (20,25,89). Furthermore, the foreskin tissue was described to have increased levels of proinflammatory cytokines including TNFα, and IFNγ (95). An inflamed environment in the male genital tract was proposed to enhance HIV acquisition. Inflammatory signals and immune activation of Langerhans cells and dendritic cells were shown to increase their susceptibility to HIV infection while immature Langerhans cells did not efficiently mediate HIV infection (96,97). Local inflammation in the skin was also observed to cause disruption in barrier integrity by tissue remodeling that causes a decrease in gap junction proteins (19). *Neisseria gonorrhoeae* (NG) was shown to augment HIV infection of resting CD4+ T cells through Toll like receptor 2 activation (98). Toll Like Receptor (TLR) triggering via *Candida albicans* and *Neisseria gonorrhoeae,* was observed to induce TNFα production in skin and vaginal biopsies (96). *Ex vivo* foreskin models showed that up to 50% of T cells could be infected with HIV after tissue was activated with TNFα and TLR-agonists, while unstimulated controls had almost no infection (96). TNFα and TLR agonists stimulation was also seen to enhance HIV replication in Langerhans cells compared to unstimulated samples (96).

To mimic what occurs in the foreskin *in vivo*, Dinh and colleagues created *ex vivo* models of foreskin and cadaveric penile tissues along with *in vivo* models of macaques to view HIV at entry sites (20). After 24 hours, it was seen that significantly higher number of virions were seen in the inner foreskin and glans tissue compared to outer foreskin. Notably, higher proportions of the virus were seen in the uncircumcised glans tissue compared to the circumcised ones (20). This suggested that the inner foreskin and the glans tissue in uncircumcised males are more prone to HIV infection through two possible mechanisms: the first is that virions are allowed to be in contact with the urethral meatus (UM) for longer time by the foreskin tissue when it covers the UM in the flaccid state. The second hypothesis

is that the foreskin tissue retained virus particles which augmented the immune response in the inner foreskin and glans leading to more uptake by HIV target cells in the tissues (20).

1.5 Urethra as an HIV target site

The penile urethra is lined with a pseudostratified non-keratinized columnar epithelium while the more distal fossa navicularis region is a stratified non-keratinized epithelium and the outermost glans region is a stratified keratinized epithelium with a high degree of stratification (99–102). The urethra is a major site of exposure and infection by bacterial and viral pathogens including *Neisseria gonorrhea, Chlamydia trachomatis*, HPV and herpes simplex virus (101,103–106). The epithelium of the urethra is populated with many CD8 T cells, natural killer cells, CD4 T cells and macrophages (100,101). The urethra was shown to be susceptible to R5 tropic HIV infection *ex vivo* (93,107). It was found that CD4+ T cells resided in the urethra in large proportions and to a lesser extent in the fossa and glans. In the three regions, most cells residing in the epithelium compartment were CD8+ T cells while the lamina propria (close to epithelium) was inhabited by both CD4+ and CD8+ T cells (108). Langerhans cells were not observed in the urethral epithelium while it was present in both fossa and glans epithelial tissues (102). CD3+ cells resided in both the epithelial and stromal compartments of the three regions with more dense population in stroma of the glans compared to the urethra and fossa. Macrophages resided in both the epithelial and stromal compartments of the urethra but only stromal compartment of the fossa and glans (102). This study showed low infection of cell associated HIV infection in the three regions. However, the infection was significantly higher in the urethra compared to the fossa and glans (102). HIV infection in the urethra was reported to preferentially target the macrophages (102) and such urethral susceptibility may explain the ~40% incomplete protection afforded by MMC against HIV acquisition.

1.6 Immune cells in the foreskin tissue

The human immune system is composed of the innate immune system and the adaptive immune system; both have the same role of protecting the body against foreign antigens which they elicit differently (109). The innate immune response is the first line of protection against antigens while the adaptive immune response elicits a response that is more specific to antigens (110). Cells involved in the innate immune response are macrophages, natural killer cells, basophils, neutrophils, dendritic cells and eosinophils while lymphocytes form the adaptive immune response (110). Lymphocytes are divided into T-lymphocytes, B-lymphocytes, and the natural killer cells (NK cells). The foreskin tissue is inhabited with a variety of immune cells that were shown to be HIV target cells; CD4+ T cells, Langerhans cells and macrophages occupying the foreskin tissue are estimated to be 22.40%, 11.50% and 2.40% of the total cell population, respectively (Figure 1.5) (111).

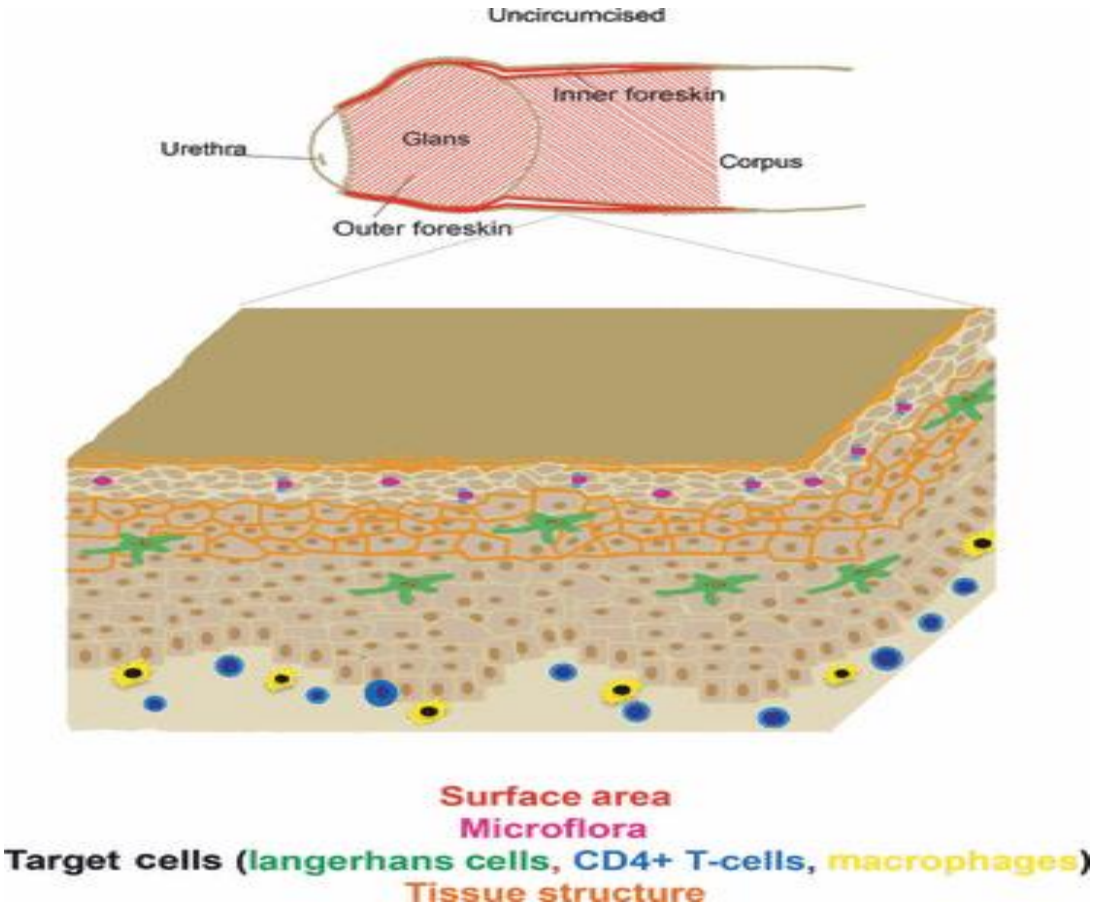

Figure 1.5: Representation of an uncircumcised penis showing potential areas of infection (red) and the change of surface microflora (Magenta) with removal of the foreskin. HIV potential target cells are shown: Langerhans cells (green), CD4+ T cells (blue) and macrophages (yellow) (90).

1.6.1 C-C chemokine receptor type 5 (CCR5) as a key factor in HIV infection

C-C chemokine receptor type 5 (CCR5) is a chemokine receptor expressed on the surface of multiple cells including macrophages, dendritic cells and T cells (112–114). CCR5 is a ligand for proinflammatory chemokines such as CCL3, CCL4 and CCL5 (RANTES) (115,116). It is one of the role-players in an effector immune response; it was shown to enhance CD4+ T cells proliferation and chemokine secretion in response to antigens and also had a role in recruiting naïve CD8+ T cells to sites where CD4+ T cells are interacting with antigen presenting cells (117,118). Furthermore, CCR5 functions as a co-receptor for HIV infection (113,119). It was observed that CD4+ T cells that co-expressed CCR5 in the foreskin were four times more abundant than compared to CD4+ cells detected in blood, suggesting that the foreskin sequestered HIV target cells and thus making it is potentially a highly susceptible site for HIV acquisition (95). CCR5-expressing CD4+ T cells have been shown to be susceptible cells for HIV-1 and it was reported that CCR5 is enriched in CD4+ T cells of the inner foreskin compared to the outer foreskin (91,119,120). In contrast to these results, a recent study observed that CD4+ T cells in the outer foreskin expressed higher levels of CCR5 and CD69. However, the study also reported the total CD4+ T cells population to be twofold higher in the inner foreskin compared to the outer foreskin. Also, the inner foreskin had higher levels of inflammatory cytokines and chemokines compared to the outer foreskin (121).

1.6.2 Langerhans cells

Langerhans cells (LCs) are a subtype of dendritic cells (DCs) and they play a role in protection against infections through being antigen presenting cells in the mucosal epithelium and epidermis of skin including the foreskin tissue (122). LCs express the markers CD1a, C-type lectin langerin and have unusual rod-shaped structures specific to LCs called Birbeck granules (123–125). LCs reside in the peripheral tissues very close to the surface of the skin (1.2% in surface epithelium versus 0.3% in submucosa) (126) and sample their environment for pathogens using their dendritic projections (122). Upon encountering antigens, LCs undergo maturation, followed by higher expression of MHC-II and co-stimulatory molecules CD80, CD86, acquisition of CD83, and down-regulation of the C-type lectin langerin (127,128). LCs maturation causes the release of IL-6, IL-8 and TNFα (127). The secretion of these cytokines and other chemokines results in the migration of LCs from the epidermis to

peripheral lymph nodes where the antigens are presented to naive T cells to initiate an immune response (128,129).

1.6.3 Role of Langerhans cells in HIV infection

Langerhans cells play a dual role during infection based on their activation state. Naïve LCs have a protective role against HIV infection by inhibiting T cell infection and degrading HIV particles (130). LCs are the first cells that capture HIV virions by langerin in naïve LCs, internalize and degrade the virus in Birbeck granules (130). On the other hand, activation of LCs by high virus concentration, pathogens or antibodies causes down regulation of langerin (124). This hinders the protective role LCs have and results in LCs being infected (Figure 1.6) (97,131). Pathogens can activate LCs through TLR interactions or response to cytokine stimulation, which indicates that coinfection decreases the protective effect of LCs due to the down regulation of langerin (96,132). Gram positive bacteria and some pathogens such as *Candida albicans* and *Neisseria gonorrhea* were seen to increase LC populations and hence HIV susceptibility by enhancing TNF-α and Toll-like receptor 2 (TLR2) agonists (96,133). LCs play an important role in HIV infection by transmitting HIV to T cells (10).

LCs express the HIV receptor CD4 and co-receptor CCR5, enabling their infection (11,134). During sexual exposure of an uninfected individual to HIV positive partner, HIV infected T cells form viral synapses with keratinocytes and infect Langerhans cells through dendrites that are extending under the superficial layers of the inner foreskin (111). These Langerhans cells then migrate to the basal membrane and infect T cells (Figure 1.7). That is how Langerhans cells are pivotal in the infection process (111).

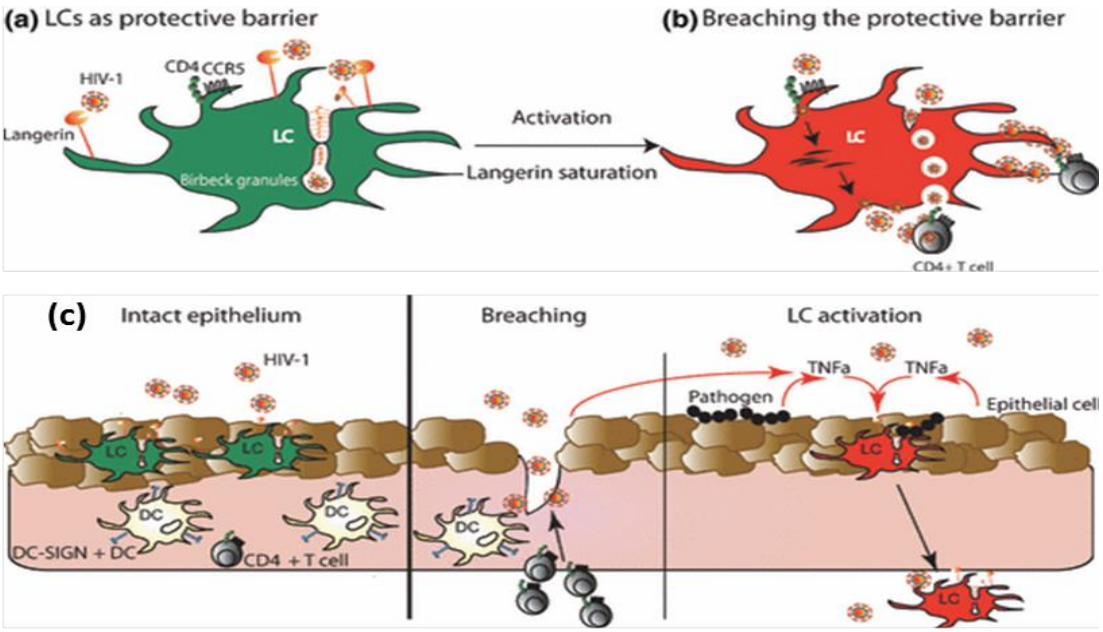

Figure 1.6: An illustration of immature (green) and activated LCs (red): A) forming protective layer to HIV through using Birbeck granules to internalize HIV. B) Activation of LCs result in downregulating langerin and infecting LCs which in turn infects CD4+ T cells. C) TNFα increases number of LCs and replication of HIV in LCs (135).

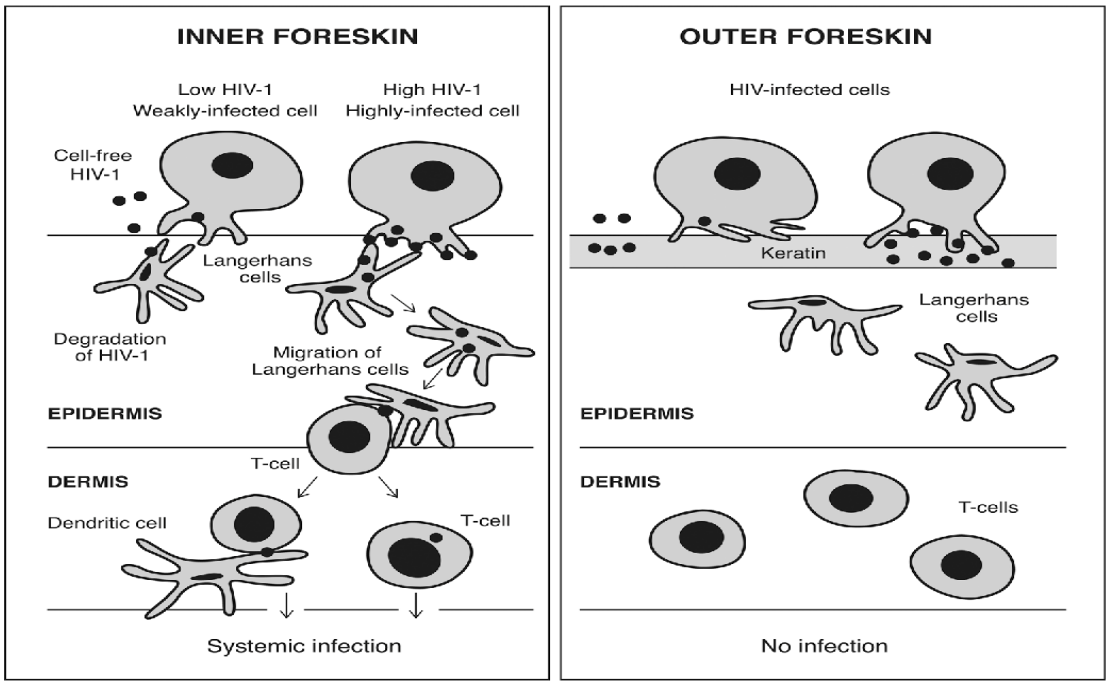

Figure 1.7: An illustration of the mediation of Langerhans cells in T cell infection in the inner and outer foreskin tissues (111).

1.6.4 Macrophages

Macrophages play an important role in the innate immune response against pathogens or damaged cells. Macrophages reside in the submucosa (0.04% reside in submucosa versus 0.02% in the surface epithelium) (126) and their main function is to scavenge and engulf antigens (136). They can naturally engulf without being activated, but when activated they start an inflammatory response represented in antigen presentation and cytokine secretion (137). Macrophages infected by HIV are very effective reservoirs for the virus that can survive for years after the primary infection (138). Macrophages also secrete Monokine Induced by γ-Interferon (MIG) that is correlated with HIV seroconversion. MIG is secreted by macrophages in response to Interferon γ (IFNγ) production and it causes recruitment of T cells in the foreskin tissue (31).

Macrophages are classified into different types according to their activation state and function: M1 type which is also known as classically activated macrophages, M2 type known as alternatively activated macrophages and regulatory macrophages (139–142). M1 macrophages differentiate under the influence of IFN-γ and TNFα and it leads to a proinflammatory pathway where they secrete IL-6, IL-12 and TNFα along with superoxide anions and oxygen and nitrogen radicals to kill pathogens (143–146). M2 macrophages develop influenced by IL-4 and IL-13 produced by Th2 cells and it leads to an anti-inflammatory, or regulatory, pathway with the secretion of IL-10 and TGF-β (139,147,148). M2 macrophages are important role players in wound healing and tissue repair (149) and can produce high levels of IL-10 (145,150,151). During acute HIV infection, macrophages have been observed to be more of an M1 inflammatory state while in chronic infection, macrophages appear to shift to an M2 state (152,153).

1.6.5 Macrophages as HIV target cells and role in latency

Macrophages co-expressing CD4+CCR5+ were observed to be the first cells to be infected with HIV in the urethral mucosa *ex vivo* following infection with cell-associated virions. Urethral T cells in humans were mostly naïve CD8+ or CD4+ cells that were not infected by HIV upon entry (102). Furthermore, macrophages were demonstrated to play an important role in HIV transmission from macrophages to CD4+ T cells (154). Macrophages play an important role in HIV latency. Infected macrophages are shown to be able to survive for long as a viral reservoir that can be reactivated (155,156). A mechanism in which macrophages

act as reservoirs for HIV-1 occurs when HIV envelope glycoprotein causes macrophages to downregulate tumor necrosis factor related apoptosis-inducing ligand (TRAIL) receptor and upregulate genes that antagonize apoptosis which allows virally infected viable macrophages to persist (157). Another mechanism for macrophages as HIV reservoir is that HIV infected macrophages are not efficiently killed by cytotoxic lymphocytes because of intrinsic resistance by the macrophages (158). Furthermore, HIV has been demonstrated to be capable of replicating in primary macrophages without signaling the innate immune system and silences IFN responses (159). HIV-1 DNA, RNA and intact virions were found in macrophages of urethral cells of HIV infected patients under suppressive ART (155). In contrast, the CD3+ T cells from the same tissue had undetected levels of HIV components (155). Furthermore, LPS stimulation caused a reactivation of HIV outgrowth in urethral cells containing macrophages but not T cells and the reactivation significantly decreased after macrophage depletion (155). Macrophages and T cells in the urethra from HIV infected patients on ART often formed conjugates in both the stroma and the epithelium compared to urethra of uninfected individuals (155).

1.6.6 T cells

The blood and tissues of a healthy human contain different subsets of T cells. T lymphocytes are developed in the thymus and are known to have a major role in the immune response. CD4+ T cells and CD8+ T cells form the major two populations of T lymphocytes (109). CD8+ T cells are known as cytotoxic T cells and are responsible for killing virus infected cells and tumor cells. CD4+ T cells are involved in many functions in the immune response such as activating the cells of the innate immunity, B-lymphocytes and cytotoxic T cells activation and also suppression of the immune response (109,160). Activation of naive CD4+ T cells occurs after interacting with antigen-MHC complex and leads to further differentiation into subtypes that elicit different immune responses according to the cytokines secreted by these T cells (109,160). CD4+ T cells can be further classified into T helper 1 (Th1) cells, T helper 2 (Th2) cells, T helper 9 (Th9) cells, T helper 17 cells (Th17), T helper 22 cells (Th22), T follicular helper cells (Tfh) and T regulatory cells (Tregs) (Figure 1.8). Each of these subsets is known for producing a distinctive set of cytokines that induce a specific immunological response (109,160).

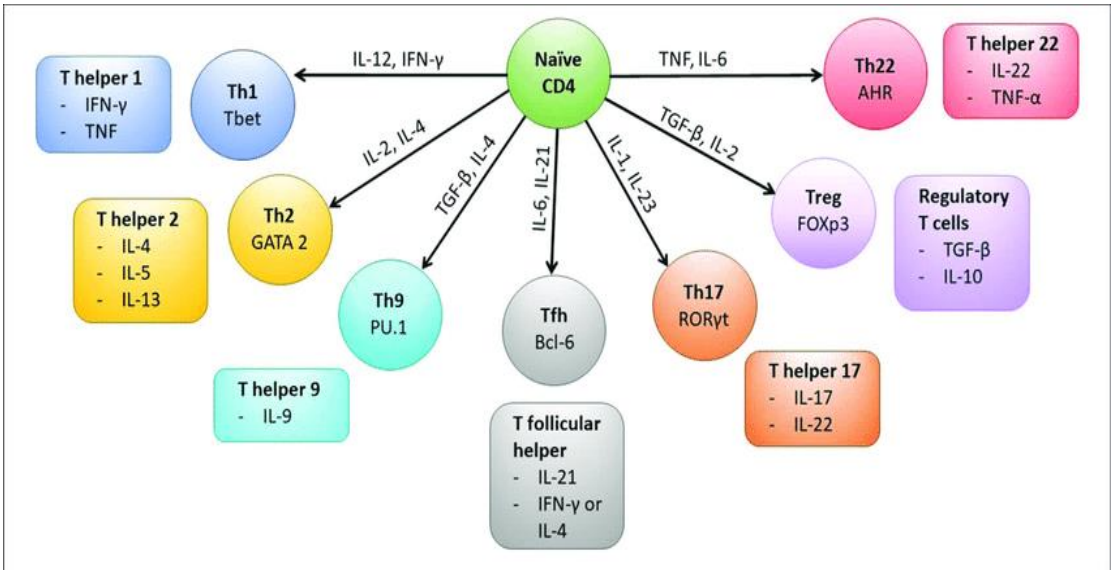

Figure 1.8: An illustration showing different T helper subsets and their main cytokine secretions (160)**.**

1.6.6.1 CD4+ T cells in the foreskin tissue

Tissue resident CD4+ T cells were reported to reside in the foreskin tissue and were predominantly an effector memory phenotype and had much higher frequency of CCR5 expression compared to CD4+ T cells in the blood (42% in foreskin tissue compared to 9.90% in blood) and IL-17 production (95). CD4+ T cell proportions differ in the inner and outer foreskin. Several studies have reported that a greater number of tissue resident CD4+ T cells reside in the inner foreskin tissue compared to the outer foreskin (24,91,120,121). However, in contrast, a study by McCoombe and short reported higher CD4 cells in the outer FS compared to the inner FS (92). Differences in these results may be because of altered conditions in the experiments such as presence of an infection or different experimental designs and analysis employed in each study. However, HIV susceptibility isn't only related to CD4+ proportions but also the state of activation and secretion of proinflammatory chemokines. Higher levels of anaerobic bacteria are known to inhabit the inner foreskin of the uncircumcised penis and most likely responsible for eliciting the elevated levels of proinflammatory cytokines, IL-17, IL-8 and RANTES, in the inner foreskin (30,121). Bacterial and viral STIs have been observed to influence the activation and density of T cell subsets in the foreskin tissue (31,50,161). CD4+ T cells were observed to be higher in the foreskin tissue of HSV-2 infected males (50). Furthermore, HSV-2 infection caused an increase in the CD8+ T cell density in the foreskin tissue (50).

1.6.6.2 Th1 cells

Th1 Cells are a subset of T cells that are known for the secretion of IFN-γ, TNF, lymphotoxin and IL-2. Naïve T cells differentiate into Th1 cells by exposure to IFN- γ and IL-12 early in the time of T cell priming (162). Th1 cells have an essential role in immune response against infections caused by intracellular bacteria. Th1 cell production of IFN- γ causes macrophages to be activated against intracellular parasites. Th1 cells express high levels of CCR5 and were found to be highly infected by R-5 tropic HIV (163).

1.6.6.3 Th2 cells and TH9 cells

Th2 cells are distinguished by their secretion of IL-4, IL-5 and IL-13 and their role in B cell immune responses while Th9 secrete IL-9 and contribute to antitumor immune defense (110,164,165). Th2 cells and Th9 cells were found to be more prone to infection with X-4 tropic than R-5 tropic strain *ex vivo* because of their expression of CXCR4 but not CCR5 (163).

1.6.6.4 T helper 17 cells

T helper 17 cells (Th17) are among the many cells that reside in the foreskin tissue and are susceptible to HIV infection because of their proinflammatory nature in mucosal immunity. Th17 cells produce IL-17A, IL-17F and TNF (166,167). The major signaling cytokines involved in Th17 cells differentiation are IL6, IL21, IL23, and TGF- β. Meanwhile, retinoic acid receptor-related orphan receptor gamma-T (RORγt) is the master regulator (168–171). Th17 cells take part in host defense against extracellular bacteria and fungi including *Klebsiella pneumonia, Candida albicans* and *Mycobacterium tuberculosis.* They are also involved in the development of autoimmune diseases (167,172–175) as well as recruitment and activation of Neutrophils (176,177).

Th17 cells were observed to be more abundant in foreskin tissue compared to blood (95). Furthermore, Th17 cells were observed to be two-fold higher in density in the inner foreskin tissue compared to the outer foreskin tissue (121). Gosselin et al. demonstrated that Th17 cells in the blood (identified as CCR4+CCR6+ T cells) were seen to be more susceptible to R5 and X4 tropic HIV infection and to have higher levels of HIV DNA in treatment naïve patients (14). Both Th17 and Th1 cells were found to be highly HIV susceptible *in vitro* and preferentially depleted *in vivo* during infection (12–14). In addition, Th17 have been seen as

a primary target for Simian immunodeficiency virus (SIV) and it made up 64% of the infected cells within 48 hours of viral acquisition (178).

1.6.6.5 T regulatory cells

T regulatory cells (Tregs) are a T cell subset that regulates the activity of other immune cells and maintain peripheral tolerance: preventing auto-reactive immune response and ensuring immunity is directed against foreign pathogens (179). Tregs express CD4+/CD25++/FoxP3+ and they exert their immune regulatory function through cell-cell interactions or cytokine release that inhibits Th1 and Th2 response (180–182). Treg cells also co-express CCR5 which makes them susceptible to HIV infection (183,184). However, HIV-infected Treg cells still maintained their suppressive role despite being infected and suppress immune activation, which might slow disease progression (184–186). Treg cells have also been described as an important HIV reservoir in patients undergoing treatment (187,188).

1.6.6.6 T helper 22 cells

T helper 22 cells (Th22) are a T cell subset that produces IL-22 and TNF but do not secrete or express IL-17 (189–191). Th22 cells co-express surface expression of CCR10, a chemokine receptor for ligands CCL27 and CCL28 (192). IL-22 is a pro-inflammatory cytokine that has a role in wound healing and keratinocyte migration to skin (193). Th22 cells constitute around 7.60% of the outer foreskin population and 5.10% of the inner foreskin population (121) and appear mostly of an effector memory phenotype (95). Th22 appear to be highly susceptible to HIV infection and are preferentially depleted in the colon of HIV positive patients compared to Th17 and Th1 cells (191).

1.7 Chemokines and cytokines in the foreskin and penile tissues

Chemokines and cytokines in the foreskin tissue have an essential role in the inflammation of foreskin tissue and potentially susceptible to STIs and HIV infection. Many chemokines and cytokines were detected in the foreskin tissue. IL-8 was detected in 60% of coronal sulcus swabs of males undergoing MMC while Monokine Induced by γ-interferon (MIG) was detected in 25% of the swabs (31). Other cytokines including GM-CSF, MCP-1, MIP3α, IL-1a and RANTES were detected in 10% of sample donors (31). IL-8 levels were noticed to

significantly decrease after MMC compared to the control group that didn't undergo circumcision. Furthermore, IL-8 detection in the coronal sulcus was correlated with a significant increase in highly HIV susceptible T cells populations; CD4+CCR5+ T cell subsets including Th17 cells, Th1 cells, and TNFα+ CD4 T cells (31). The seroconversion rates in the control group that didn't undergo circumcision has been seen to increase when more than one of the cytokines were detected in the coronal sulcus swabs (31). IL-8 and MIG were specifically correlated with higher HIV acquisition in males (31). MMC was reported to decrease IL-8 levels significantly which might potentially decrease HIV acquisition. IL-8 and MIG are pro inflammatory cytokines that are involved in the recruitment of immune cells to inflamed tissues (31).

The epithelium of the inner foreskin tissue of sexually active men was reported to harbor higher concentration of the pro-inflammatory cytokines GM-CSF, IFN-γ, IP-10, and RANTES (119). IP-10, GM-CSF, RANTES and IFN-γ were four-fold, three-fold, two-fold and 1.25 fold higher compared to the outer foreskin, respectively (119). This suggests an increased inflammation in the inner foreskin tissue compared to the outer foreskin tissue. Zhou et al. demonstrated that HIV inoculation induced higher RANTES levels in the inner foreskin. The high RANTES levels were observed to mediate T-cells recruitment to the epidermis of the inner foreskin tissue and promotes formation of LC-T cells conjugates; this study suggests the inflammatory process involved in the higher susceptibility of the inner foreskin tissue to HIV (194). Many chemokines were observed to be highly expressed in the inner foreskin compared to the outer foreskin (91). Out of 84 genes assessed, 28 genes were significantly expressed higher in the inner foreskin tissue including CCL27, CXCL12, and TLR4 (91). However, other chemokines including CXCL10, TLR2 and TYMP were significantly higher in the outer foreskin as opposed to the inner. CCL27 was ∼7 fold higher in the inner foreskin compared to the outer foreskin; this was in correlation with CD4+CCR5+ cells estimated higher in density in the epithelium of the inner foreskin (91). CCL27 is a chemokine that is predominantly expressed in the skin by keratinocytes and is involved in homing of memory T cells and Langerhans cells to the skin (195). It was observed to be produced upon stimulation of keratinocytes with TNFα (196). CCL27 is the ligand for CCR10 receptor which is expressed on a variety of HIV susceptible cells including Th22 cells and Langerhans cells (191,192,197). CCL27/CCR10 have a paramount role in tissue repair, skin homeostasis and inflammatory responses (192).

Despite the protective role MMC has against STIs and HIV acquisition, there still remains target sites in the male genital tract that facilitate infection including the glans penis and the urethra (102,198). All penile regions (penis glans, urethra and fossa) were observed to be able to spontaneously produce pro-inflammatory and anti-inflammatory cytokines such as IL-17 and IL-22 and other important intermediaries in the infection process (108). The glans penis contains higher proportions of activated NK cells and effector CD8+ cells which makes it a preferential site for HIV infection after the foreskin tissue (108). Multiple cytokines were found in the urethra, fossa and glans of the penis (108). IFN-γ-secreting cells, CD4+ cells expressing both IL-4 and IL-5 were detected in the three tissues and to a lesser extent TNFα secreting cells, IL-2 secreting cells (108). IFNγ, TNFα and IL-2 production was detected in low amounts (less than 2% of CD4+ T cells) in all three penile regions (108). Proportions of IL-17 and IL-22 were considerably lower in the glans penis, fossa and urethra than in the inner or the outer foreskin tissue (108). Urethra, fossa and glans were also observed to have a wide range of cytokines including RANTES, IL-13, CCL28 (high levels) and MCP-1, TRAIL, and CCL25 (in intermediate concentrations) and CCL27, MIP-3α, Etoaxin, MCP-4 and IL-4 (low levels) (121). TGF-β1, SDF-1α, MCP-1, IL-8 and IL-7 were found to be present in high concentrations in the seminal fluid of fertile males. IL-5, IL-13, MIP-1B, IL-1α and β, RANTES, IL-6, IL-17, MIP-1β, IFN-α and G-CSF were also detected in low concentrations (<150 pg/ml)(199). The roles of some of these chemokines has been described in literature to increase HIV susceptibility or recruit more immune cells to skin. MIG, MIP-3α and IP-10 have been observed to increase HIV uptake in resting CD4+ T cells without requiring the cells to be activated (200). CCL28 is the ligand for CCR10 along with CCL27 and is involved in homing of T cells to skin (201). Furthermore, MCP-1 is a key chemokine in the regulation of the migration and infiltration of macrophages and memory T cells (202,203). The male genital tract is an active immune site with both innate and adaptive immune responses along with chemokine production (204).

1.8 Fluorescence techniques in measuring tissue-resident immune cells

The discovery of fluorescence and fluorescence labeled substances is one that enabled a breakthrough in all aspect of cell biology, molecular biology and immunology; this subsequently led to the development of the first fluorescent microscope in 1913 by Heinrich Lehmann (205). Fluorescence microscopy enables the examination of fluorescent cells and tissues using a microscope; whether these tissues were intrinsically fluorescent or through staining with an extrinsic fluorescent dye (206). It has allowed a wide range of applications and uses over other forms of microscopy with high sensitivity and specificity.

1.8.1 Immunofluorescence imaging

Immunofluorescence (IF) imaging is a technique that uses different immunofluorescence labeled antibodies to visualize cells in the tissue and how they might be localized among other tissue compartments (207). IF imaging allows visualizing spatial distribution and expression of markers in the tissue. It is an important tool in viewing tissues and organs as a system and not as separate cells (207).

1.8.2 Flow cytometry

Flow cytometry is a tool that uses lasers to analyze different characteristics of cells (208). It is powerful in characterizing immune cells in single cell suspensions and it can characterize wider ranges of surface and intracellular markers compared to microscopy (208). It defines cells into different populations using cell size, granularity and fluorescence labeled antibodies. It enables interrogation of multiple different markers expressed by a single cell and allows understanding immunological environment in a tissue beyond spatial distribution of cells (208). It can identify immune cells that express many different markers (i.e. Th1, Th2, Th17 and Th22) along with identifying differentiation of cells (208).
We have used both immunofluorescence imaging and flow cytometry to characterize CD4+ T cells in the foreskin tissue and how it responds to exogenous stimulation by chemokines.

1.9 Rationale of the project

MMC has been reported to decrease HIV susceptibility and the risk of acquiring other STIs (35–37). The observed reduced risk of STI infection due to the removal of the foreskin tissue is postulated to be associated to the abundance of HIV target cells recruited to foreskin tissue during an inflammatory response, however the mechanism for this is poorly defined. Previously, increased level of CCL27 expression in the inner FS tissue was associated with higher frequency of CD4+CCR5+ which are quintessential HIV-1 target cells (8,89,90). CCL27 is a chemokine involved in tissue repair and homeostasis and is involved in T cells homing to skin (195,209). In this study we hypothesized that CCL27 secreted during tissue damage and/or inflammation takes part in the recruitment of CD4+ T cells to the epithelium of the foreskin tissue and that exogenous exposure to CCL27 will result in recruitment of these cells to the epithelium of the foreskin tissue. Furthermore, CCL27 was previously observed to be upregulated in the inner FS relative to outer FS, suggesting a possible mechanism for increased HIV acquisition via the inner compared to outer FS. Therefore, using immunofluorescence we aimed to characterize the response of CD4+ T cells to CCL27 exogenous exposure and the role of CCL27 in the recruitment of HIV target cells (CD3+CD4+ T cells) in the epithelium of the foreskin tissue. Moreover, given that CCL27 is the ligand for CCR10 receptors found on Th22 cells and LCs (192,197), we aimed to phenotype the immune cells recruited under the influence of CCL27 using multi parameter flow cytometry.

1.10 Hypothesis

This dissertation hypothesized that CCL27 higher expression in the inner foreskin was responsible for the recruitment of CD4+ T cells in the epithelium of the inner foreskin tissue and that exogenous exposure to CCL27 would have an impact on the increase in the density of CD3+CD4+ T cells in the epithelium of the foreskin tissue.

1.11 Aims and objectives

Aim 1: to determine the impact of CCL27 on recruiting CD3+CD4+ T cells to the foreskin epithelium.

Objective of aim 1: to use immunofluorescence microscopy to assess the changes in CD3+CD4+ T cell density in the epithelium of the foreskin tissue under the influence of exogenous exposure to CCL27.

Aim 2: to compare two methods of counting CD3+CD4+ cells; manual counting and semi-automated counting.

Objective of aim 2: to use Softworx software on the Deltavision microscope for manual counting and PIPSQUEAK macro on ImageJ for semi-automated counting of dually labelled cells and compare the two methods using different statistical analysis methods.

Aim 3: to use multiparameter flow cytometry to characterize T cell subsets isolated from foreskin tissue under the influence of CCL27.

Objective of aim 3: to use multiparameter flow cytometry panel: CD45, CD3, CD4, CCR5, CCR4, CCR6 and CCR10 to characterize and quantify live T cells in the foreskin tissue.

Chapter 2: Materials, methods and titration of chemokines

Table of contents

2.1 Study participants

Participants enrolled into the study were all adults undergoing voluntary MMC from the Western Cape Province and MMC is conducted in one of the collaborating clinics in Cape Town. The following inclusion criteria were applied for participants:

Participants were scheduled for Voluntary MMC, were adults >18 years, HIV-1 seronegative, had no symptomatic STIs or lesions and provided an informed consent to collect foreskin samples.

The following exclusion criteria were applied:

Participants who did not meet inclusion criteria, had an unknown HIV-1 status or HIV-1 seropositive, had symptomatic STI or visible lesion or where informed consent was not obtained.

A total of 18 foreskin samples were analyzed in this dissertation. Immunofluorescence microscopy utilized foreskin samples from 11 donors (11 inner foreskin tissues and 4 outer tissues). However, three inner foreskin samples derived from one donor were excluded due to disintegration of tissue which prevented quantification of cells. We used samples derived from 7 donors for the flow cytometry analysis. This sub-study, including laboratory protocols and the use of human foreskins, was reviewed and approved by the University of Cape Town's Faculty of Health Sciences Human Research Ethics Committee (HREC REF 382/2021 under the main study HREC REF number 071/2017).

2.2 Sample collection

Foreskin tissues were collected in the clinics after performing MMC. Foreskins were immediately stored in sterile 50 mL conical tubes [Greiner Bio-One (Lasec Cat. No.: P1TUB0138-00050)] containing 20 ml of RPMI 1640 media (Sigma Cat. No.: R8758-500ml) supplemented with 10% Heat inactivated Fetal Calf serum [Gibco (Life Technologies Cat. No.: F10493-106)] and 1% penicillin-streptomycin [Gibco (Life Technologies Cat. No.: 15140-122)]. The tissues were transported to UCT laboratories as soon as possible after MMC, to reduce negative effects on tissue viability. Upon reaching the laboratories of the University of Cape Town, samples were rinsed with Phosphate buffer serum PBS supplemented with 1% penicillin-streptomycin [Gibco (Life Technologies Cat. No.: 14040-

0910] and the excess fat tissue and blood vessels were removed using sterile scalpel and forceps. After the removal of all excess adipose tissue, the inner and outer foreskin were separated as shown in Figure 2.1 and further sectioned into ~1cm^2 smaller sections.

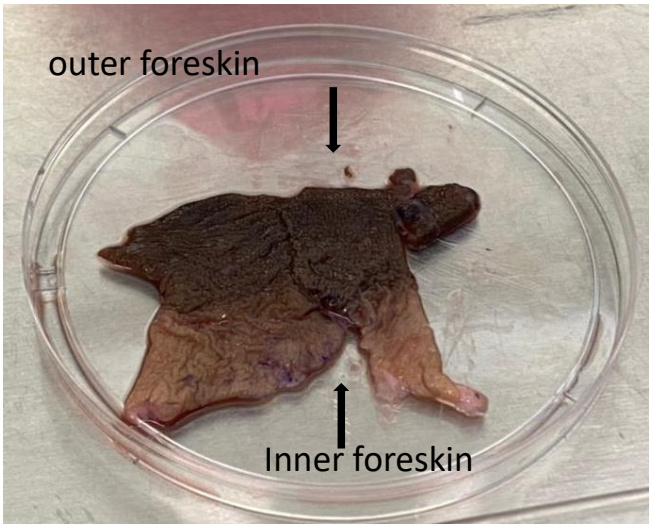

Figure 2.1: A foreskin tissue sample (inner and outer).

2.3 Exposure of Foreskin tissue to TNF and CCL27

The inner and outer foreskin tissues were sectioned into 1 cm^2 sections and transferred to a 48 well plate (Lasec Cat. No.: P1PLA044C-000048). To determine the effect of CCL27 on foreskin T cells recruitment in the epithelium of the foreskin tissue, three conditions were tested; unstimulated (1 ml of RPMI 1640 supplemented with 10% FCS and 1% pen-strep), TNFα as a positive control (23) (100 ng/ml TNFα in 1 ml RPMI 1640 supplemented with 10% FCS and 1% penicillin-streptomycin) and CCL27 [R&D (Whitehead scientific Cat. No.: 376-CT-025)] (400 ng/ml in 1 ml RPMI 1640 supplemented with 10% FCS and 1% pen-strep). All experiments were set up in a blinded manner. The samples were incubated for 48 hours at 37 ºC, 5% CO_2. Tissue sections were then rinsed in PBS, embedded in tissue freezing medium [Leica biosystems (SMM Africa Cat. No.: 14020108926), placed into regular cryomolds and frozen at -80 ^{o}C, until further analysis.

2.4 Sectioning and staining of foreskin tissue

Cryomolds containing tissue freezing media embedded tissues were transferred to a cryostat machine (Leica CM1860). Tissue sections were cut at 12 µm thickness and transferred onto slides (Marienfeld Cat.No.: 0810000). Two to three tissue sections were placed on each slide and then transferred to the -40°C freezer till staining. At the time of the staining, tissue sections were allowed to thaw at room temperature for ten minutes then hydrophobic pen was drawn around each tissue section and PIPES-formaldehyde fixative was added to the slides (3 ml PIPES buffer+ 1 ml methanol free formaldehyde) (Thermo fisher scientific Cat. No.: 28906). After washing in three coplin jars (Sigma Aldrich Cat.No.: S5516) with PBS, tissues were blocked with 10% normal donkey serum (supplemented with 0.10% Triton X-100 and 0.10% Sodium Azide) for 1 hour at room temperature. The tissue sections were incubated with primary antibodies against human CD3 (undiluted) (Table 2.1) for 1 h at 37 °C and were washed three times in PBS then incubated for 30 min at room temperature with donkey anti-rabbit Alexa Fluor 488 (FITC) (1:500) then washed. The tissue sections were then incubated with primary antibodies against human CD4 (1:50) (Table 1) for 1 h at 37 °C and were washed three times in PBS then incubated for 30 min at room temperature with donkey anti-mouse Alexa Fluor 647 (1:500) then washed. Tissue sections were counterstained with HOECHST (1 µl in 20 ml PBS) for 5 min at room temperature to visualize nuclei. A fourth wash was added at the end using fresh PBS to decrease background in the images. Tissues were air dried and then mounted using fluorescent mounting medium MOWIOL (MERCK Cat. No: 475904) with antifade and covered with coverslips (marienfeld Cat.No.: 0107222) ensuring no air bubbles form. The edges of the coverslips were sealed with fast drying clear nail polish. After ensuring that the nail polish was dry, slides were stored in slide boxes (Leica, Cat. No. 71459-B) at 4°C until imaging.

Table 2.1: List of Antibodies used in immunofluorescence staining.

Antibody	Fluorophore	Cat. No.	Company	Dilution
Anti CD3 rabbit anti human	NA	Ab21703	Abcam	Neat
Anti CD4 mouse anti human	NA	C1805-100TST	SIGMA	1:50
Secondary CD3 (Donkey anti-rabbit)	Alexa Fluor 488	711-546-152	AEC Amersham	1:500
Secondary CD4 (Donkey anti-mouse)	Alexa Fluor 647	715-607-003	Jacksons	1:500
HOECHST (DAPI)	NA	H1399	LTC Tech South Africa	1:20000

2.5 Immunofluorescence microscopy

Images were collected on a Deconvolution microscope using a DeltaVision RT system on Olympus IX71 microscope and inspected using a SoftWorX software. Images were captured on a digital camera (CoolSNAP HQ; Photometrics) using a ×60 objective. Thirty z-sections, 0.50 µm apart, were collected per image field. Panels of 9 images were collected to visualize the density of the target cells (CD3+CD4+) across the epithelium of the inner and outer foreskin tissue explants. To determine CD3+CD4+ cell density in each sample, 10 images were collected for each experimental condition. Panel images were acquired to include the epithelium and lamina propria. Surface area of the epithelium was highlighted for measurement and CD3+ CD4+ cells were highlighted on each of the layers manually. Data were uploaded to collaborators at Northwestern University, Chicago, to analyze the files using Integrative Data Language to calculate surface area and calculate the counted dually positive cells in the epithelium. The number of CD3+CD4+ cells in each image was divided by the surface area to calculate density of cells per mm^2 of tissue. A total of 650 images were collected. As negative controls, corresponding slides were concurrently stained with universal isotype control (Rabbit IgG and mouse IgG1) along with HOECHST only slides. The images were also analyzed using PIPSQUEAK/ImageJ.

2.6 Image analysis using ImageJ

We exported the images generated on the Deltavision RT system and analyzed them using ImageJ 1.53f and PIPSQUEAK AI (version 5.2.1, Rewire neuro), a macro added to ImageJ that enables semi-automated counting of double positive cells. It automatically detected the single labeled cells in both Alexa 488 and Alexa 647 channels and then merged them to detect and count the dually labeled cells. We analyzed 16 inner foreskin tissue samples (6 unstimulated samples and 5 TNFα 100ng/ml and CCL27 400ng/ml exposed samples) and 6 outer foreskin tissue samples. This was used for comparison between manual and semi-automated counting methods.

2.7 Cell extraction by migration of spontaneously migrating cells

Inner and outer foreskin cells were allowed to spontaneously migrate out of the tissue into the culture medium under the three conditions (unstimulated, TNFα 100ng/ml exposed or CCL27 400ng/ml exposed). The tissue was split into three parts and cut into 1 cm^2 sections that were incubated in R10 media (RPMI 1640 supplemented with 10% FCS and 1% pen-strep), TNFα as a positive control (100 ng/ml TNFα in RPMI 1640 supplemented with 10% FCS and 1% pen-strep) and CCL27 (400 ng/ml in RPMI 1640 supplemented with 10% FCS and 1% pen-strep) for 48 hours at 37° C. After 48 hours, the migrated cells from the inner and outer foreskin tissues were harvested into single cell suspensions and counted using TC20 cell counter (BIO RAD, Model no. TC20TM Automated Cell counter) and viability recorded. Cells were stained for flow cytometry.

2.8 Separation of epidermis and dermis layers using Dispase enzyme

A portion of tissues exposed to chemokines as described in section 2.7 were washed in PBS and placed in 4 mls of 5U/ml Dispase II [Roche (Sigma Cat. No.: 04942078001)] in Hanks buffer salt solution [Gibco (Thermo fisher scientific Cat. No: 14170120)] was added to divided petri dishes (lasec Cat. No: 18090H) for 18 hours at 4° C to separate epidermal sheets from the remaining hypodermis layer. Figure 2.2 shows the placement of cells in Dispase solution with the orientation of epidermis facing the lid of the plate. Following 18 hours of dispase treatment, epidermis and dermis were separated using forceps and used to compare spontaneous cell migration or liberase tissue digestion. For spontaneous cell

migration, the epidermis and dermis layer were separately placed in culture plates containing 4 ml RPMI 1640 supplemented with 10% FCS and 1% pen-strep for 48 hours at 37° C. Alternatively, the epidermis and dermis were placed in Liberase for digestion into single cell suspensions.

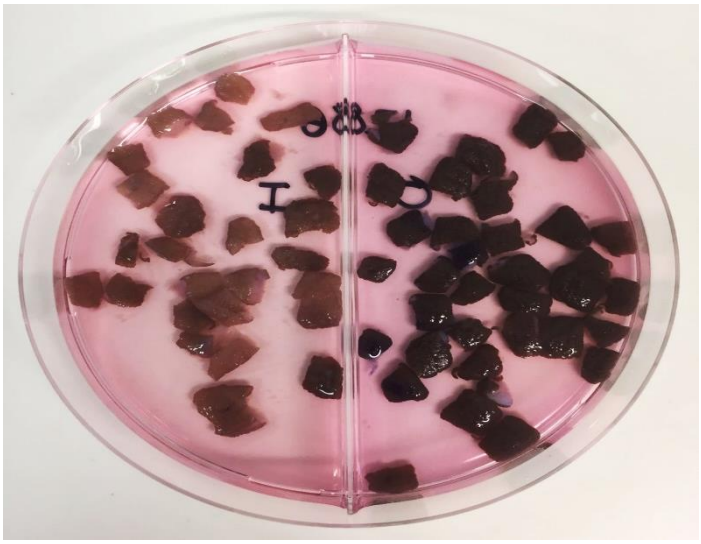

Figure 2.2: Inner and outer foreskin tissue sections placed in Dispase 5 U/ml for 18 hours.

2.9 Liberating cells from the foreskin tissue

Epidermal sheets of inner and outer foreskin tissue after Dispase treatment were placed in Liberase 5U/ml (Sigma Aldrich Cat.No: L313453) for 3 hours in 37^{o}C and then single cell suspensions were collected using 70 µm cell strainers [Corning (Sigma Aldrich Cat. No: CLS431751-50EA)]. Cells were washed with PBS, centrifuged at 400g for 5 minutes and supernatant discarded. Cells were resuspended in PBS and counted using TC20 cell counter and viability recorded.

2.10 Flow cytometry staining

Foreskin cells were transferred to a 96-well plate at a concentration of 2×10^{6} cells per well. Cells were stained with the viability marker VIVID [Invitrogen (Thermo Fisher Scientific Cat.No: 34955)] using 50 µl of vivid solution (stock is diluted at 1:40 then 1 µl to 49 µl of PBS). The plate was incubated in the dark at room temperature for 20 min. Cells were washed once with 100 µl of Facs buffer and centrifuged at 400 g for 5 minutes. Supernatant was removed and 50 µl of surface staining monoclonal antibody cocktail was added (CD45, CD3, CD4) (table 2.2). The plate was incubated at room temperature for 20 min in the dark.

Cells were washed once with 100 µl of Facs buffer and centrifuged at 400 g for 5 minutes. Supernatant was removed and 50 µl of CCR staining monoclonal antibody cocktail was added (CCR5, CCR4, CCR6, CCR10) (table 2.2). The plate was incubated at 37^{o}C for 20 min and covered with foil. Cells were washed once with 100 µl of Facs buffer and centrifuged at 400 g for 5 minutes. Supernatant was removed and cells resuspended in 200 µl FACS lysis buffer (1 ml lysis solution in 10 ml distilled water). Cells were transferred to labeled 5 ml Facs tubes. Th17 cells are denoted as cells expressing CD45+, CD3+, CD4+, CCR4+, CCR5+ and CCR6+ while Th22 are CD45+, CD3+, CD4+, CCR4+, CCR5+, CCR6+ and CCR10+. Samples were acquired within 24 hours of staining using BD LSRII flow cytometer. 500000 events were acquired. Data were analyzed using FlowJo analytical software version 10.7.1 (FlowJo, LLC).

Antibody Panel:

Table 2.2: Antibody panel used in flow cytometry experiment.

Antibody	Fluorophore	Clone	Cat. No.	Company	Dilution
CD45	BV786	HI30	563716	BD Biosciences	1 µl in 50 µl Facs buffer.
CD3	APC/Cy7	UCHT1	300426	Biolegend	1 µl in 50 µl Facs buffer.
CD4	Alexa Fluor 700	SK3	344622	Biolegend	1 µl in 50 µl Facs buffer.
CCR5	PE/CY7	J418F1	359108	Biolegend	0.625 µl in 50 µl Facs buffer.
CCR4	BV-605	L291H4	359418	Biolegend	1.5 µl in 50 µl Facs buffer.
CCR6	BV711	G034E3	353436	Biolegend	1.5 µl in 50 µl Facs buffer.
CCR10	APC	1B5	564771	BD Biosciences	0.625 µl in 50 µl Facs buffer.

2.11 Statistical analysis:

Statistical analysis was conducted using GraphPad Prism 8® (GraphPad Software, San Diego California USA). Non-parametric Mann-Whitney U test was used for unpaired data while non-parametric Wilcoxon matched pairs was used for paired data. Paired t-test was used for paired parametric Log_{10} transformed data. For correlation analysis, Spearman rank correlation test was used to measure strength of correlation between two counting methods (manual counting and semi-automated counting). Bland-Altman plots (difference plots) were used to measure difference between manual and semi-automated counting methods. A p-value <0.05 was considered statistically significant.

2.12 Titration of chemokines:

We titrated the concentrations of chemokines used to induce cell recruitment in the foreskin tissue explants and used MIP1α 100 ng/ml, TNFα 100 ng/ml, CCL27 100 ng/ml and CCL27 400 ng/ml. Preliminary data showed low efficacy of MIP1α 100 ng/ml and CCL27 100 ng/ml in stimulating foreskin tissue explants. Based on these findings, we opted to continue the experiment with TNFα 100 ng/ml as a positive control and CCL27 400 ng/ ml as our tested chemokine. Figure 2.3 shows representative images of titration results. Figure 2.3 shows representative images comparing MIP1a, TNFα and the 2 concentrations of CCL27. In Figure 2.4, each data point represents a field of view (FOV) in foreskin tissue samples (~10 per sample) acquired via the Deltavision microscope. Figure 2.4a show TNFα 100 ng/ml to be a superior positive control compared to MIP1α (Median density of CD3+CD4+ in TNFα 100 ng/ml was 202.10 cells/mm^2, IQR: 146.10-268 compared to 133.30 cells/mm^2, IQR: 78.52-202.10 in unstimulated tissues, p=0.003, Median density of CD3+CD4+ in MIP1α 100 ng/ml was 167.80 cells/mm^2, IQR: 85.73-254.40, p=0.171). Meanwhile, CCL27 400 ng/ml Induced higher CD3+CD4+ cell recruitment compared to CCL27 100 ng/ml (Median density of CD3+CD4+ in CCL27 400 ng/ml was 175.10 cells/mm^2, IQR: 112.40-259.20 compared to 133.30 cells/mm^2, IQR: 78.52-202.10 in unstimulated tissues, p=0.061, Median density of CD3+CD4+ in CCL27 100 ng/ml was 132.30 cells/mm^2, IQR:.97.91-210.80, p=0.460).

In the outer foreskin (Figure 2.4b), TNFα 100 ng/ ml and MIP1α had limited impact on the density of CD3+CD4+ T cell (Median density of CD3+CD4+ in TNFα 100 ng/ml was 33.18 cells/mm^2, IQR: 0-190.10 compared to 34.72 cells/mm^2, IQR:0-79.31 in unstimulated tissues, *p*=0.330, Median density of CD3+CD4+ in MIP1α 100 ng/ml was 34.80 cells/mm^2, IQR: 0-91.71, *p*=0.785). Both CCL27 400 ng/ml and CCL27 100 ng/ml had limited impact on the density of CD3+CD4+ T cell (Median density of CD3+CD4+ in CCL27 400 ng/ml was 27 cells/mm^2, IQR: 0-72.38 compared to 34.72 cells/mm^2, IQR: 0-79.31 in unstimulated tissues, *p*=0.644, Median density of CD3+CD4+ in CCL27 100 ng/ml was 0 cells/mm^2, IQR:.0-67.05, *p*=0.138). We concluded that TNFα 100 ng/ml and CCL27 400 ng/ml are the optimal chemokines and concentrations for downstream experiments and analysis.

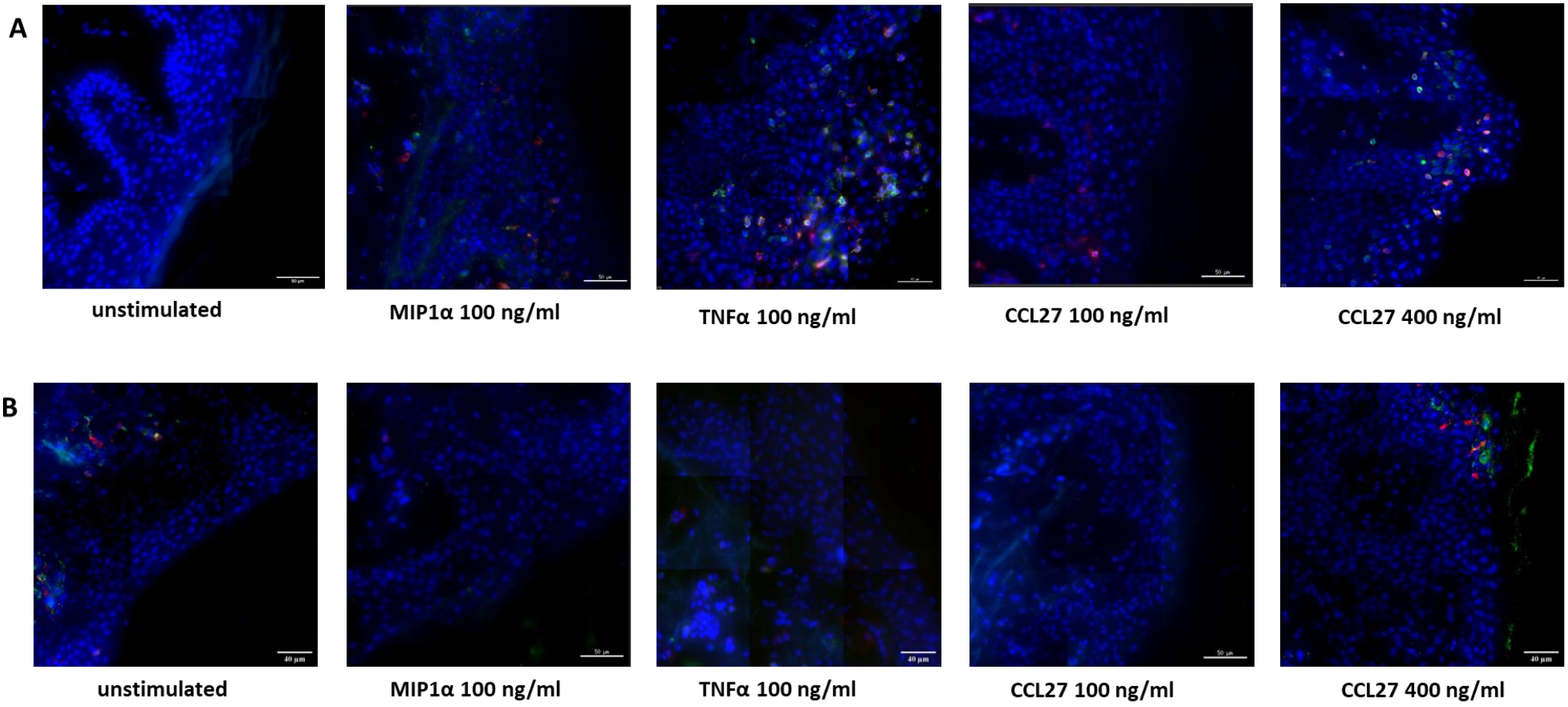

Figure 2.3 Representative images from the titration of chemokines. A) Representative images of unstimulated, MIP1α 100 ng/ml, TNFα 100 ng/ml, CCL27 100 ng/ml, CCL27 400ng/ml exposed tissues in the inner foreskin. B) Representative images of unstimulated, MIP1α 100 ng/ml, TNFα 100 ng/ml, CCL27 100 ng/ml, CCL27 400ng/ml exposed tissues in the inner foreskin.

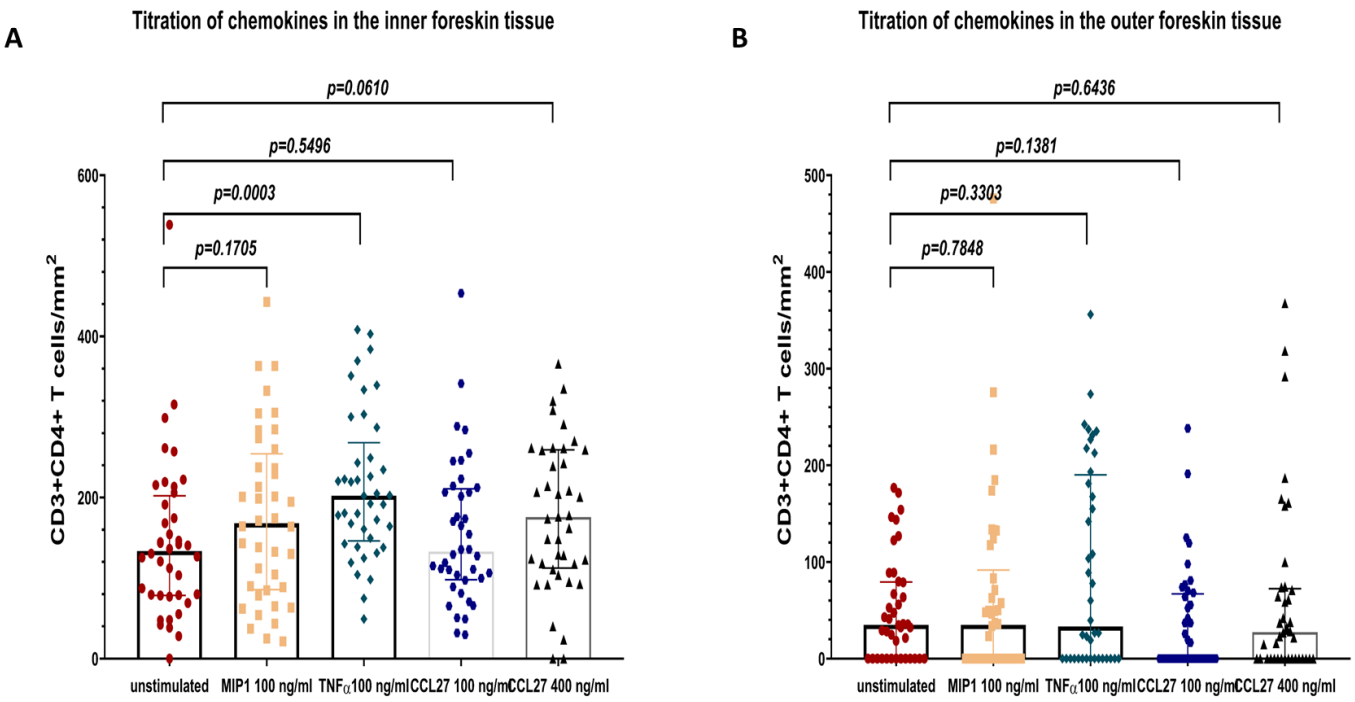

Figure 2.4: Titration of chemokines in the inner and outer foreskin tissues. A) Titration results in the inner foreskin tissue (n=40). B) Titration results in the outer foreskin tissue (n=40).

Chapter 3: Immunofluorescence imaging of the foreskin tissue under the influence of TNFα and CCL27

Table of contents

3.1 Introduction

The foreskin tissue has been shown to be a site rich in Langerhans cells, Macrophages and T cells which express CD4 and CCR5 as stated in section 1.6 in the literature review. The foreskin tissue has also been shown to be rich in proinflammatory chemokines and cytokines including RANTES, IL-8, MIG and MCP-1 as stated in section 1.7, page 21. In section 1.3.2, page 5 in the literature review, we have indicated that the foreskin tissue has been shown to increase susceptibility to different infections including HPV, HSV-2, MG and HIV. Studies have observed that the inner foreskin was a more favorable site for HIV infection compared to the outer foreskin tissue (section 1.2.1, page 3 in literature review). We aimed to understand if the inner foreskin tissue has a potential to be infected with HIV by examining numbers of HIV target cells in the tissue. Prior findings by our lab have assessed levels of chemokines in both inner and outer foreskins (91)(section 1.7, page 20). Twenty-eight of these genes were significantly more upregulated in the inner foreskin such as CCL27 and CXCL12. However, other genes including TLR4, CXCL10, TLR2 and TYMP were more predominant in the outer foreskin compared to the inner foreskin. Chemokine C-C ligand 27 (CCL27) had ~7 fold increase in the inner foreskin compared to the outer foreskin tissue (91). CCL27 is a chemokine that is produced by keratinocytes and has been shown to be involved in homing of memory T cells in skin (195,201). CCL27 is also the ligand for CCR10 that is expressed on the surface of Th22 cells and Langerhans cells (192,197). These cells were observed to reside in the foreskin tissue and are important role players in HIV infection (111,121,194). CCL27 upregulation in the inner foreskin tissue was found to be correlated with increased CD4+CCR5+ cell populations in the epithelium of the inner foreskin compared to the outer foreskin (91). We hypothesized that CCL27 protein elevation would influence the number of CD3+CD4+ T cells in the epithelium of the inner and outer foreskin tissue, and that the exogenous exposure of tissue explants to CCL27 will cause a recruitment of CD3+CD4+ T cell populations from the dermis of the tissue to the epidermal layers where it would be more prone to HIV infection. To test this hypothesis, we exogenously exposed inner and outer foreskin tissue explants to TNFα, an inflammatory cytokine mainly produced by macrophages and monocytes and has a role in inflammatory responses, and CCL27 and performed immunofluorescence imaging on the tissue to compare density of CD3+CD4+ T

cells across the three conditions: unstimulated, TNFα exposed and CCL27 exposed foreskin tissue explants.

3.2 Experimental design

Figure 3.1 shows the experimental design illustrating the chronological process involved in generating the output data starting from obtaining the foreskin samples to ultimately generating immunofluorescent images. The steps involved included: (i) processing foreskin samples, (ii) exposure to chemokines, (iii) snap freezing, (iv) tissue sectioning and (v) staining for imaging.

Figure 3.1: The experiment design for measuring chemokines impact on the density of CD3+CD4+ T cells in the inner and outer foreskin tissue.

3.3 Results

3.3.1 Selection criteria

Samples were collected from HIV negative adults undergoing MMC. Seeing that CCL27 upregulation in the inner foreskin tissue was associated with higher density of CD4+CCR5+ T cells (section 1.7, page 21 in literature review), we wanted to understand a mechanism for possible cell movement into the tissue and measure the impact of exogenous exposure to CCL27 on the inner and outer foreskin tissue explants. Exogenous TNFα was used as a positive control. Ten inner foreskin samples and 4 outer foreskin samples were used for this experiment.

3.3.2 Unstimulated explants of inner and outer foreskin tissue

We compared 10 inner and 4 outer foreskin tissue explants in their untreated condition (cultured in R10 media for 48 hours). Each of the tissues had approximately 10 FOVs taken from different areas of the tissue and cells were counted on the Deltavision microscope. In the untreated foreskin tissue, CD3+CD4+ T cells were found to be present in both the epithelium of the inner and outer foreskin consistent with previous findings showing the foreskin tissue to be inhabited with CD4+ T cells as mentioned in section 1.6.6.1, page 18 in literature review (9,24,92,121). Our findings from inner foreskin tissue sections from all images generated for the 10 donors (~10 images per donor per condition) showed the median of CD3+CD4+ T cells in the epithelium of the inner foreskin tissue to be 60.08 cells/mm2 (IQR: 24.47-126.40 cells/mm2) while for the outer foreskin tissue of the 4 donors was 34.72 CD3+CD4+ T cells/mm^2 (IQR: 0-79.31 cells/mm^2) (Figure 3.2a). The median densities were compared using Mann-Whitney test, and there was a significant difference between inner and outer foreskin (p=0.022). We observe the spread of the density of CD3+CD4+ T cells from across the 10 samples in the inner foreskin in Figure 3.2b showing variations in the density of CD3+CD4+ T cells across individuals. We then chose 4 samples from the inner foreskin tissue and 4 samples from the outer foreskin tissue and plotted the means of all the images taken from each donor per condition and conducted Mann-Whitney test. Figure 3.2c shows higher median density of CD3+CD4+ T cells in the inner foreskin (127.50 cells/mm^2, IQR: 89.22-219.5 cells/mm^2) compared to outer foreskin tissue explants

(36.52 cells/mm^2, IQR:18.29-96.65 cells/mm^2; p=0.057). These results suggest a trend of higher densities of CD3+CD4+ T cells in the inner foreskin tissue explants compared to the outer foreskin in the untreated tissue explants. However, the small sample size compared in the inner and outer foreskin may be a factor in the results not being significant.

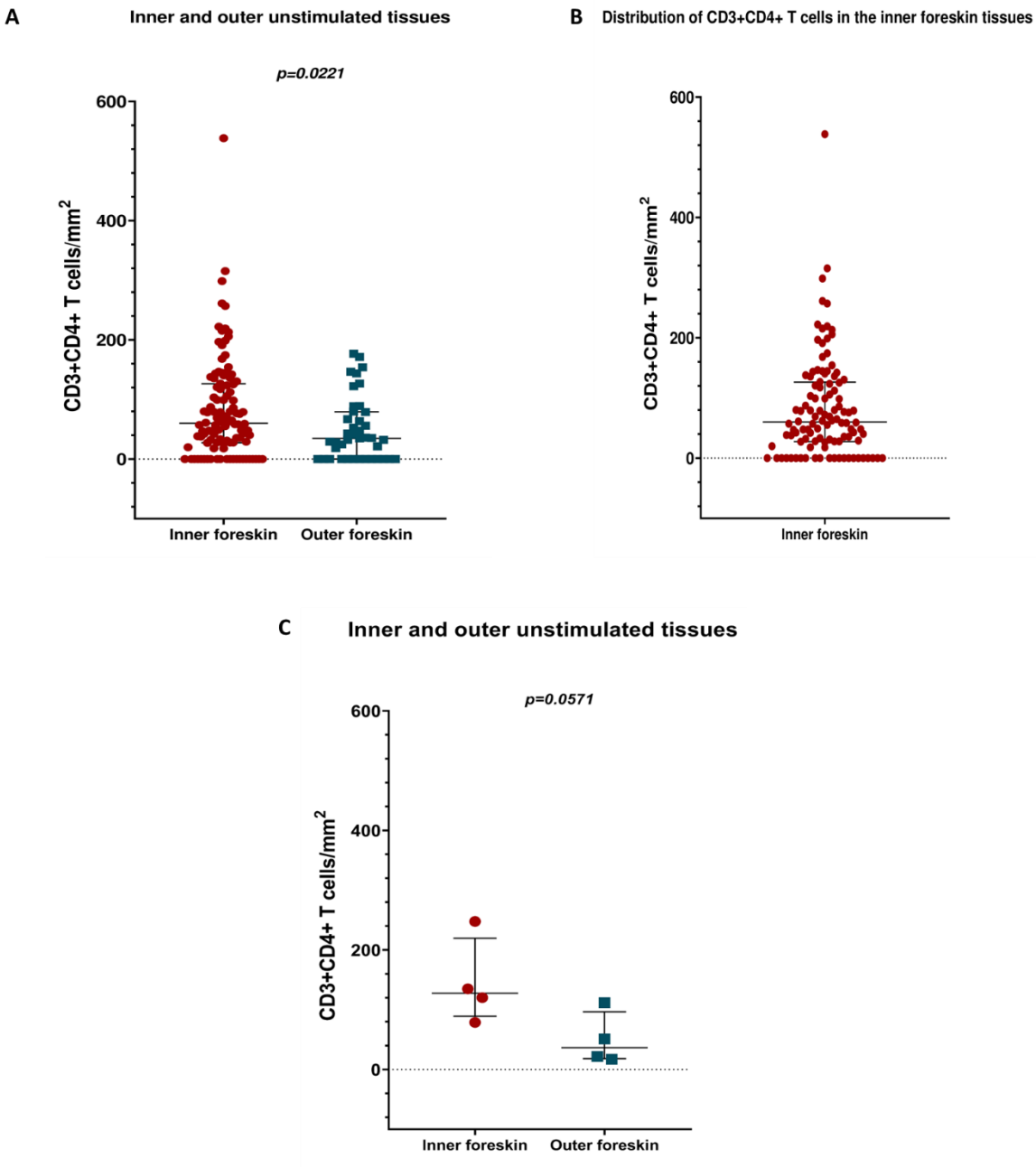

Figure 3.2: Comparing *ex vivo* CD4+ T cell/mm^2 between inner and outer foreskin tissue in the unstimulated tissues. A) Number of CD3+CD4+ T cells in the epithelium of 10 untreated inner and 4 outer foreskin tissue explants (n=108 for the inner foreskin, n=41 for the outer foreskin). B) Number of CD3+CD4+ T cells in the epithelium of 10 inner foreskin tissue explants (n=108). C) Means of densities of CD3+CD4+ T cells in 4 inner foreskin tissue and 4 outer foreskin tissue explants (means of ~10 images per sample per condition were taken, n=4).

3.3.3 Frequency distribution of CD3+CD4+ density in the foreskin tissue in response to chemokines

Figure 3.3 shows the frequency distribution of the number of CD3+CD4+ T cells in the inner and outer foreskin tissues across the unstimulated, TNFα exposed and CCL27 exposed tissue explants. The distribution in Figure 3.3a and 3.3b shows the data points are not normally distributed in the inner and outer foreskin tissue samples, respectively. Non-parametric statistics were thus used to analyze the data (Mann-Whitney test). In Figure 3.3a, we noted 21% of unstimulated explants had the count of 0-25 cells/mm2 compared to 4% and 9% in TNFα and CCL27 exposed tissues, respectively. Cell counts of 25-75 cells/mm2 in the unstimulated tissue were also higher (32%) compared to TNFα (12%) and CCL27 exposed tissues (4%). However, in the higher counts, TNFα and CCL27 exposed tissues recorded higher percentages compared to unstimulated. These results highlight that there were increased number of cells with the exposure of tissues of the inner foreskin to TNFα and CCL27. Figure 3.3b shows that in the outer foreskin tissue samples, 73% of the unstimulated tissues counts, 55% of TNFα exposed tissues counts and 80% of CCL27 exposed tissues counts fall within 0-75 cells/mm^2. This suggests a limited effect of CCL27 and TNFα on the densities of CD3+CD4+ T cells in the outer foreskin tissue.

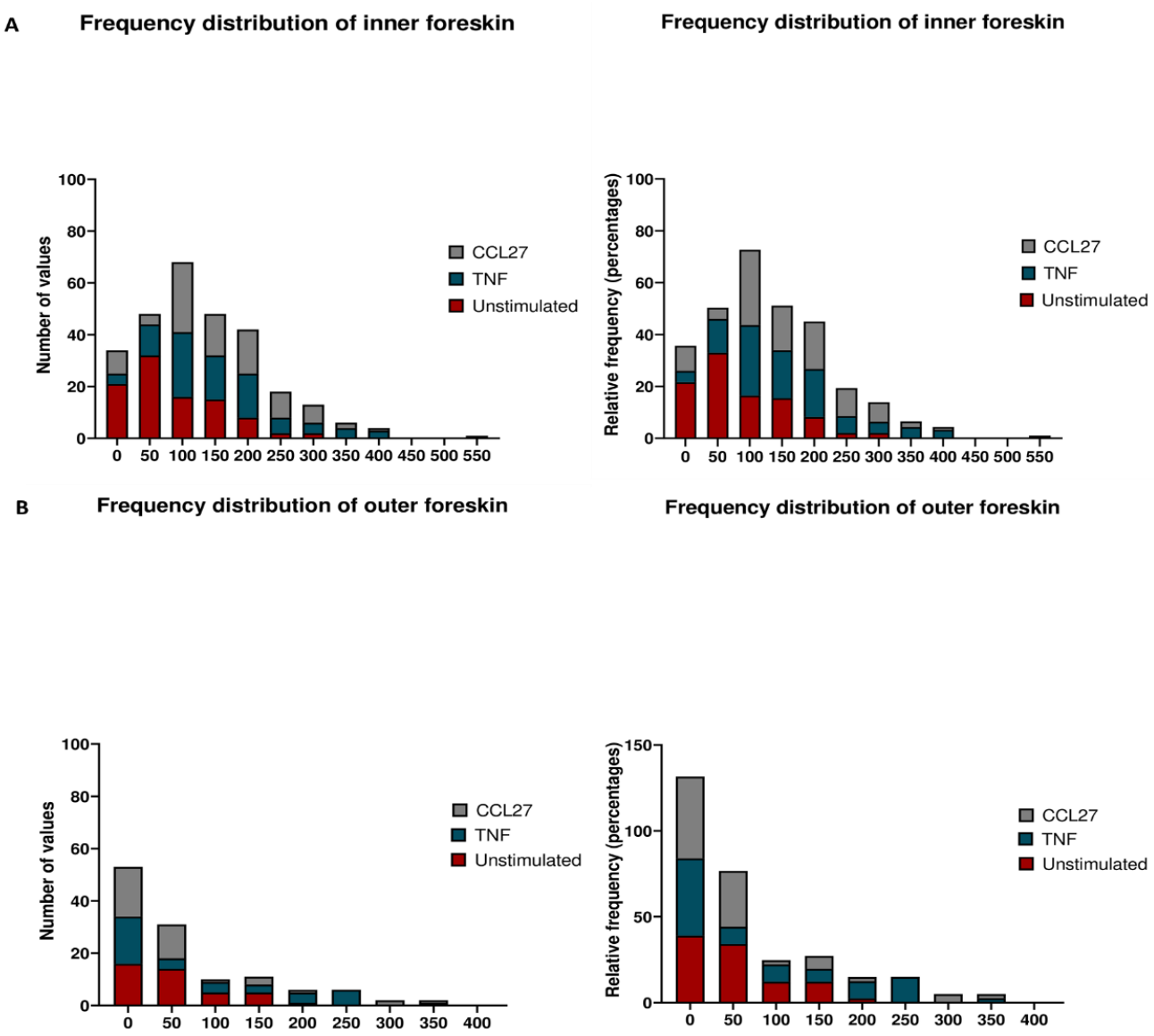

Figure 3.3 Frequency distribution in the inner and outer foreskin tissues. A) Frequency distribution of density of CD3+CD4+ cells in the inner foreskin tissue explants across unstimulated, TNFα and CCL27 exposed samples. B) Frequency distribution of density of CD3+CD4+ cells in the outer foreskin tissue explants across unstimulated, TNFα and CCL27 exposed samples.

3.3.4 Impact of TNFα and CCL27 exposure of inner and outer foreskin tissue explants on CD3+CD4+ T cell population in the epithelium

We next compared samples from 9 inner foreskin tissue explants and 4 outer foreskin tissue explants (∼10 images per donor) across the three conditions tested (unstimulated, TNFα 100ng/ml and CCL27 400ng/ml).

CD3+CD4+ T cell population in the epithelium of the inner foreskin tissue after TNFα and CCL27 exposure

Figure 3.4 (A, B and C) shows representative images of the dually positive CD3+CD4+ T cells in the epithelium of the inner foreskin tissue explants in unstimulated, TNFα exposed and CCL27 exposed tissues, respectively. Images in the left-hand side show CD3-ALEXA 488 labeled cells, images in the middle show CD4-ALEXA 647 labeled cells and the images on the right-hand side are dually labeled CD3+CD4+ cells which are our target cells. Figure 3.4 (D, E and F) show isotype controls for CD3, CD4 and HOECHST only staining, respectively. It is observed in Figure 3.5 that after exposing 9 inner foreskin tissue explants to exogenous TNFα 100 ng/ml or CCL27 400 ng/ml, a significant increase in the number of CD3+CD4+ T cells in the epithelium of the inner foreskin tissue occurred. In Figure 3.5a, we compared cell median density from 9 donors (∼10 images per donor) using Mann Whitney test and it showed a significant increase in the median density of CD3+CD4+ T cells in the inner foreskin tissue explants after exposure to TNFα (138.20 cells/mm^2, IQR: 89.31-208.70 cells/mm^2) compared to unstimulated tissue (62.07 cells/mm^2, IQR:27.85-136 cells/mm^2; P<0.0001) and CCL27 (147.40 cells/mm^2, IQR:93.03-208.30 cells/mm^2) to unstimulated tissue explants (62.07 cells/mm^2, IQR:27.85-136 cells/mm^2; P<0.0001). We then calculated the average cell density for each donor from the 10 images captured and compared the median cell density among the 3 conditions using Mann-Whitney test. Similarly, median cell densities were observed to be significantly higher in the TNFα exposed tissues (134.80 cells/mm^2, IQR: 109.30-206.60 cells/mm^2) compared to unstimulated tissue explants (78.88 cells/mm^2, IQR: 33.02-127.50 cells/mm^2; p=0.035) and significantly higher in the CCL27 exposed tissue (164.80 cells/mm^2, IQR: 140.30-184.90 cells/mm^2) compared to unstimulated tissue explants (78.88 cells/mm^2, IQR: 33.02-127.50 cells/mm^2; p=0.008) (Figure 3.5b). The differences in p values in 3.5a and 3.5b is due to taking the means of all images taken per donor to account for 10 data points as 1 data point per donor per condition.

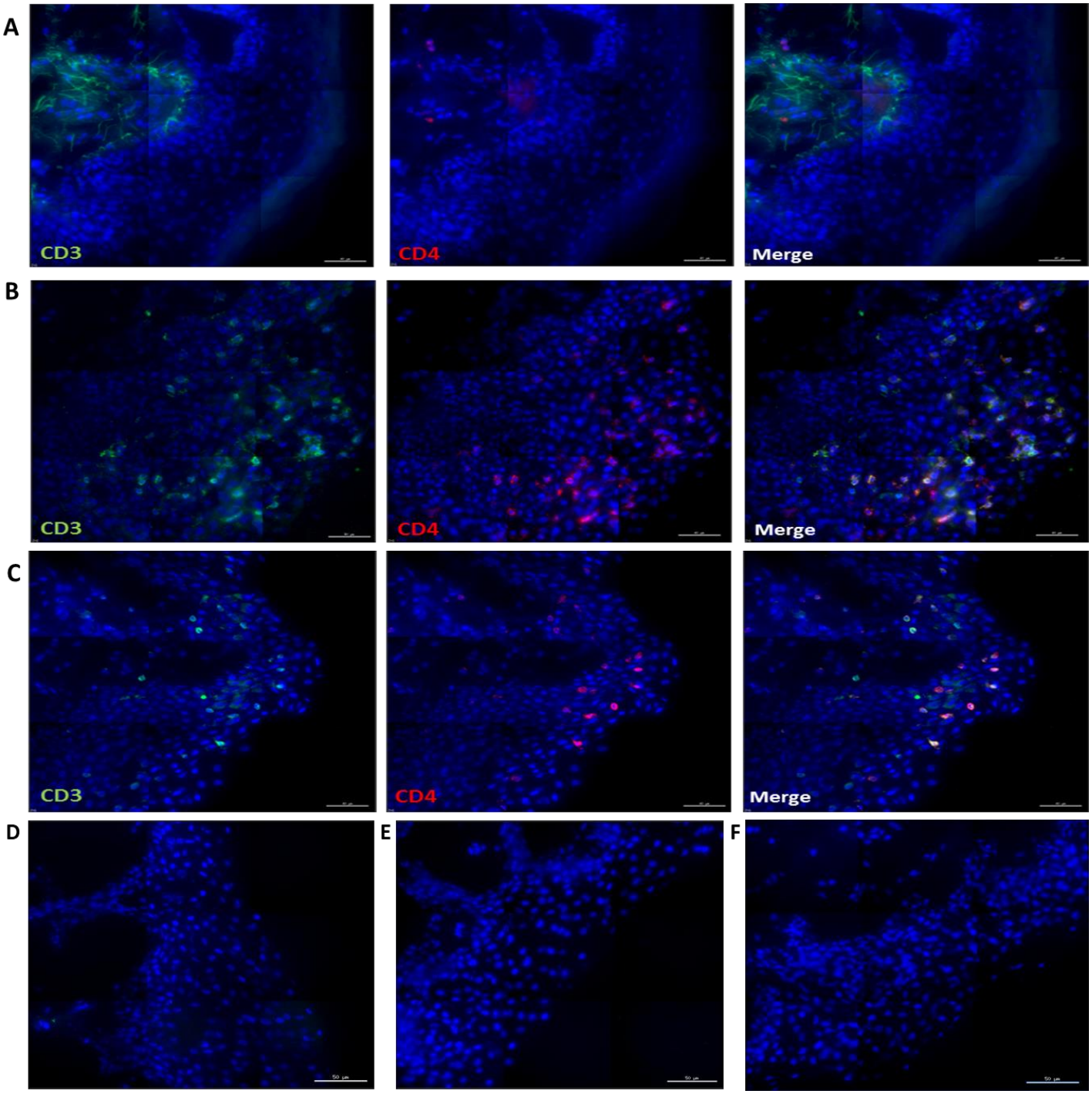

Figure 3.4 Immunofluorescent images of the inner foreskin tissue in three conditions showing CD3, CD4 and the merged staining. A) Unstimulated tissue with CD3 (left), CD4 (middle) and merged images (right). B) TNFα exposed tissues with CD3 (left), CD4 (middle) and merged images (right). C) CCL27 exposed tissues with CD3 (left), CD4 (middle) and merged images (right). D) Isotype control for Rabbit IgG1 (CD3). E) Isotype control for Mouse IgG1 (CD4). F) HOECHST only control.

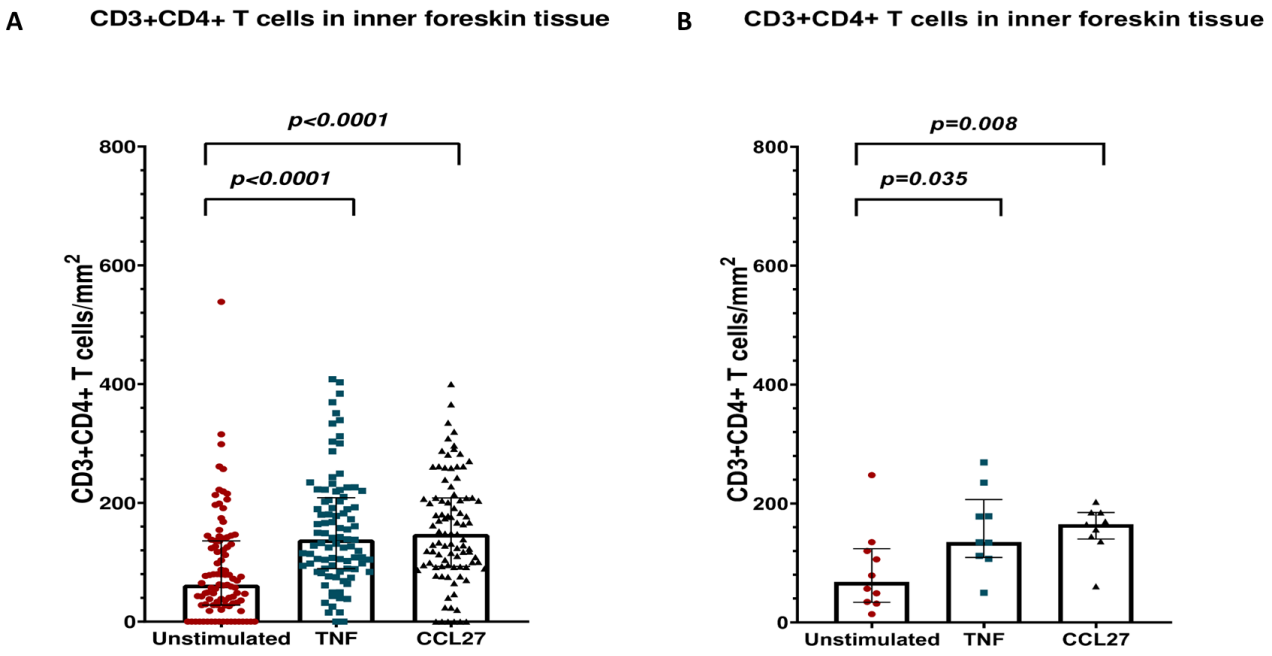

Figure 3.5: A) CD3+CD4+ T cell counts in all images (~10 images per donor) across unstimulated (n=97), TNFα exposed (n=92) and CCL27 exposed inner foreskin tissue (n=93). B) CD3+CD4+ T cell counts using the mean number of cells across unstimulated (n=10), TNFα exposed (n=9), and CCL27 exposed inner foreskin tissue (n=9).

CD3+CD4+ T cell population in the epithelium of the outer foreskin tissue after TNFα and CCL27 exposure

We compared outer foreskin tissue explants from 4 donors across the three conditions tested (unstimulated, TNFα 100ng/ml and CCL27 400ng/ml) to see the impact of CCL27 on the outer foreskin tissue. We hypothesized that exogenous CCL27 will recruit CD3+CD4+ T cells in the epithelium of the outer foreskin despite the low expression of CCL27 in the outer foreskin tissue compared to the inner foreskin tissue. Exogenous CCL27 exposure, however, did not have a significant impact on CD3+CD4+ T cell density in the outer foreskin tissue. Figure 3.6 (A, B and C) shows representative images of the double positive CD3+CD4+ T cells in the epithelium of the outer foreskin tissue explants in unstimulated, TNFα exposed (100 ng/ml) and CCL27 exposed (400 ng/ml) respectively. Figure 3.6 (D, E and F) shows isotype controls for CD3, CD4 and HOECHST only staining, respectively. Figure 3.7 depicts that after exposing 4 outer foreskin tissue explants to exogenous TNFα 100 ng/ml and CCL27 400 ng/ml, no significant increase in the median density of CD3+CD4+ T cells in the epithelium of the tissue was observed contrary to inner foreskin tissue. Figure 3.7a shows the median density of CD3+CD4+ T cells in the outer foreskin tissue explants after exposure to TNFα

(33.18 cells/mm^2, IQR: 0-190.10 cells/mm^2) compared to unstimulated tissue (34.72 cells/mm^2, IQR:0-79.31 cells/mm^2; *P*=0.330) and CCL27 (27.66 cells/mm^2, IQR:0-73.04 cells/mm^2) to unstimulated tissue explants (34.72 cells/mm^2, IQR:0-79.31 cells/mm^2; *P*=0.735). Mann Whitney test was conducted.

We then plotted the means of the images of each of the 4 donors in the three conditions (Figure 3.7b), conducted Mann-Whitney test and compared the density of CD3+CD4+ T cells in the TNFα and CCL27 exposed tissue explants compared to the unstimulated tissue explants. Figure 3.7b shows the median density of CD3+CD4+ T cells in TNFα exposed tissues (65.12 cells/mm^2, IQR: 7.30-202.80 cells/mm^2) compared to unstimulated tissue explants (36.52 cells/mm^2, IQR: 18.29-96.65 cells/mm^2; *p>0.999*) and in the CCL27 exposed tissues (24 cells/mm^2, IQR: 11.35-149.40 cells/mm^2) compared to unstimulated tissue explants (36.52 cells/mm^2, IQR: 18.29-96.65 cells/mm^2; *p*=0.686).

Collectively, these results show that exogenous CCL27 and TNFα resulted in increased numbers of CD4+ T cells in the inner foreskin, but not the outer foreskin.

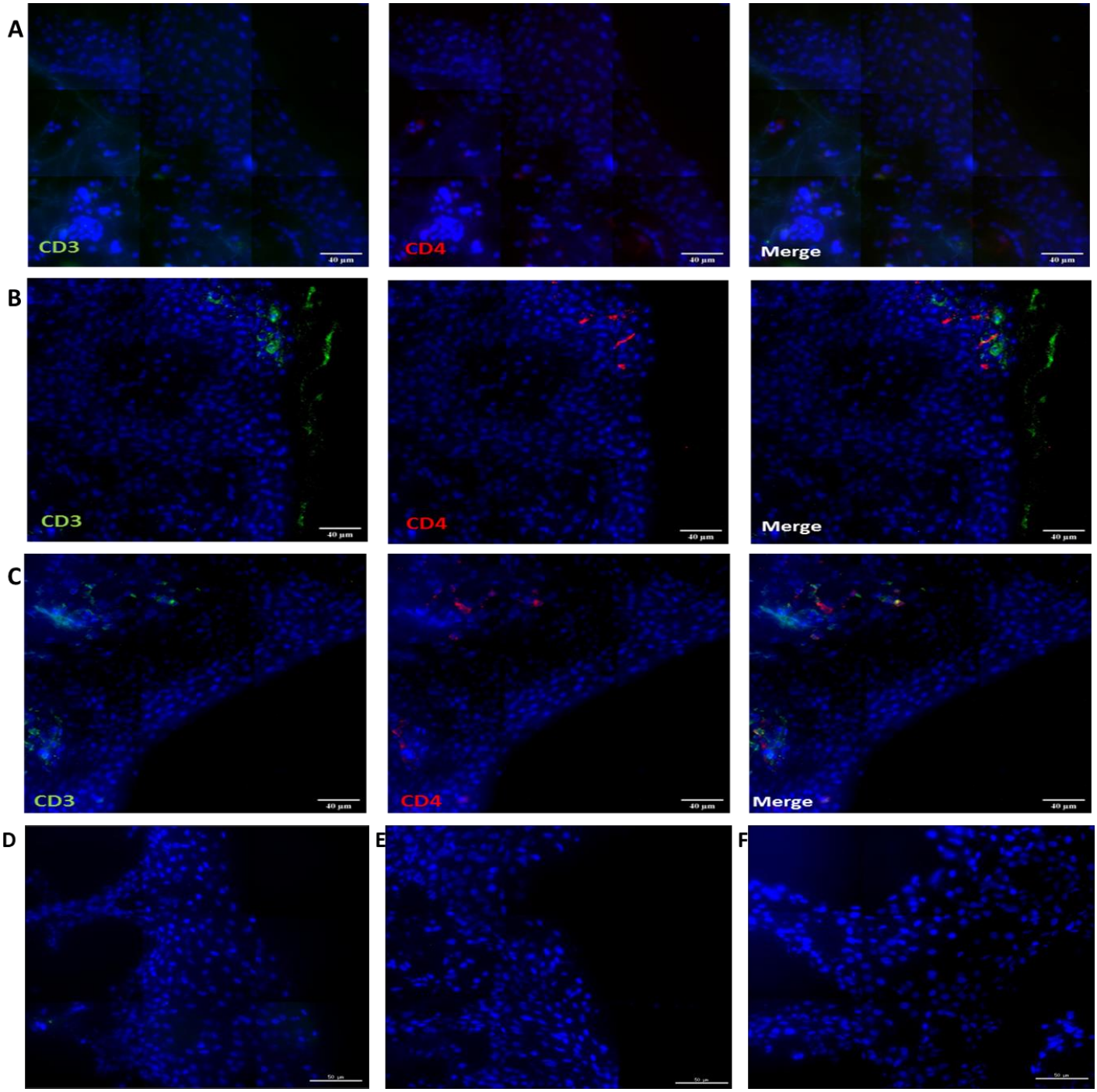

Figure 3.6: Immunofluorescent images of the outer foreskin tissue in three conditions showing CD3, CD4 and the merged staining. A) Unstimulated tissue with CD3 (left), CD4 (middle) and merged images (right). B) TNFα exposed tissues with CD3 (left), CD4 (middle) and merged images (right). C) CCL27 exposed tissues with CD3 (left), CD4 (middle) and merged images (right). D) Isotype control for Rabbit IgG1 (CD3). E) Isotype control for Mouse IgG1 (CD4). F) HOECHST only control.

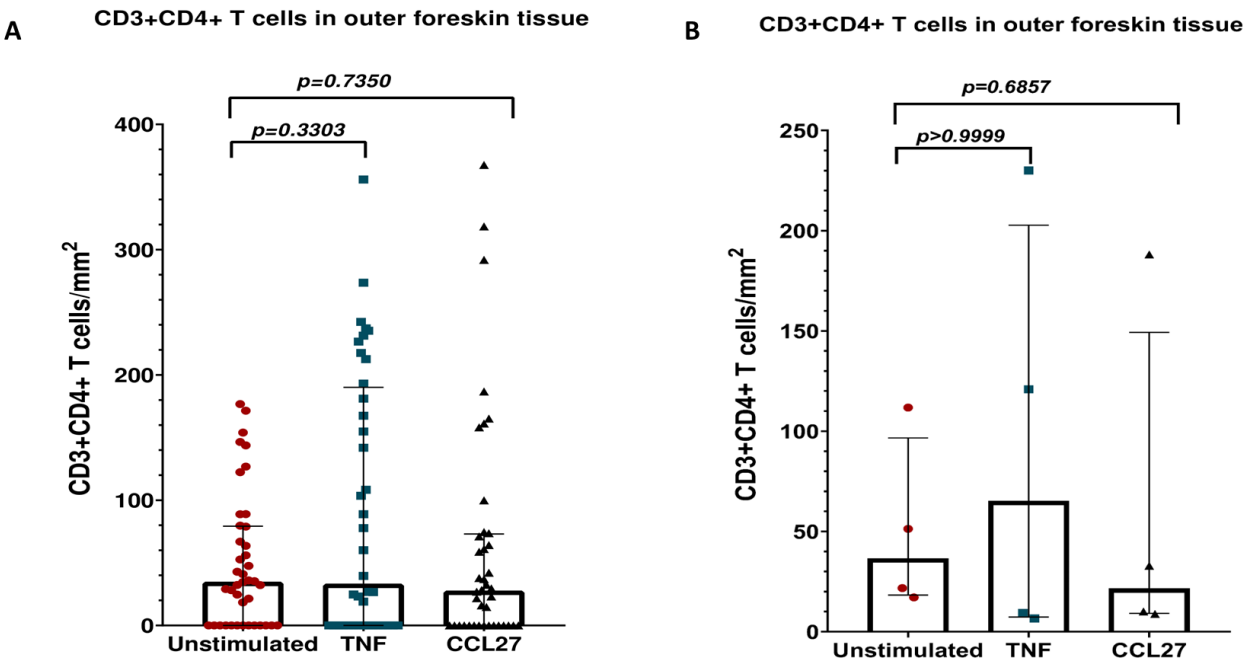

Figure 3.7: A) CD3+CD4+ T cell counts in all images (~10 images per donor) across unstimulated (n=41), TNFα exposed (n=40) and CCL27 exposed outer foreskin tissue (n=40). B) CD3+CD4+ T cell counts using the mean number of cells across unstimulated, TNFα exposed and CCL27 exposed outer foreskin tissue (n=4 for each condition).

3.3.5 Semi-automated counting method using ImageJ software

The analysis of the numbers of dually positive cells (CD3+CD4+ cells) in the inner and outer foreskin tissue images was initially conducted using a manual counting method by highlighting the dually positive cells and then analysis using an interactive program designed using IDL (Interactive Data Language). IDL calculated the number of cells which were manually counted and the surface area of the epithelium of each tissue explant. Figure 3.8 illustrates how the cells were manually highlighted and then recorded. To validate the counting method, we used a semi-automated counting method to detect the double positive cells in each channel (FITC and CY5 channels). ImageJ is a Java-based image processing program developed at the National Institutes of Health (NIH) (210). We used ImageJ and PIPSQUEAK AI, a macro added to ImageJ, that enables semi-automated counting of double positive cells to automatically detect the single labeled cells in both FITC and CY5 channels and then merge them to determine cells that co-expressed CD3 and CD4 and count the dually labeled cells (Figure 3.9). Counting using PIPSQUEAK AI was manually verified to

remove the possibility of false positives. Both counting methods were conducted blinded through assigning the conditions different codes by a third party; unblinding only occurred after all counting was done for analysis purposes. We compared both methods of counting to view correlation and differences. We counted 16 inner foreskin tissue samples: 6 unstimulated samples, 5 TNFα exposed samples and 5 CCL27 exposed samples (~10 images per sample) and 6 outer foreskin tissue samples: (2 unstimulated samples, 2 TNFα exposed samples and 2 CCL27 exposed samples).

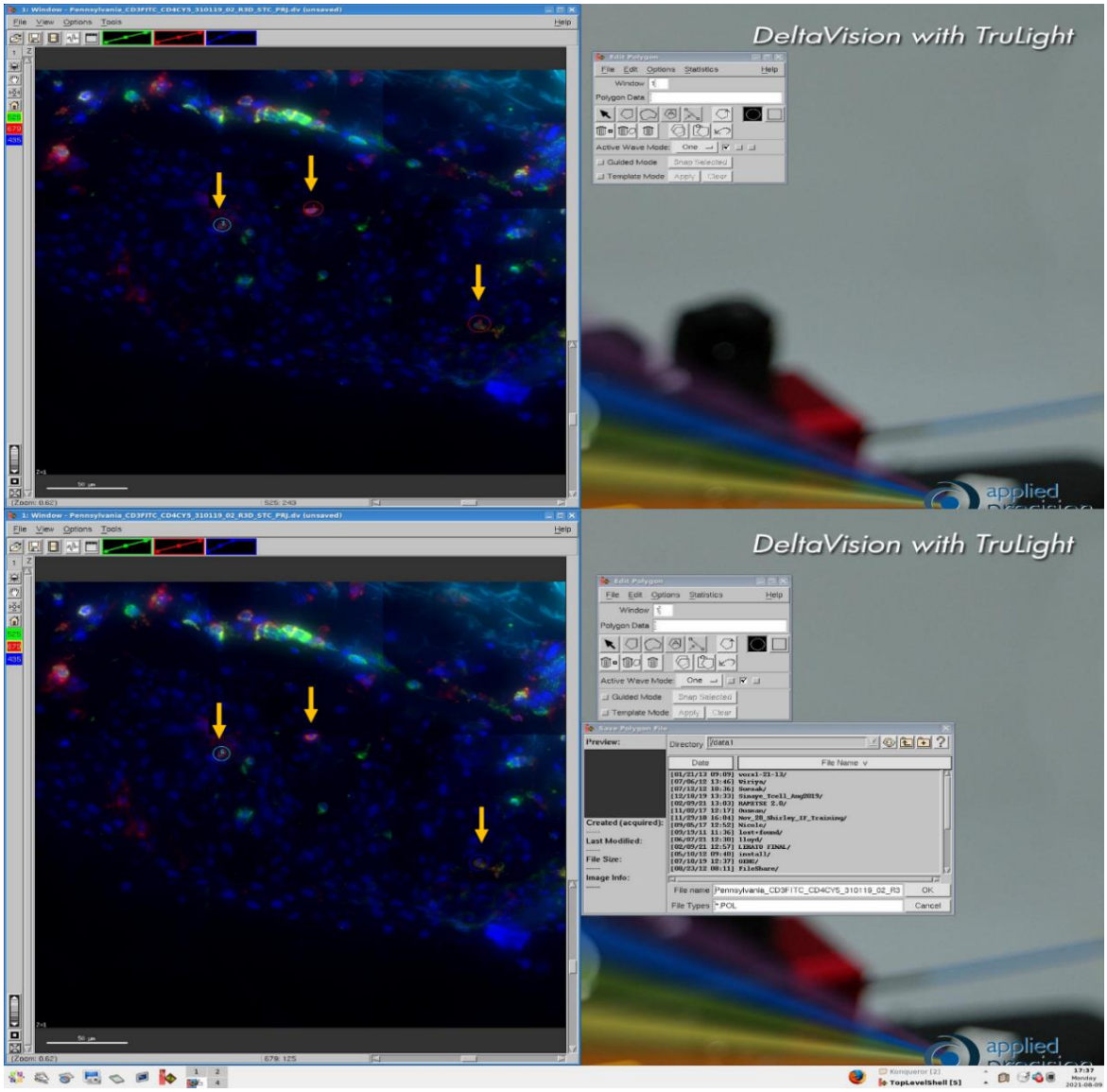

Figure 3.8: Illustration of manual counting of double positive CD3+CD4+ cells on the Softworx software.

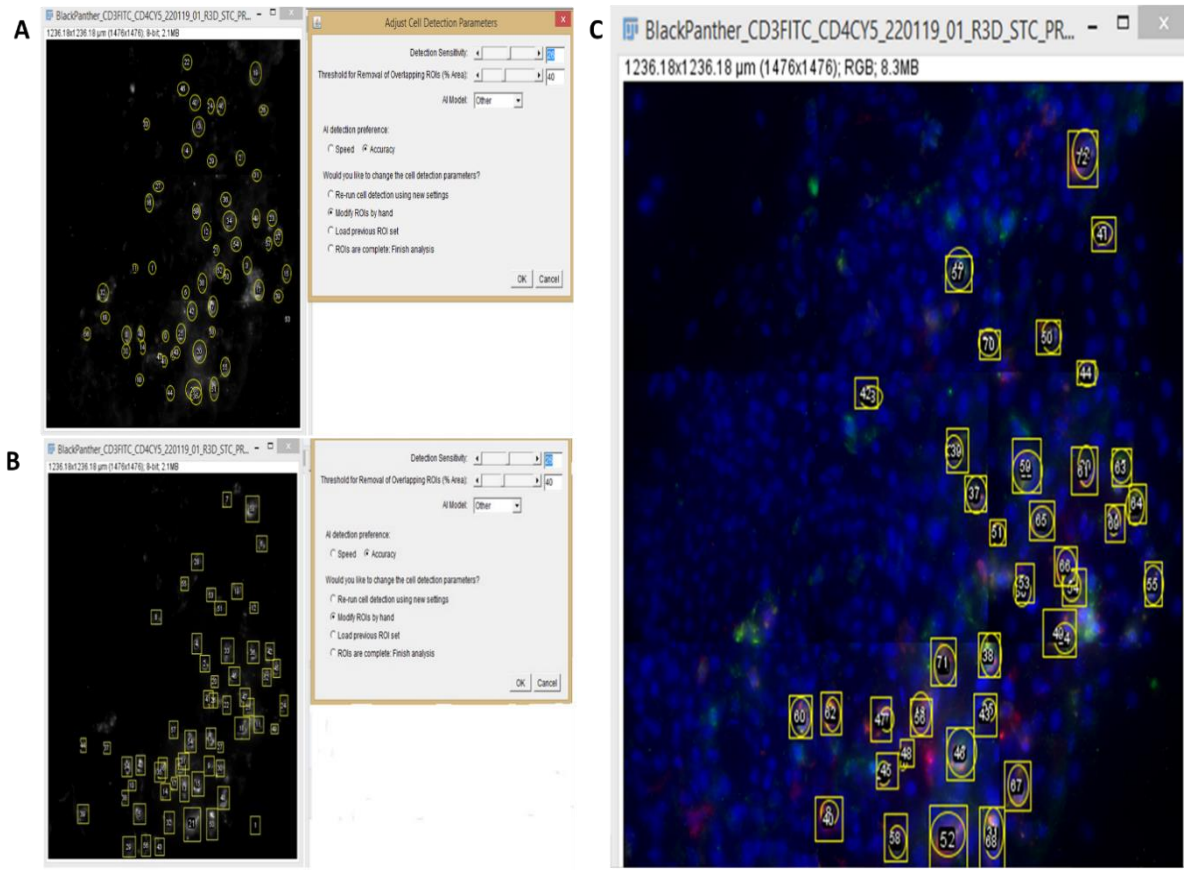

Figure 3.9: Illustration of the semi-automated counting using PIPSQUEAK/ImageJ. A) software detecting and counting CD3+ cells. B) software detecting and counting CD4+ cells. C) software merging the two counts to detect colocalization.

3.3.5.1 Frequency distribution of the manual and semi-automated counting in the inner and outer foreskin samples

We generated frequency plots to compare the distribution of CD3+CD4+ T cell numbers determined using the manual counting method versus the semi-automated counting method. Figure 3.10 shows the frequency plots in the inner foreskin tissue for both the manual and semi-automated counting methods. In Figure 3.10a, samples from the inner and outer foreskin tissues were not normally distributed across the two counting methods. Log_{10} transformed cell counts were plotted from the inner and outer foreskin samples to compare manual and semi-automated counts on the same scale and reduce skewness in the data (Figure 3.10b). After plotting log_{10} transformed data, the frequency distribution in this tissue assumed a more Gaussian distribution. It was also apparent that the manual counting method was possibly enumerating more cells than the semi-automated method.

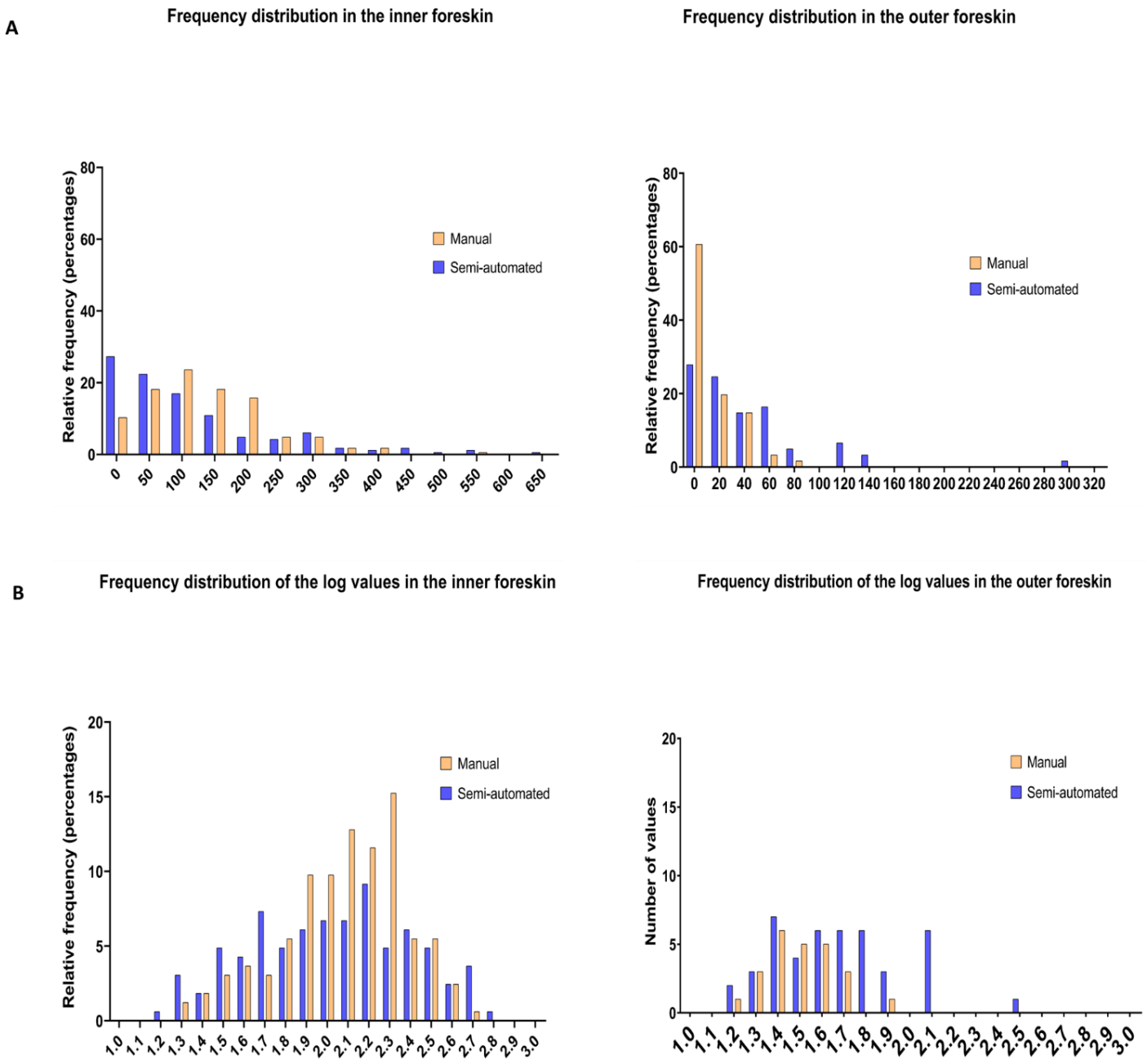

Figure 3.10: Frequency distribution in the inner foreskin between manual and semi-automated counting methods. A) Frequency distribution of counts of CD3+CD4+ cells in the inner (left) and outer (right) foreskin tissue explants across manual and semi-automated methods of counting. B) Frequency distribution of $\log_{10}$ counts of CD3+CD4+ cells in the inner (left) and outer (right) foreskin tissue explants across manual and semi-automated methods of counting.

3.3.5.2 Comparison between manual and semi-automated counting methods

To further compare the two methods of counting and access the significance of their discrepancies, a parametric paired T test of the log-transformed data determined from the manual and semi-automated counting methods was used to evaluate significant difference between the two counting methods.

Figure 3.11 shows the paired T test conducted on the two methods of counting in each of the three conditions (unstimulated, TNFα and CCL27) along with the total collated conditions in the inner foreskin tissue. There was a significant difference in the counts between the manual and semi-automated counting methods in all conditions (*P* values are 0.0009 in both unstimulated tissues and TNFα exposed tissues and <0.0001 in both CCL27 exposed tissues and in the collated conditions).

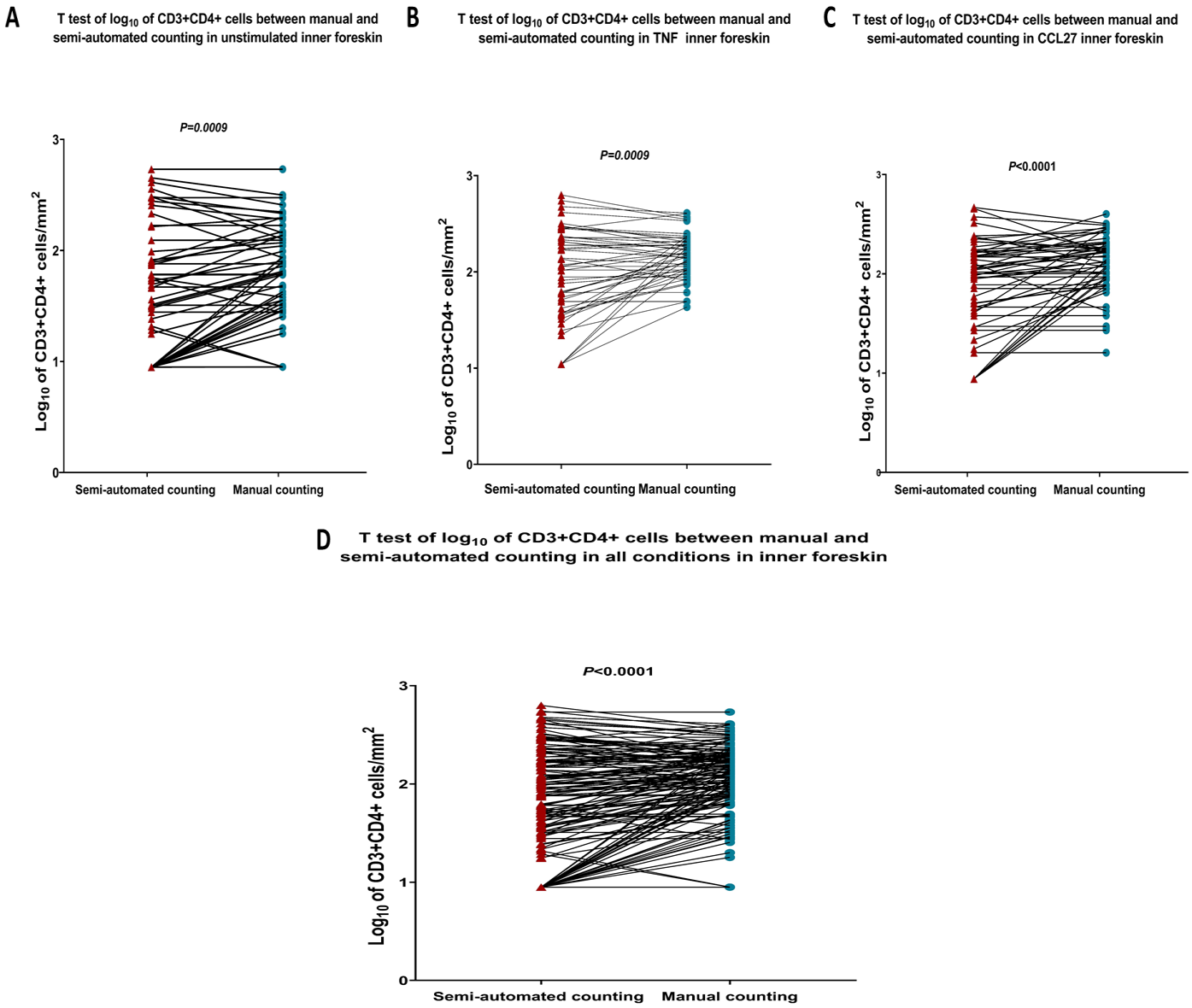

Figure 3.11: Paired T test of log_{10} values in manual and semi-automated counting in three conditions of the inner foreskin tissue. A) Paired T test of log_{10} values in unstimulated inner foreskin between manual and semi-automated counting (n=63). B) Paired T test of log_{10} values in TNFα exposed inner foreskin between manual and semi-automated counting (n=50). C) Paired T test of log_{10} values in CCL27 exposed inner foreskin between manual and semi-automated counting (n=52). D) Paired T test of log_{10} values in total conditions in the inner foreskin between manual and semi-automated counting (n=165).

Figure 3.12 shows significant differences in all three conditions along with the collated conditions between the semi-automated method and manual method of counting (*P* values are 0.001 and 0.0002 in unstimulated and TNFα exposed tissues and <0.0001 in both CCL27

tissues and collated conditions) which indicated that the two methods are estimating different numbers of cells across all conditions in the outer foreskin tissue.

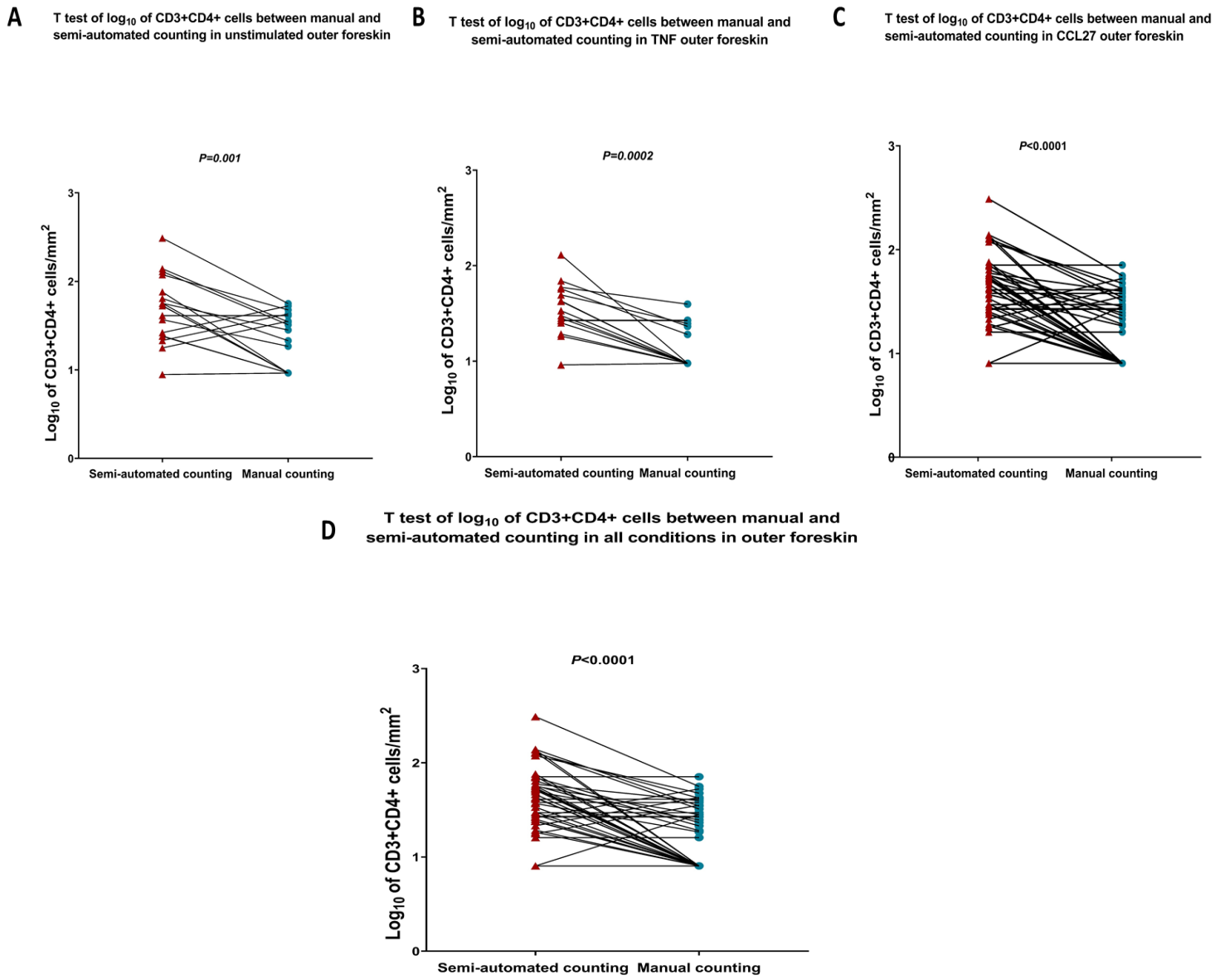

Figure 3.12: Paired T test of log_{10} values in manual and semi-automated counting in three conditions of the outer foreskin tissue. A) Paired T test of log_{10} values in unstimulated outer foreskin between manual and semi-automated counting (n=21). B) Paired T test of log_{10} values in TNFα exposed outer foreskin between manual and semi-automated counting (n=20). C) Paired T test of log_{10} values in CCL27 exposed outer foreskin between manual and semi-automated counting (n=20). D) Paired T test of log_{10} values in the outer foreskin between manual and semi-automated counting (n=61).

3.3.5.3 Correlation plots

To understand the relationship between the counting methods, correlation plots between the $\log_{10}$ transformed data points (~10 images per donor per condition) in the manual (using Softworx software) and the semi-automated method (PIPSQUEAK/ImageJ) were made.

Correlation plots in the inner foreskin tissue

Figure 3.13 shows the Spearman correlation of the counting between unstimulated, addition of exogenous TNFα and exogenous CCL27 in the inner foreskin tissue. In the unstimulated inner foreskin tissue, we observed a high degree of positive correlation between the manual counting and ImageJ semi-automated counting with a coefficient of relativity (R) of 0.84 and the coefficient of determination (R^2) being 0.70; *p<0.0001* (Figure 3.13a). In the TNFα exposed inner foreskin, both coefficient of relativity (R) and coefficient of determination (R^2) was lower (0.64 and 0.41 respectively) showing moderate degree of positive correlation between the manual and semi-automated counting methods; *p<0.0001* (Figure 3.13b). The same occurs in the CCL27 exposed inner foreskin with coefficient of relativity (R) and coefficient of determination (R^2) becoming 0.64 and 0.41 respectively; *p<0.0001* (Figure 3.13c). conducting correlation analysis on the total conditions in the inner foreskin showed a large positive coefficient of relativity (R) and coefficient of determination (0.78 and 0.61 respectively; *p<0.0001*). Coefficient of relativity is seen to be lower in the TNFα and CCL27 samples where higher numbers of cells were recorded. These correlation plots show a trend across the 4 conditions, where the manual method of counting is enumerating higher number of double positive cells compared with the semi-automated method when the numbers of tissue-resident cells were low in density (log values between 1-2) and the semi-automated counting method enumerating higher numbers of double positive cells compared to manual when the cells are higher in density (log values between 2-3).

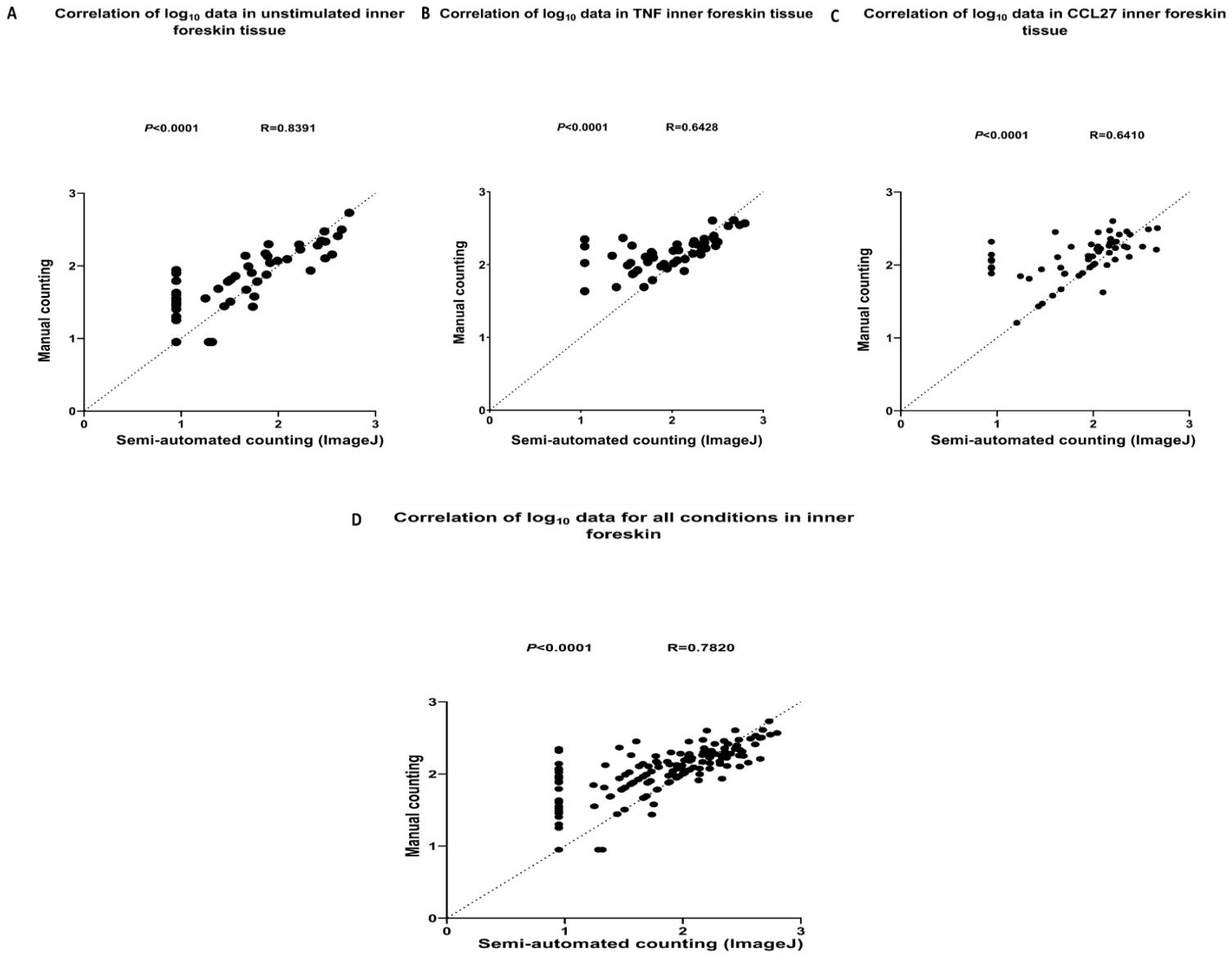

Figure 3.13: Correlation plots of log_{10} values between manual and semi-automated counting in three conditions of the inner foreskin tissue. A) Correlation of log_{10} values in unstimulated inner foreskin between manual and semi-automated counting (n=63). B) Correlation of log_{10} values in TNFα exposed inner foreskin between manual and semi-automated counting (n=50). C) Correlation of log_{10} values in CCL27 exposed inner foreskin between manual and semi-automated counting (n=52). D) Correlation of log_{10} values in all conditions in the inner foreskin between manual and semi-automated counting (n=165).

Correlation plots in outer foreskin tissue

We also plotted CD3+CD4+ T cell density (log_{10} cells/mm2) in the outer foreskin tissue between manual and semi-automated methods of counting. Here, the two methods showed weak correlation across all the conditions as indicated by R<0.5. These observations could be

due to lower sample size and thus not sufficiently powered to detect significant correlation. Figure 3.14 shows the weak correlation between the two counting methods in the outer foreskin tissue. In the unstimulated outer foreskin tissue (Figure 3.14a), the coefficient of relativity (R) between the manual counting and ImageJ semi-automated counting is 0.4109 while the coefficient of determination (R^2) is 0.17; p=0.064. In the TNFα exposed outer foreskin, coefficient of relativity (R) and coefficient of determination (R^2) are 0.46 and 0.21 respectively; p=0.064 (Figure 3.14b). In the CCL27 exposed outer foreskin, the coefficient of relativity (R) and coefficient of determination (R^2) were lower with values of 0.25 and 0.07 respectively; p=0.060 (Figure 3.14c). In the collated conditions in the outer foreskin, the coefficient of relativity (R) and coefficient of determination were 0.40 and 0.16 respectively; p=0.064 (Figure 3.14d). The weak correlation across the outer foreskin samples suggests different cell counts recorded using the two methods. Across all Figures, semi-automated counting estimated higher counts compared to the manual counting method. This could be due to observer's bias in the outer foreskin tissues which had lower cell counts (despite blinded experiments). Due to the number of donors compared being low, no clear conclusion can be made about the cell counts in the outer foreskin across the two different counting methods.

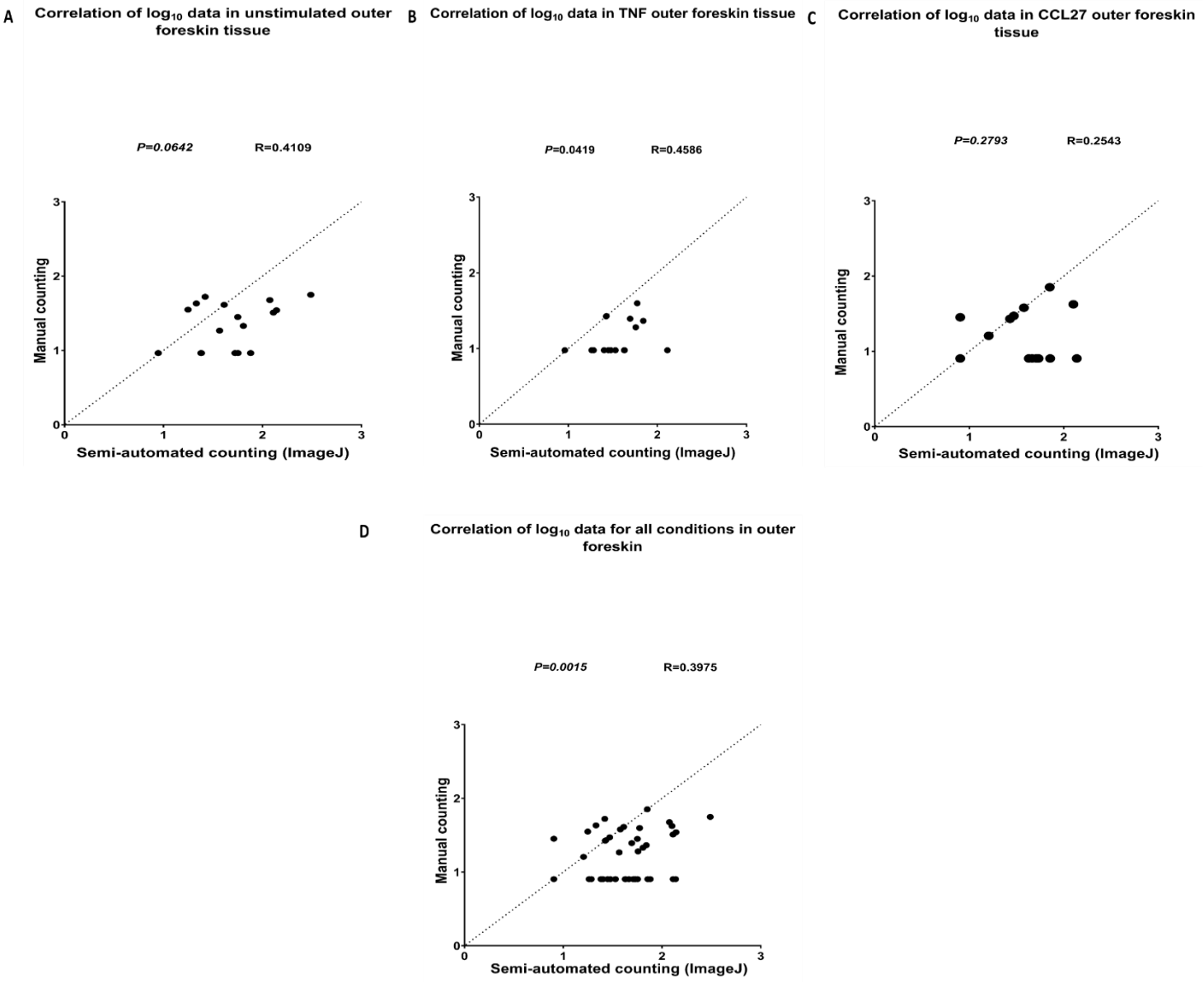

Figure 3.14: Correlation plots of log_{10} values in manual and semi-automated counting in three conditions of the outer foreskin tissue. A) Correlation of log_{10} values in unstimulated outer foreskin between manual and semi-automated counting (n=21). B) Correlation of log_{10} values in TNFα exposed outer foreskin between manual and semi-automated counting (n=20). C) Correlation of log_{10} values in CCL27 exposed outer foreskin between manual and semi-automated counting (n=20). D) Correlation of log_{10} values in all conditions in the outer foreskin between manual and semi-automated counting (n=61).

3.3.5.4 Difference plots (Bland-Altman)

Although correlation plots assessed the relationship between the counting methods, it did not provide a measure of difference between the two counting methods. Difference plots were first explained by Bland and Altman in 1983 (211). They created a method to measure

agreement between two quantitative variables by constructing limits of agreement using both the mean and standard deviation (*s*) of the differences between the two variables. The difference plots depict an XY scatter plot where Y is the difference between the variables measured for the two methods (A-B) and X is the average of these two measurements ((A+B)/2). Using the Bland-Altman plots, 95% of the data points should be within ±2 standard deviations of the mean difference (212). Calculation of these differences also provides more insight into how the two counting methods show signs of bias (212). The term bias in the plots refer to the average of the differences between two methods. In two completely congruent methods or those having minimum differences, the bias should be zero or a small value. When the bias value is negative, it means the second method (B) measures higher units than the first method (A) while a bias that has a positive value means that method (A) measures higher units than method (B) (212). The units of bias between two methods represent the average of the differences between each of the paired samples to show which method is measuring higher units relative to the other method. The maximum acceptable bias is dependent on each experimental outcome and prior defining of acceptable thresholds (212).

Difference plots between manual and semi-automated counting method in the inner foreskin

Figure 3.15 shows the difference plots for all conditions in the inner foreskin. Here, it is noticed that almost all the points in the four graphs are within the limits of agreement which highlights that the two methods of counting CD3+CD4+ T cells (manual and semi-automated method) are correlated. We see that the bias (average of the difference) in the unstimulated inner foreskin is -1.539 (Figure 3.15a), which indicates agreement between the two methods since the average of the differences has a low value. When investigating the other two conditions (Figure 3.15b and 3.15c), the average of differences (bias) increased showing that the manual method of counting is measuring 13.56 and 38.72 units more than the semi-automated method in TNFα and CCL27 exposed tissues respectively. It can be observed from Figure 3.15 across all graphs (A,B, C and D) that the results are leaning towards being estimated higher by the manual method of counting when the number of cells is lower (<100 CD3+CD4+ T cells/mm2) while they are leaning towards being estimated higher by the semi-

automated method of counting compared to the manual method when the number of cells in the tissue is higher (> 200 CD3+CD4+ T cells/mm2).

Figure 3.15d shows the difference plot for the total conditions in the inner foreskin, the manual counting is measuring 16.90 units more than the semi-automated counting method and we notice the same trend of the manual counting estimating higher number of cells when the cell count in the tissue is low or medium (<100 CD3+CD4+ T cells/mm2).

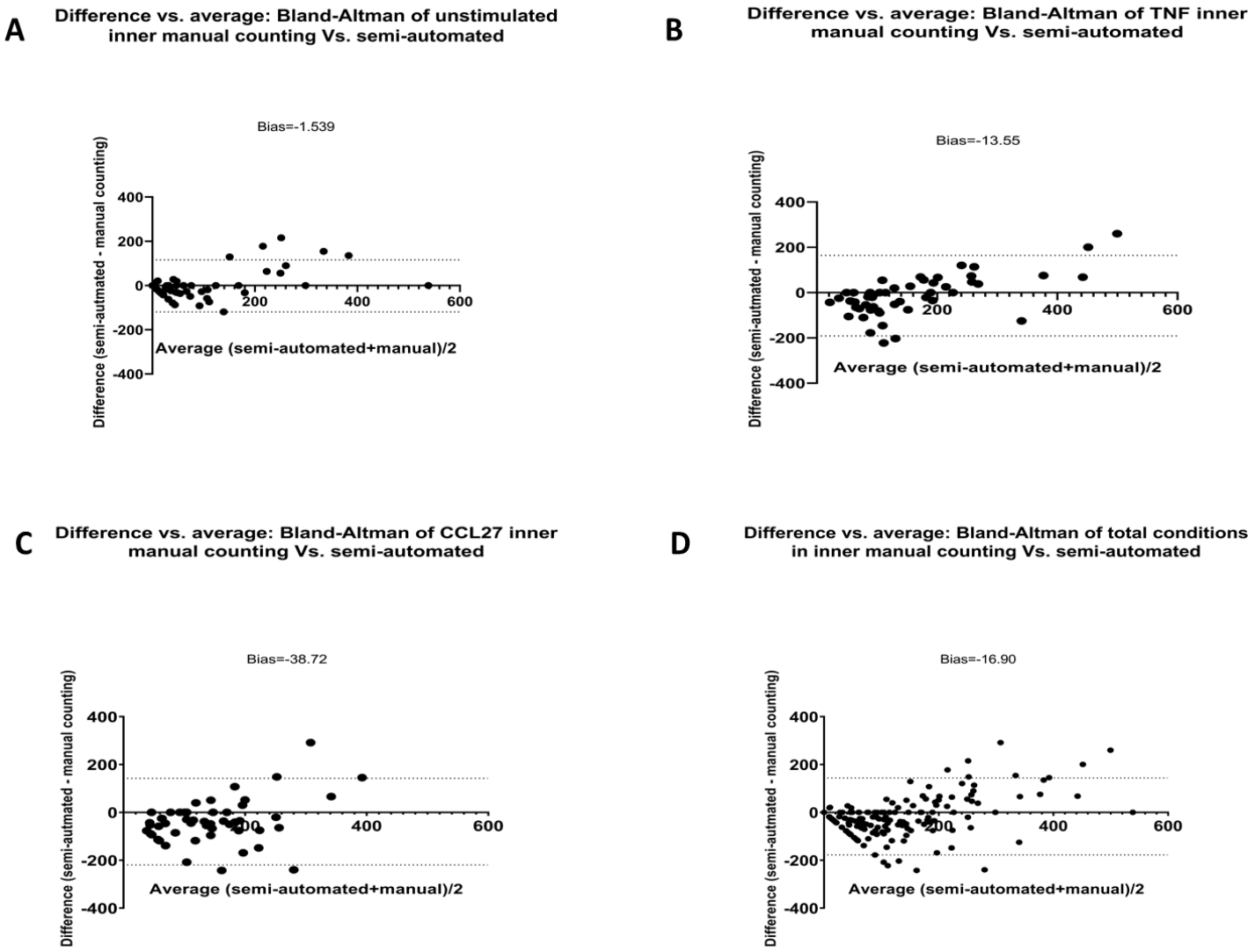

Figure 3.15: Bland-Altman plots between manual and semi-automated counting in three conditions of the inner foreskin tissue. A) Bland-Altman plots in unstimulated inner foreskin between manual and semi-automated counting (n=63). B) Bland-Altman plots in TNFα exposed inner foreskin between manual and semi-automated counting (n=50). C) Bland-Altman plots in CCL27 exposed inner foreskin between manual and semi-automated counting (n=52). D) Bland-Altman plots in total conditions in the inner foreskin between manual and semi-automated counting (n=165).

Difference plots between manual and semi-automated counting method in the outer foreskin

Figure 3.16 highlights the difference plots in the outer foreskin tissue. In the difference plots for the outer foreskin, it was noticed that the results in the four graphs are also within the limits of agreement which highlights that the two methods of counting CD3+CD4+ T cells (manual method and semi-automated method) are indeed correlated. We see that the bias in the four graphs in the outer foreskin takes a positive sign indicating higher counts in the semi-automated counting method compared to the manual count unlike the inner foreskin tissue. Bias in the three conditions is 39.75, 24.92 and 22.96 respectively while in the total conditions in the outer foreskin bias is 29.38.

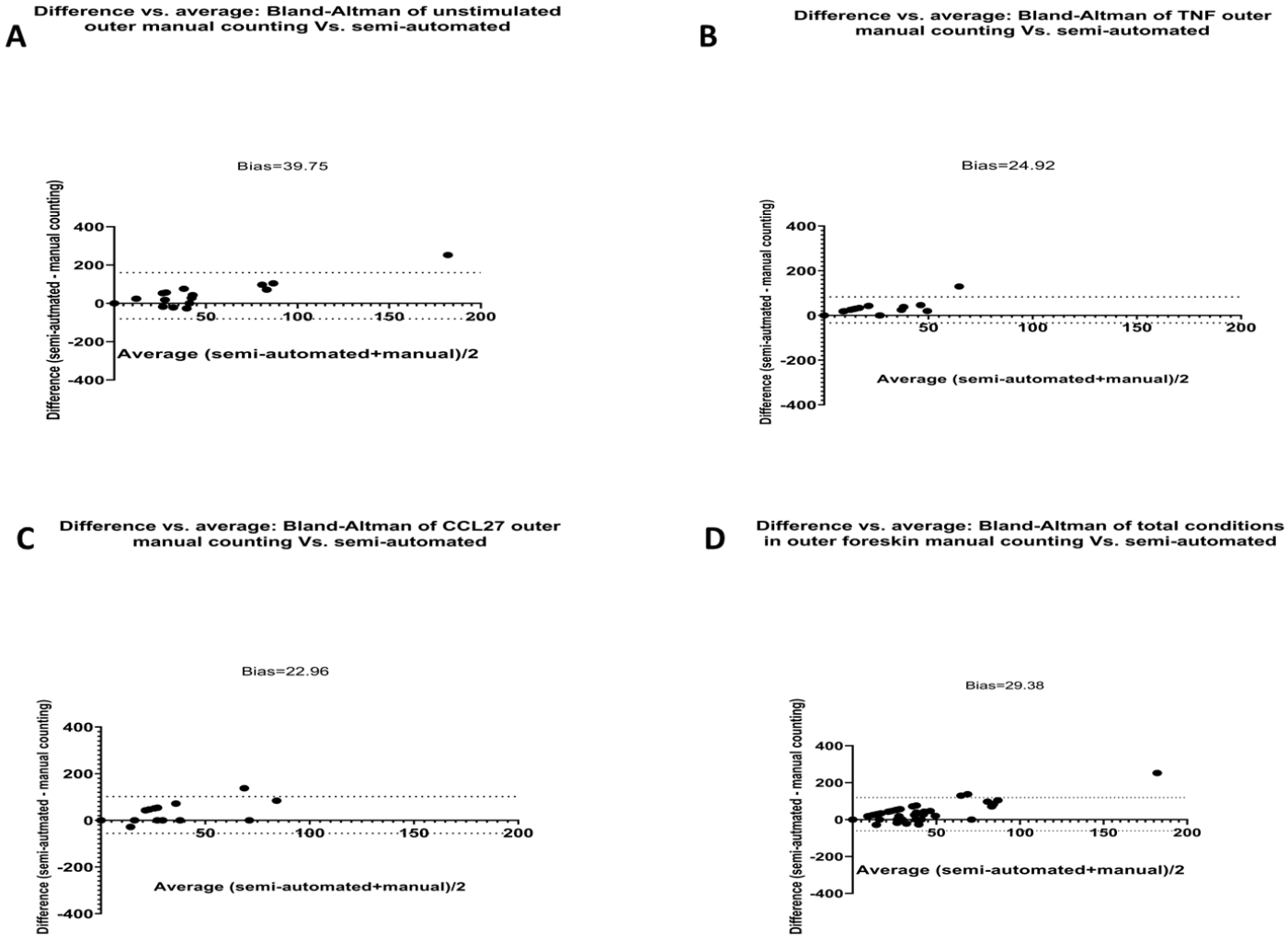

Figure 3.16: Bland-Altman plots between manual and semi-automated counting in three conditions of the outer foreskin tissue. A) Bland-Altman plots in unstimulated outer foreskin between manual and semi-automated counting (n=21). B) Bland-Altman plots in TNFα exposed outer foreskin between manual and semi-automated counting (n=20). C) Bland-Altman plots in CCL27 exposed outer foreskin between manual and semi-automated counting (n=20). D) Bland-Altman plots in total conditions in the outer foreskin between manual and semi-automated counting (n=61).

3.3.5.5 Statistical analysis of inner foreskin samples counted by manual and semi-automated methods

We chose 4 paired inner foreskin samples and compared the medians across unstimulated, TNFα exposed and CCL27 exposed samples and conducted Mann Whitney test. Our aim was to see if both methods would give approximate statistical results. Figure 3.17a shows the data plotted from the 4 donors (~10 images per donor). We observed that p values decrease, and significance increases in the manual counting compared to the semi-automated counting in both the comparisons of unstimulated and TNFα (*P*=0.001 in the manual counting compared to *p=0.062)* and in unstimulated compared to CCL27 exposed (*p*=0.0004 and *p*=0.139 in manual counting and automated, respectively). The median densities of CD3+CD4+ T cells in the manually counted samples compared to semi-automated counted samples were as follows: 74 cells/mm^2, IQR: 32.80-149.80 in manual vs 48 cells/mm^2, IQR: 0-179.90 in unstimulated tissues, 130.2 cells/mm^2, IQR: 95.5-217.7 in manual vs 85 cells/mm^2, IQR: 37-185.70 in semi-automated counting in TNFα treated tissue explants and 138.70 cells/mm^2, IQR:96.80-201.59 in manual vs 98.50 cells/mm^2, IQR:41.50-171.50 in semi-automated counting in CCL27 treated tissue explants. This indicates that the two counting methods gave different results for the same samples analyzed.

We next plotted the mean number of CD3+CD4+ T cells in each donor across the three conditions and conducted Mann-Whitney test on the samples. Figure 3.17b shows that *p* values increase in the semi-automated counting compared to the manual counting in the comparison of unstimulated and TNFα exposed (*P*=0.200 and *P*=0.343 in manual counting and automated, respectively*)* and the comparison between unstimulated and CCL27 exposed (*p*=0.343 and *P*=0.486 in manual counting and automated, respectively). The median densities of CD3+CD4+ T cells in the manually counted samples compared to semi-automated counted samples were as follows: 81.30 cells/mm^2, IQR: 37.80-212.30 in manual vs 48.80 cells/mm^2, IQR: 27-270 in unstimulated tissues, 134.50 cells/mm^2, IQR: 117.30-235.40 in manual vs 102.70 cells/mm^2, IQR: 46-283.80 in semi-automated counting in TNFα treated tissue explants and 157 cells/mm^2, IQR:138.30-181 in manual vs 100 cells/mm^2, IQR:62.70-227 in semi-automated counting in CCL27 treated tissue explants. We noticed the trend that across all results of the manual vs. semi-automated, manual counting had higher

count of cells compared to the semi-automated. This can be attributed to bias that occurred in the manual counting.

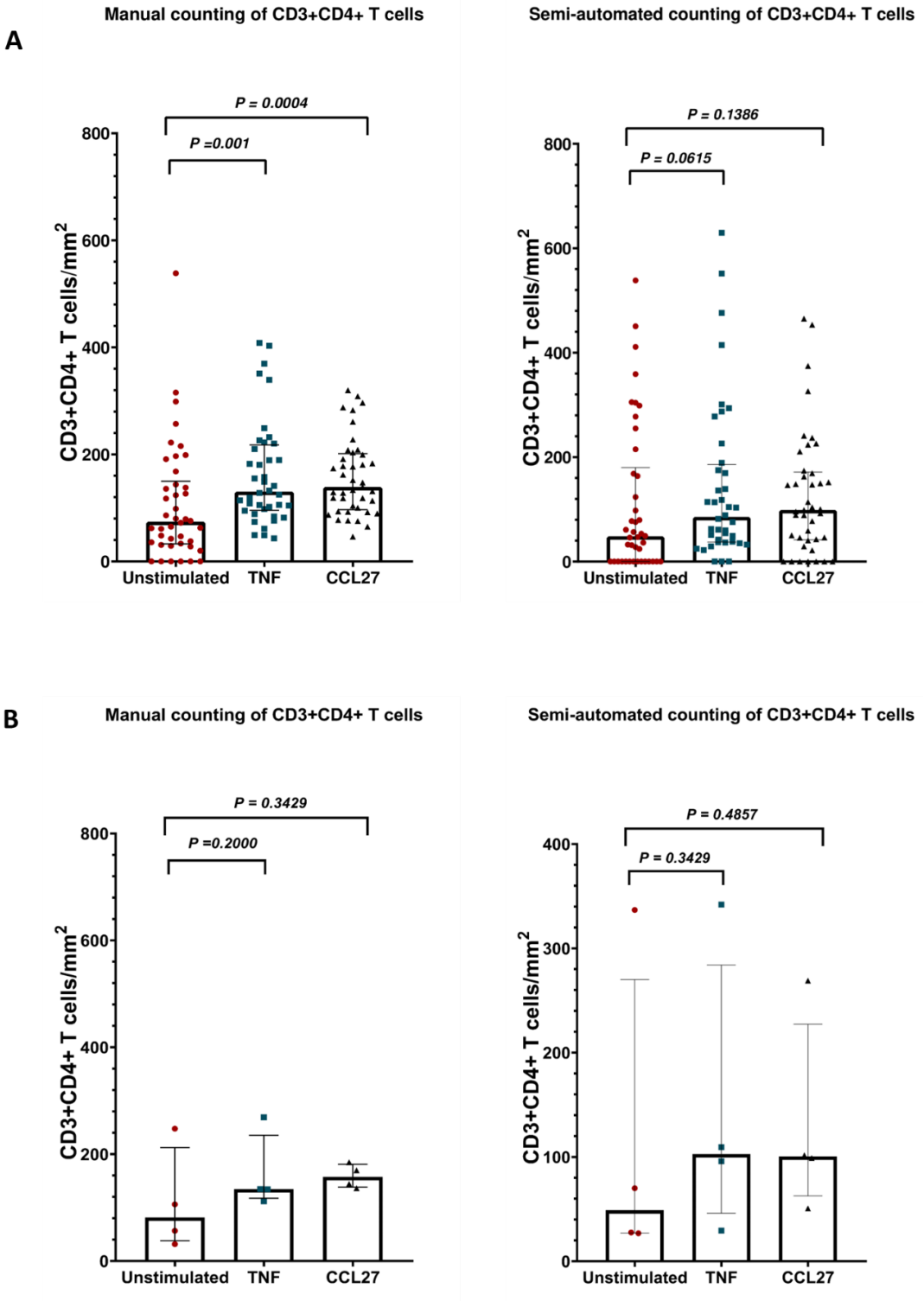

Figure 3.17: Mann-Whitney test in the three conditions in the inner foreskin when cells are counted manually and semi-automatically. A) Mann-Whitney test in the manual counting method compared to the semi-automated method in the unstimulated (n=42), TNFα exposed (n=40) and CCL27 exposed tissues(n=41). B) Mann-Whitney test on the mean number of cells in the manual counting method compared to the semi-automated method (n=4 for each condition).

3.3.5.6 Single positive cell densities in the semi-automated counted samples

CD3+ cells are known to be either T helper cells when expressing CD4 marker as well, T cytotoxic cells when expressing CD8 marker or MAIT cells. CD8+ T cells are known to reside in the foreskin tissue and an influx of CD8+ T cells was observed in recently infected HIV+ men (95,213). CD4+CD3- cells residing in the foreskin tissue are potentially T cells, Langerhans cells or macrophages. Langerhans cells and macrophages have been shown to reside in the foreskin tissue and to have a role in HIV infection (126,194).

We investigated the numbers of CD3+CD4+ cells which are T helper cells in the foreskin tissue under the influence of chemokines. However, other cells subsets that express CD3+ or CD4+ in the absence of the other marker inhabit the foreskin tissue. CD3+CD4- cells are potentially T cytotoxic cells or MAIT cells while CD4+CD3- cells might be Langerhans cells or macrophages. These cells have different roles in HIV infection (95,126,194,213). Hence, we wanted to view the effect of TNFα and CCL27 on the densities of CD3+CD4- and CD4+CD3- cells. We compared the number of CD3+CD4- cells and CD4+CD3- cells in the inner foreskin tissue explants of 4 donors (extracted from the PIPSQUEAK analysis). We first plotted the data points from all FOVs from the 4 donors and conducted Mann Whitney test (~10 images per donor per condition). Figure 3.18a shows the density of CD3+CD4- and CD4+CD3- cells in the inner foreskin tissue across unstimulated, TNFα exposed and CCL27 exposed tissue explants. It shows the median density of CD3+CD4- cells to be 209 cells/mm^2, IQR:109.90-354.70 in TNFα treated tissues compared to unstimulated explants (89 cells/mm^2, IQR:35.30-294; p=0.135) and the median density of CD3+CD4- cells in CCL27 treated tissues to be 143.50 cells/mm^2, IQR: 86.90-203.80 compared to unstimulated explants (89 cells/mm^2, IQR:35.30-294; $p=0.$319). It also shows the median density of CD4+CD3- cells to be 135.20 cells/mm^2, IQR:73.58-227.10 in TNFα treated tissues compared to unstimulated explants (101.90 cells/mm^2, IQR:79.55-150.30; p=0.364) and the median density of CD4+CD3- cells in CCL27 treated tissues to be 178 cells/mm^2, IQR: 118.20-246.20 compared to unstimulated explants (135.20 cells/mm^2, IQR:73.58-227.10; p=0.002). We see a significant difference in the density of CD4+CD3- cells after exposure to CCL27 which suggests CCL27 might have an impact on LCs and macrophages in the inner foreskin tissue as well as T cells. However, the number of donors compared is low (4 donors per condition) which warrants caution in interpreting results.

We then plotted the data points showing the mean number of CD3+CD4- or CD4+CD3- from the 4 donors and conducted Mann-Whitney test. Figure 3.18b shows the density of CD3+CD4- and CD4+CD3- cells in the inner foreskin tissue across unstimulated, TNFα exposed and CCL27 exposed tissue explants. The median density of CD3+CD4- cells was 257.70 cells/mm^2, IQR:87.28-334.2 in TNFα treated tissues compared to unstimulated explants (133.70 cells/mm^2, IQR:45.16-405.50; p=0.686) and the median density of CD3+CD4- cells in CCL27 treated tissues to be 134 cells/mm^2, IQR: 101-303.3 compared to unstimulated explants (133.70 cells/mm^2, IQR:45.16-405.50; p=0.886). It also shows the median density of CD4+CD3- cells to be 172 cells/mm^2, IQR:76.89-210.70 in TNFα treated tissues compared to unstimulated explants (124.80 cells/mm^2, IQR:93.39-148.10; p=0.686) and the median density of CD4+ cells in CCL27 treated tissues to be 215.80 cells/mm^2, IQR:145.40-280.50 compared to unstimulated explants (172 cells/mm^2, IQR:76.89-210.70; p=0.200).

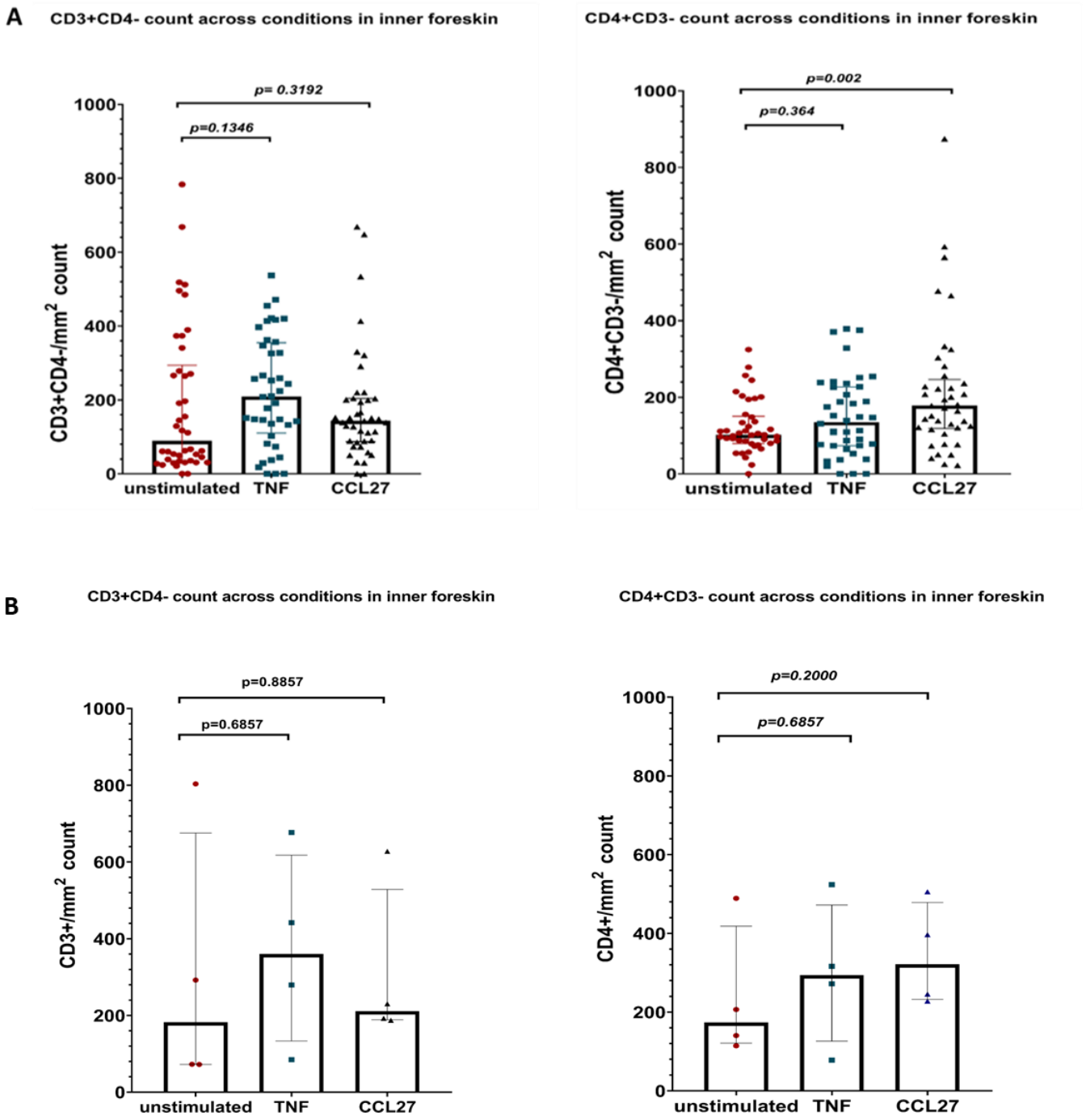

Figure 3.18: Single positives CD3+ and CD4+ counts in the inner foreskin under the influence of TNFα and CCL27. Figure A shows data points plotted from ~10 FOVs in 4 donors for each condition while Figure B shows data points from the mean of values of all FOVs per condition. A) CD3+CD4- and CD4+CD3- counts in 4 paired samples in unstimulated (n=42), TNF exposed (n=40) and CCL27 exposed tissues (n=41). B) CD3+CD4- and CD4+CD3- counts in 4 paired samples after taking the mean of all images for each donor per condition (n=4 for each condition).

3.4 Discussion

The foreskin tissue has been observed to have increased susceptibility to different STIs including HPV, MG, HSV-2 (50–52,59). It has also been observed that the inner foreskin tissue has an increased susceptibility to HIV infection (20,23,194,214). Furthermore, the foreskin tissue is a proinflammatory site due to being rich in CD4+ T cells, Langerhans cells and macrophages (95,111). CD4+ T cells were shown to be twofold higher in the inner foreskin compared to the outer foreskin and proinflammatory cytokine levels were also significantly higher in the inner foreskin tissue compared to the outer foreskin including IL-17, IL-8, RANTES and IL-1β (121). We aimed in this chapter to better understand how the proinflammatory environment of the foreskin tissue, through exploring CCL27 in the inner foreskin, might lead to recruitment of CD4+ T cells to the epithelium of the foreskin tissue.

Our findings showed a trend in higher density of CD4+ T cells in the inner foreskin tissue compared to the outer foreskin tissue. These results are consistent with findings observing CD4+ T cells to be significantly higher in the inner foreskin tissue compared to the outer foreskin (20,121). Then we observed the impact of exogenous exposure to CCL27 and TNFα on the recruitment of CD4+ T cells in the inner and outer foreskin. Both TNFα and CCL27 caused a significant increase in the density of CD4+ T cells in the inner foreskin tissue compared to unstimulated tissue explants (p=0.004 for TNFα exposed compared to unstimulated explants and p=0.027 for CCL27 exposed compared to unstimulated explants). Meanwhile, TNFα and CCL27 did not cause a significant change in the density of CD4+ T cells in the outer foreskin tissue explants. This is consistent with finding by Fahrbach et al. regarding inner and outer foreskin responses to external stimulation (23). In their findings, MIP1α and TNFα exposure caused significant increase in the number of CD4+ T cells in the inner foreskin tissue, but not the outer (23). The reasons for the lower response of the outer foreskin tissue to exposure to chemokines compared to the inner foreskin are not clear. A plausible mechanism might be the significantly higher numbers of proinflammatory chemokines and cytokines in the inner foreskin compared to the outer foreskin including MIG, IL-8, RANTES and IL1β, IL-17, GM-CSF, IFN-γ, IP-10 and CCL27 (119,121). This is of importance because many of these chemokines were reported to have different roles in increasing HIV susceptibility (31,91,200). The upregulation of these chemokines was also accompanied by higher CD4+CCR5+ cells in the epithelium of the inner foreskin tissue

compared to the outer foreskin (91,119). The difference in cytokine levels between the inner and outer foreskin tissue is of importance because IL-8 and MIG have been reported to be directly linked to HIV seroconversion (31). Notably, IL-8 levels in the penis decreased significantly after MMC (31). Furthermore, IP-10, MIG have been found to directly affect HIV uptake and latency in resting CD4+ T cells (200). CD207+ LC cells were also found to be enriched in the inner foreskin and to co-express CCR5 compared to the outer foreskin tissue (120). This suggests higher inflammatory environment in the inner foreskin tissue compared to the outer foreskin which might lead to higher response to chemokines that cause homing of T cells (TNF and CCL27) due to the pre-existing inflammatory chemokines in the inner foreskin; this might lead to increased response to exogenous exposure to chemokines and increased recruitment of immune cells including CD4+ T cells in the inner foreskin compared to the outer foreskin. The increased density of CD4+ T cells under the influence of these chemokines might also suggest a higher susceptibility to HIV in the inner foreskin due to the abundance of target cells in the inner foreskin tissue. However, one limitation to the comparison in the outer foreskin is the small sample size which might have contributed to the results not being significant.

In this chapter, we also wanted to compare two different counting techniques (manual and semi-automated counting techniques) to measure differences between the two methods and how this affects the cell counts. We observed a strong correlation between the two methods of counting which is an expected outcome since the two methods achieve the same purpose in counting dually positive cells. However, further analysis showed difference in the counts between the two methods, specifically in the inner foreskin. We observed agreement in the two methods for the untreated tissues of the inner foreskin (when cells estimated are usually few). However, higher counts in the manual counting method compared to the semi-automated counting in the stimulated tissues were noticed when the number of cells was relatively lower (<100 cells/mm^2). Higher number in the semi-automated counting compared to the manual methods were estimated in higher numbers of cells (> 200 cells/mm^2). We also showed that by comparing paired samples from unstimulated tissues compared to TNFα and CCL27 treated tissues (section 3.3.5.5), each of the two counting methods produced a different p value. These differences could be due to many reasons. First, the manual counting was conducted on the coloured images while the

semi-automated counting used grey scale images to detect cells (including the validation done after the software highlighted the cells). This might be in favour of less biased results coming from semi-automated counting since erroneous counts might have occurred in the manual method where background was considered a cell. Although the conditions and tissue type (inner and outer foreskin) in the two methods were blinded, observer bias might have been involved and led to overestimation or underestimation of numbers of cells in either method. To be able to precisely compare the two methods, we suggest including different observers to do the counting to minimize the bias. We also suggest keeping one method of counting consistent throughout an experiment to minimize conflicted results. However, underestimation of cells was also a possibility when the signal was not very strong. Autofluorescence may have caused errors in quantification. However, this is unlikely since quantification occurred in the epithelium of the foreskin tissue where autofluorescence was minimal.

Finally, we measured the numbers of CD3+CD4- cells and CD4+CD3- cells in the inner foreskin tissue from our semi-automated counting files. When comparing 4 data points (mean of 10 images per donor) from the 4 donors, we observed the CD3+CD4- cell counts to be non-significant across unstimulated, TNFα exposed and CCL27 exposed tissues. CD4+CD3- cells were relatively higher in CCL27 exposed samples compared to unstimulated tissues, although non-significant. This could be due to the low number of donors compared (4 donors) and more donors might provide more clarity on how TNFα and CCL27 might affect single positive CD3+CD4- cells and CD4+CD3- cells. CD3+ cells are known to be either T helper cells when expressing CD4 marker, T cytotoxic cells when expressing CD8 marker or MAIT cells. CD8+ T cells are known to reside in the foreskin tissue and an influx of CD8+ T cells was observed in recently infected HIV+ men (95,213). Meanwhile, CD4+ cells residing in the foreskin tissue are potentially T cells, Langerhans cells or macrophages. Langerhans cells and macrophages have been shown to reside in the foreskin tissue and to have a role in HIV infection (126,194). Although results regarding CD4+CD3- cells were non-significant, the trend suggests recruitment of Langerhans cells and/or macrophages in the inner foreskin under the influence of TNFα and CCL27 along with T cells recruitment that we observed in this chapter. Staining with only CD3 and CD4 markers is one limitation to this finding and further experiments are required with CD1a, CD207 (langerin) and CD11c staining to inspect

the impact of TNFα and CCL27 on LCs and macrophage density in the epithelium of the foreskin tissue. In summary, we showed an increased number of CD3+CD4+ T cells in the inner foreskin compared to the outer. We also showed that exogenous exposure to TNFα and CCL27 resulted in recruitment of CD4+ T cells in the inner foreskin but not the outer foreskin tissue. Furthermore, we observed that CD4+ T cell density had a trend of being higher in the inner foreskin compared to the outer and CD4+ T cell density increased under the influence of TNFα and CCL27. We also showed potential bias regarding differences in counting methods and how they may affect the results and suggesting consistent counting throughout experiments.

Chapter 4: Impact of CCL27 chemokine exposure on foreskin tissues and cells phenotype and function

Table of contents

4.1 Introduction

CCL27 chemokine had a significant effect on the number of CD3+CD4+ T cells in the epidermis of the inner foreskin tissue using *ex vivo* models and immunofluorescence imaging. Multi-parameter flow cytometry was used to measure the impact of CCL27 on specific T cell populations and marker expression in both the epidermis and dermis of the foreskin tissue. Th17 and Th22 cells are cells that reside in the foreskin tissue and are known for their susceptibility to HIV and production of inflammatory chemokines (166,167,189–191). Flow cytometry was used to focus on the impact of CCL27 exposure on both frequency of cells and marker expression in the inner and outer foreskin and thus complement the immunofluorescence results. However, due to limiting factors such as low cell yields, low viability and/or loss of marker expression altogether; the outcomes from these flow cytometry experiments were inconclusive and are interpreted with caution.

4.2 Experimental design

Overall, 4 sets of experiments were conducted, and they had different designs and objectives:

1. **impact of TNFα and CCL27 on foreskin cells from tissues digested with Liberase.**

Objective: to measure Th17 and Th22 frequencies in the inner and outer foreskin cells following digestion of foreskin tissue with Liberase enzyme and treatment with CCL27. In this experiment, foreskin tissue samples were digested with Liberase then the liberated cells were treated by TNFα or CCL27 (Figure 4.1a).

2. Impact of TNFα and CCL27 on spontaneously migrated cells from whole tissue foreskin samples.

Objective: to measure Th17 and Th22 cell frequencies and markers expressed in the inner and outer foreskin in whole tissue samples. In this experiment, foreskin tissue samples were exposed to chemokines (TNFα and CCL27) for 48 hours then cells were stained and acquired (Figure 4.1b).

3. Spontaneous migration following chemokine exposure and Dispase treatment.

Objective: to compare the differences in frequencies of Th17 and Th22 cells isolated from epidermis and dermis of the foreskin tissues treated with TNFα and CCL27 relative to unstimulated controls. In this experiment, foreskin tissue samples were exposed to chemokines for 48 hours, followed by Dispase digestion for 18 hours to separate the epidermis and dermis, after which cells were migrated in RPMI for 48 hours (Figure 4.1c).

4. Effect of Dispase digestion and prolonged cell culturing on foreskin cell markers.

Objective: to determine the effect of Dispase and prolonged incubation on cell surface markers (CD45, CCR4 and CCR6) isolated from the foreskin tissue. In this experiment, FS tissues were treated with HBSS (control) or Dispase for 18 hours. Then both the cells migrated from the whole tissue controls or the Dispase treated tissues in RPMI and then harvested completely after 24 hours (to allow regain of markers cleaved under the effect of Dispase (215)), 48 hours and 96 hours (Figure 4.1d).

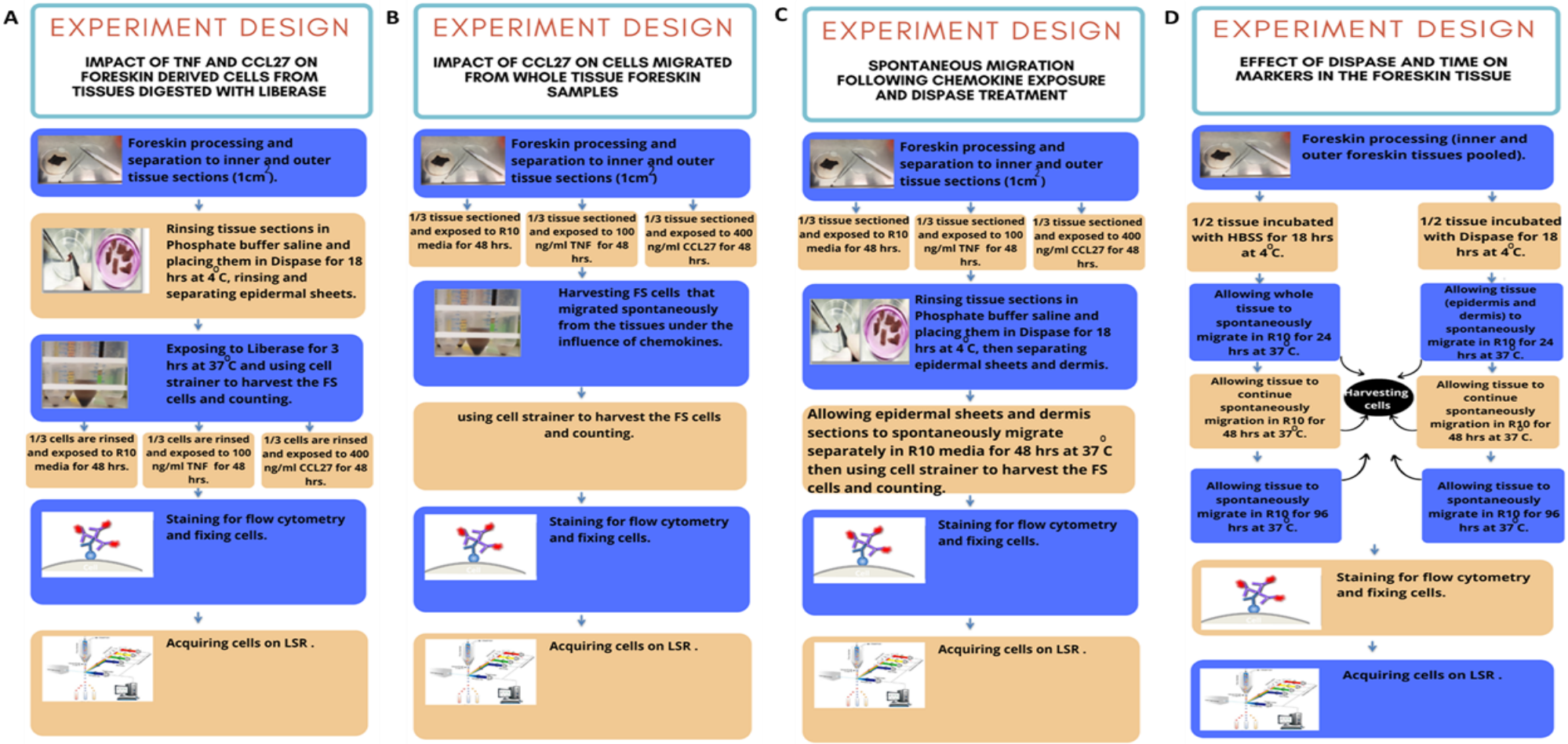

Figure 4.1: A) Experiment design to show impact of TNF and CCL27 on cells isolated from Liberase digested FS tissues. B) Experiment design to show impact of TNF and CCL27 on spontaneously migrated cells from whole tissue foreskin samples. C) Experiment design showing spontaneous migration following chemokine exposure then Dispase treatment. D) Experiment design to show the effect of Dispase and prolonged culturing time on the markers in the foreskin tissue.

4.3 Gating strategy:

The proportion of Th17 and Th22 cells were obtained using the gating strategy shown in Figure 4.2.

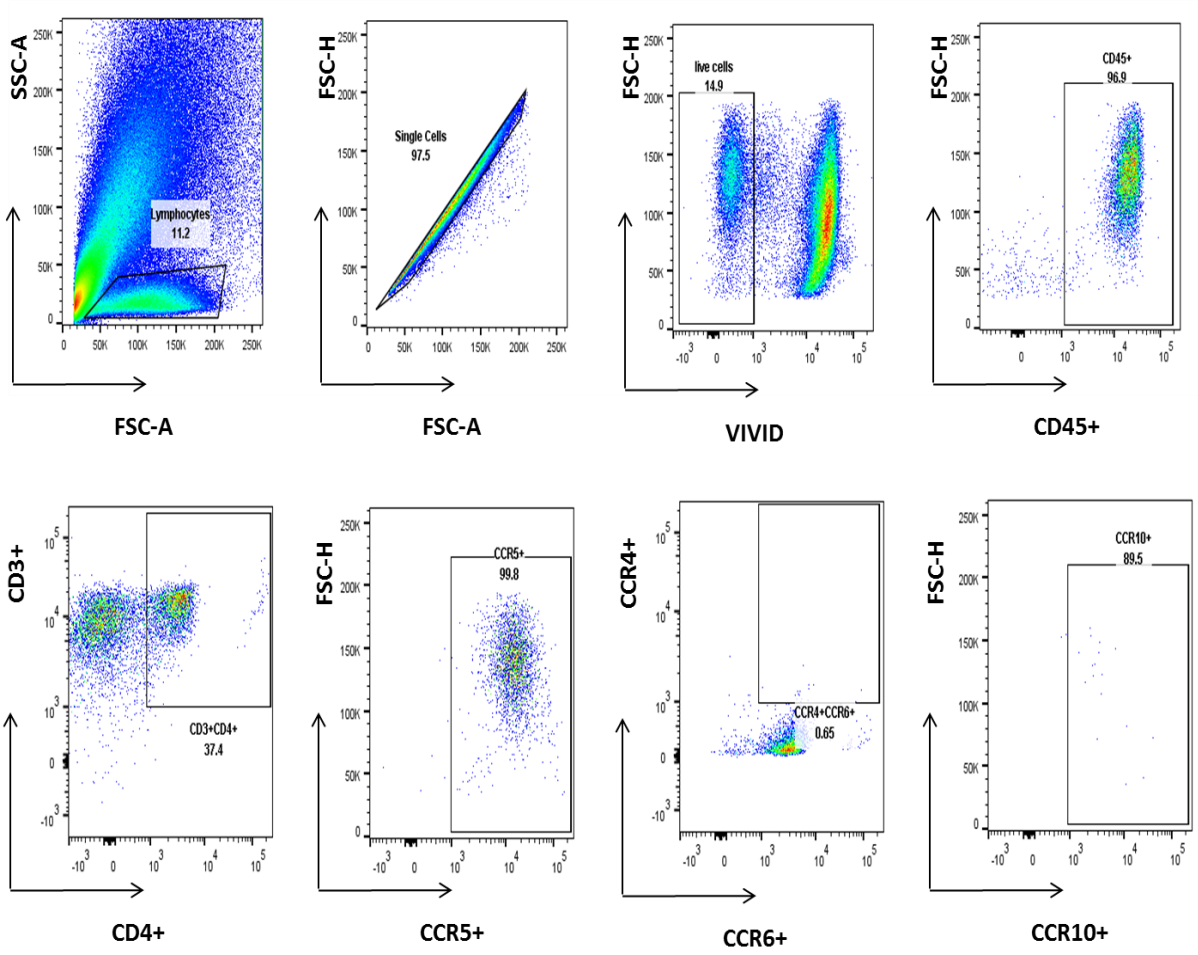

Figure 4.2: Gating strategy for the experiments

4.4 RESULTS

4.4.1 Impact of TNFα and CCL27 on foreskin cells from foreskin tissues digested with liberase

The objective of this experiment was to determine the impact of CCL27 on the frequencies of Th17 and Th22 cells in the epidermal sheets of the inner and outer foreskin tissue. Th17 cells were identified as cells that were expressing CD3+CD4+CCR5+CCR4+CCR6+ and Th22 cells were identified as cells that were expressing CD3+CD4+CCR5+CCR4+CCR6+CCR10+.

Figure 4.3 shows representative flow plots of the following populations: (**CD3+CD4+, CD3+CD4+CCR5+, CD3+CD4+CCR5+CCR4+CCR6+, CD3+CD4+CCR5+CCR4+CCR6+CCR10+).**

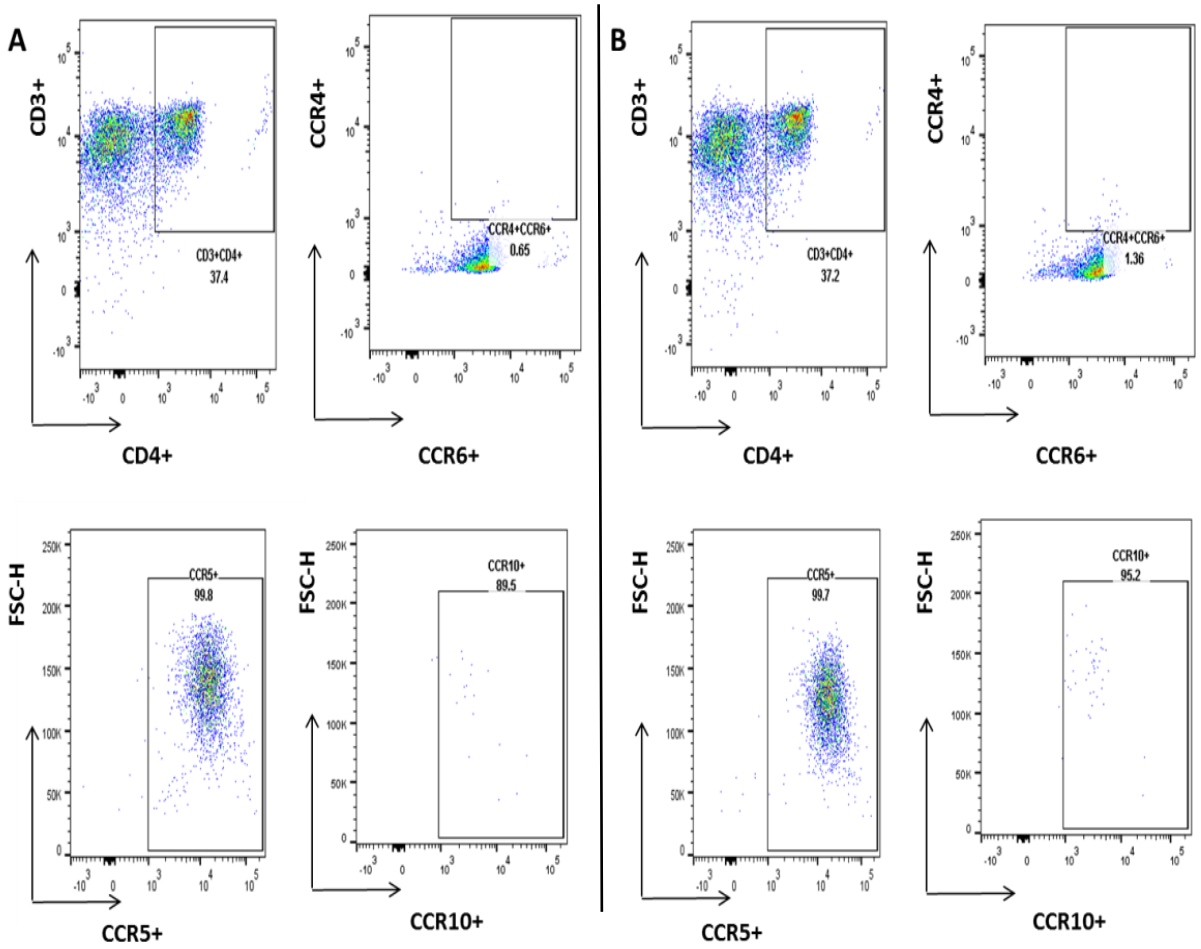

Figure 4.3: Flow plots showing: A) CD3+CD4+, CD3+CD4+CCR5+, CD3+CD4+CCR5+CCR4+CCR6+, CD3+CD4+CCR5+CCR4+CCR6+CCR10+ populations in the unstimulated inner foreskin cells B) CD3+CD4+, CD3+CD4+CCR5+, CD3+CD4+CCR5+CCR4+CCR6+, CD3+CD4+CCR5+CCR4+CCR6+CCR10+ populations in the CCL27 exposed inner foreskin cells.

We could observe that the low cell yield and viability in this method affected the experiment (only 1 million cells were stained, ~20000 to 50000 events were acquired and viability was less than 20% in the inner foreskin and less than 5% in the outer foreskin and cell numbers were not enough to include TNFα exposed cells in the inner foreskin). Table 4.1 shows the low number of events of CD3+CD4+, CD3+CD4+CCR5+, CD3+CD4+CCR5+CCR4+CCR6+, CD3+CD4+CCR5+CCR4+CCR6+CCR10+ cells in both the inner and outer foreskin samples which makes the results less reliable to describe the impact of TNFα and CCL27 on foreskin cells. One donor was used for the optimization of this experiment. However, we designed the next experiment to improve the measured outcomes and improve viability and number of cells acquired.

Table 4.1: Number of events of CD3+CD4+, CD3+CD4+CCR5+, CD3+CD4+CCR5+CCR4+CCR6+, CD3+CD4+CCR5+CCR4+CCR6+CCR10+ in both the inner and outer Liberase treated foreskin sample.

Population	Unstimulated		TNF exposed		CCL27	
	Inner	Outer	Inner	Outer	Inner	outer
CD3+CD4+ cells	2948	150	___	4	3109	10
CD3+CD4+CCR5+ cells	2941	146	___	2	3099	9
CD3+CD4+CCR5+CCR4+CCR6+ cells	19	1	___	0	42	0
CD3+CD4+CCR5+CCR4+CCR6+CCR10+ cells	17	1	___	0	40	0

4.4.2 Impact of TNFα and CCL27 on spontaneously migrated cells from whole tissue foreskin samples

We aimed at recovering the optimal cell yield required for evaluating the impact of CCL27 on FS tissue, two experiments in sections 4.4.2 and 4.4.3 were conducted from the same 4 donors and compared. The following experiment aimed to improve the outcome and number of cells compared to the first experiment and enable analysis of proportions and marker expression changes occurring post exposure to chemokine. It is worth noting that number of samples in the experiment is low (4 donors) which warrants caution in interpreting the results. Table 4.2 shows the mean number of events acquired in each of the populations of CD3+CD4+, CD3+CD4+CCR5+, CD3+CD4+CCR5+CCR4+CCR6+ and CD3+CD4+CCR5+CCR4+CCR6+CCR10+ and shows cell numbers are also quite low.

Table 4.2 Number of events of CD3+CD4+, CD3+CD4+CCR5+, CD3+CD4+CCR5+CCR4+CCR6+, CD3+CD4+CCR5+CCR4+CCR6+CCR10+ in both the inner and outer foreskin whole tissue samples.

Population	Unstimulated		TNF exposed		CCL27	
	Inner	Outer	Inner	Outer	Inner	outer
CD3+CD4+ cells	649±397.80	578±410.20	1398±1421	379±242.30	1403±1598	181± 68.22
CD3+CD4+CCR5+ cells	568±366.2	442±296	1228±1269	317±215.5	1228±1467	147±52.44
CD3+CD4+CCR5+CCR4+CCR6+ cells	192±176.4	147±127.1	251±253.4	108±77.5	263±219.8	45±14.8
CD3+CD4+CCR5+CCR4+CCR6+CCR10+ cells	47±52.62	39±51.21	44±56.13	22±12	33±39.69	10±4.9

4.4.2.1 Impact of TNFα and CCL27 on frequency of spontaneously migrated cells from whole tissue foreskin.

We compared median frequencies of T cell subsets in the FS cells spontaneously migrating from the FS tissue samples under three conditions (unstimulated, TNFα and CCL27) in 4 donors. Figure 4.4 shows representative flow plots of frequencies of T cells migrating under the impact of TNFα and CCL27 exposed sample. Figures 4.5 and 4.6 show no significant differences in the median frequencies of all cell populations measured when comparing unstimulated cells (control) to CCL27 and TNFα treated cells from both the inner and outer foreskins. In the inner foreskin, the median CD3+CD4+ cells frequencies of CD45+ population in the unstimulated FS samples were 38.40% (IQR: 25-61.85) compared to TNFα exposed FS samples (42.65%, IQR: 29.75-59.68, *P*=0.375) and CCL27 exposed FS samples (40.90%, IQR: 22.25-64.95, *p*=0.625) (Figure 4.5a). The median frequency of CCR5+ cells of CD3+CD4+ population in the unstimulated FS samples were 87.20% (IQR: 61.15-92.25) compared to TNFα exposed FS samples (88.55%, IQR: 63.73-88.85, *P>0.999*) and CCL27 exposed FS samples (86.60%, IQR: 68.98-90.73, *p>0.999*) (Figure 4.5b). Th17 cells (CCR4+CCR6+) frequency of CD3+CD4+ population was 27.75% (IQR: 8.19-45.90) in unstimulated FS samples compared to TNFα exposed FS samples (24.45%, IQR: 8.67-38.38, *P*=0.625) and CCL27 exposed FS samples (27.90%, IQR: 7.96-46.10, *p>0.999*) (Figure 4.5c). Finally, Th22 cells (CCR4+CCR6+CCR10+) frequency of CD3+CD4+ population in the unstimulated FS samples was 8.76% (IQR: 1.68-12.60) compared to TNFα exposed FS samples (5.35%, IQR: 0.96-7.67, *P*=0.250) and CCL27 exposed FS samples (4.92%, IQR: 0.75-7.39, *p*=0.125) (Figure 4.5d).

It is worth noting that the number of samples is low (4 donors). Hence, the results should be interpreted with caution. No conclusions can be confidently made from these results due to the low number of donors.

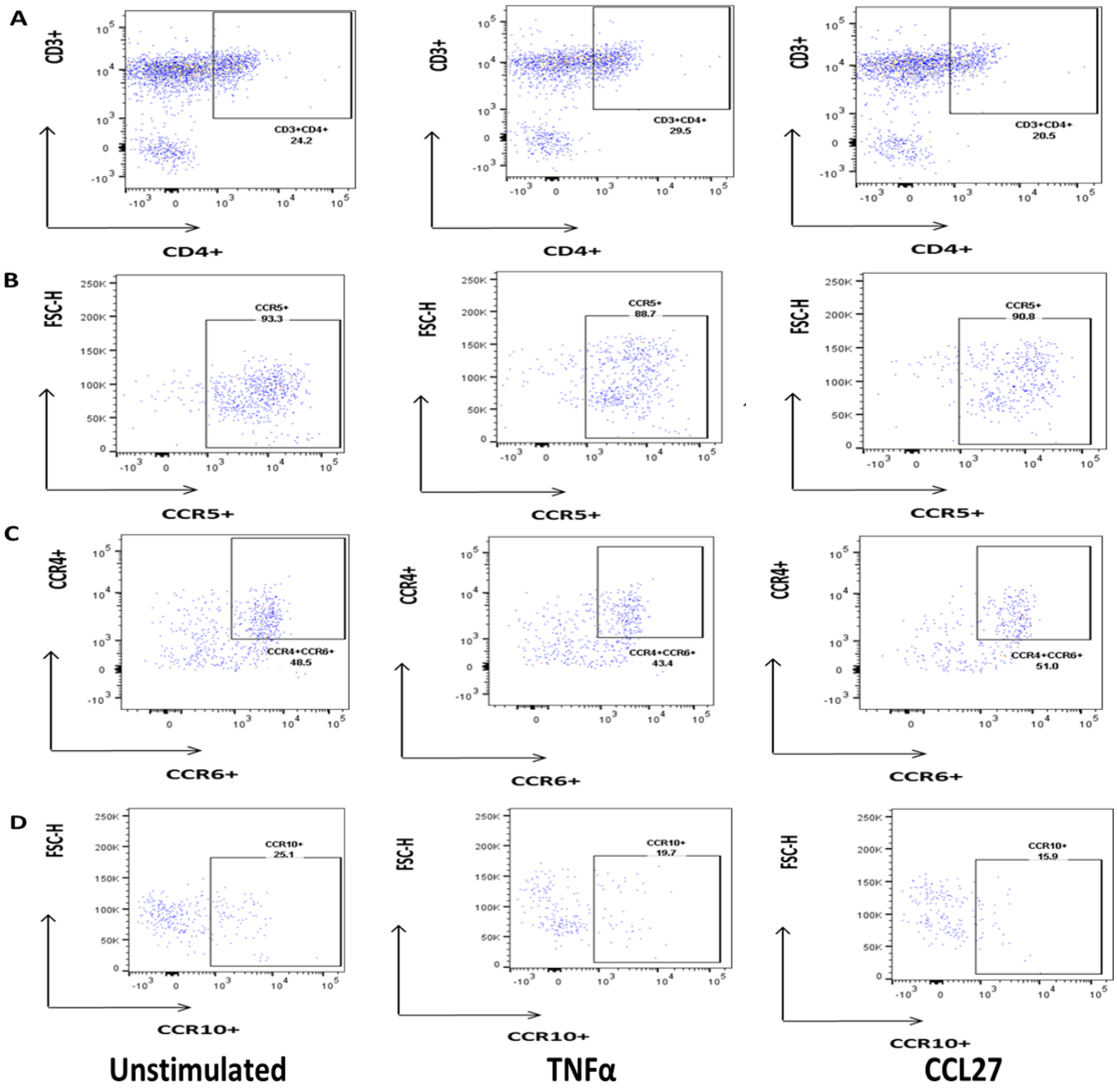

Figure 4.4: Representative flow plots for spontaneous migration from Whole tissue samples under the impact of TNFα (positive control) and CCL27 exposed sample in the inner foreskin. A) CD3+CD4+ population across the three conditions. B) CD3+CD4+CCR5+ population across the conditions. C) CD3+CD4+CCR5+CCR4+CCR6+ population across the conditions. D) CD3+CD4+CCR5+CCR4+CCR6+CCR10+ population across the conditions.

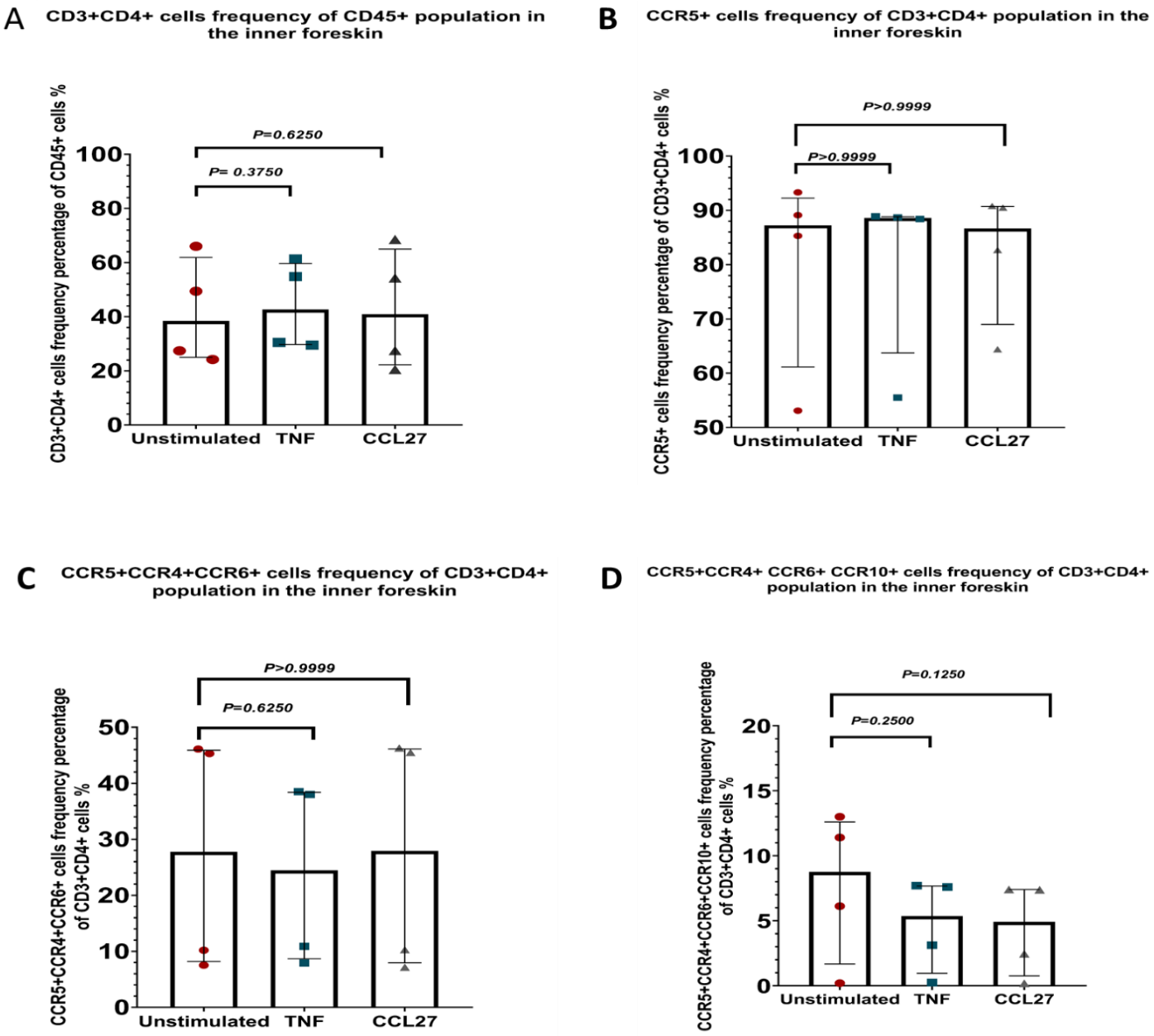

Figure 4.5: Difference in frequency of spontaneously migrating cells from whole tissue foreskin samples from the inner foreskin of 4 samples (n=4 for each condition). A) CD3+CD4+ frequency of CD45+ population. B) CCR5+ frequency of CD3+CD4+ population. C) CCR4+CCR6+ frequency of CD3+CD4+ population. D) CCR4+CCR6+CCR10+ frequency of CD3+CD4+ population.

In the outer foreskin, the median CD3+CD4+ cells frequencies of CD45+ population in the unstimulated FS samples were 37.25% (IQR: 20.55-52.45) compared to TNFα exposed FS samples (35.70%, IQR: 23-60.60, *P*=0.500) and CCL27 exposed FS samples (31.60%, IQR: 28.05-40.63, *p>0.999)* (Figure 4.6a). The median frequency of CCR5+ cells of CD3+CD4+ population in the unstimulated FS samples were 75.65% (IQR: 61.88-88.23) compared to TNFα exposed FS samples (84.90%, IQR: 68.30-91.70, *P*=0.500) and CCL27 exposed FS samples (79.40%, IQR: 75.68-88.23, *p*=0.500) (Figure 4.6b). Th17 cells (CCR4+CCR6+) frequency of CD3+CD4+ population was 21.60% (IQR: 15.40-37.33) in unstimulated FS

samples compared to TNFα exposed FS samples (28.20%, IQR: 14.60-39.40, *P*=0.750) and CCL27 exposed FS samples (22.90%, IQR: 22.90-29.50, *p>0.999*) (Figure 4.6c). Finally, Th22 cells (CCR4+CCR6+CCR10+) frequency of CD3+CD4+ population in the unstimulated FS samples was 4.68% (IQR: 2.30-12.93) compared to TNFα exposed FS samples (5.37%, IQR: 5.34-7.58, *P*=0.750) and CCL27 exposed FS samples (4.45%, IQR: 3.65-5.98, *p>0.999*) (Figure 4.6d). These results investigate proportions of cells that spontaneously migrate under the influence of chemokines and show no significant difference, but the experiment did not investigate recruitment of T cell populations in the epithelium of foreskin tissue under the influence of these chemokines.

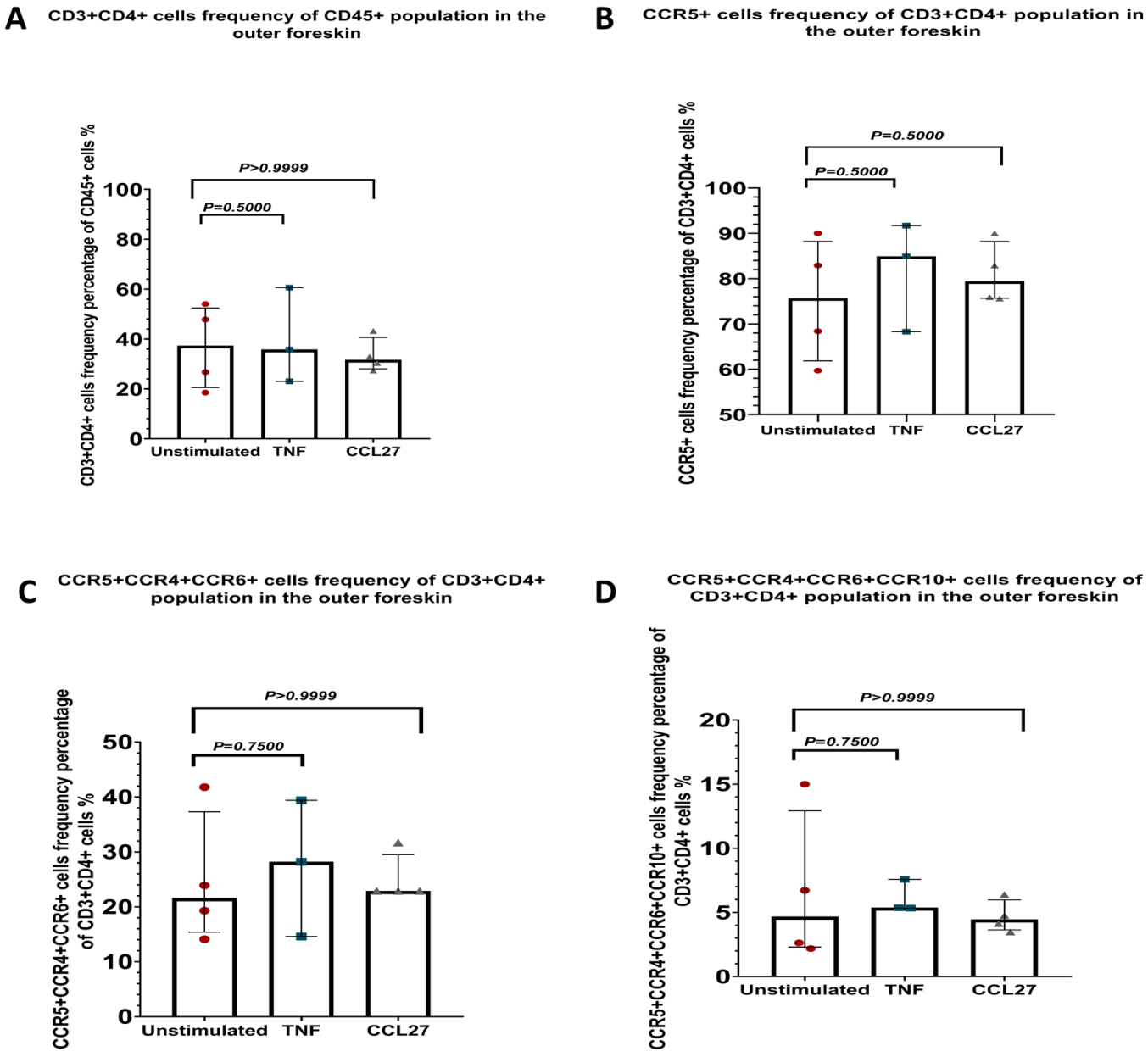

Figure 4.6: Difference in cell proportions in whole tissue crawled foreskin samples from the outer foreskin of 4 samples (n=4 for each condition). A) Statistical analysis of CD3+CD4+ frequency of CD45+ population. B) Statistical analysis of CCR5+ frequency of CD3+CD4+ population. C) Statistical analysis of CCR4+CCR6+ frequency of CD3+CD4+ population. D) Statistical analysis of CCR4+CCR6+CCR10+ frequency of CD3+CD4+ population.

4.4.2.2 Impact of CCL27 on marker expression in Whole tissue migrated foreskin cells

We wished to validate if the increase in density of CD3+CD4+ cells in the foreskin tissue (observed in chapter 3) was due to merely an increase in marker expression caused by chemokine exposure or due to recruitment of T cells from the deeper layers of the foreskin tissue to the epithelium. Hence, we created histograms to measure mean fluorescence intensity of CD3, CD4, CCR5, CCR4, CCR6 and CCR10 markers across unstimulated samples, TNFα exposed and CCL27 exposed whole tissue foreskin samples. We measured mean fluorescence intensity (MFI) for each marker to compare differences occurring in single marker expressions due to chemokine exposure. Figure 4.7 shows representative histograms of the markers in the inner and outer foreskin tissues.

A

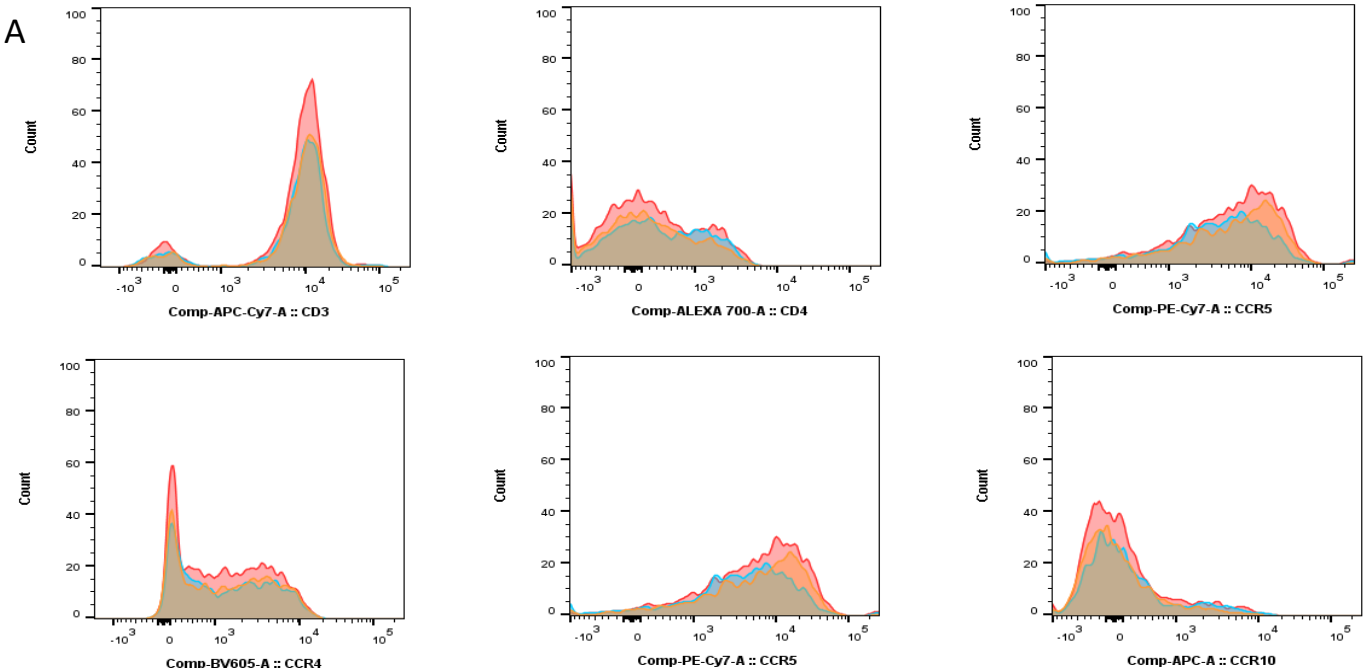

Sample Name	Subset Name	Count
Whole tissue with CCL27	CD45+	1915
Whole tissue with TNF	CD45+	1829
Whole tissue unstimulated	CD45+	2583

B

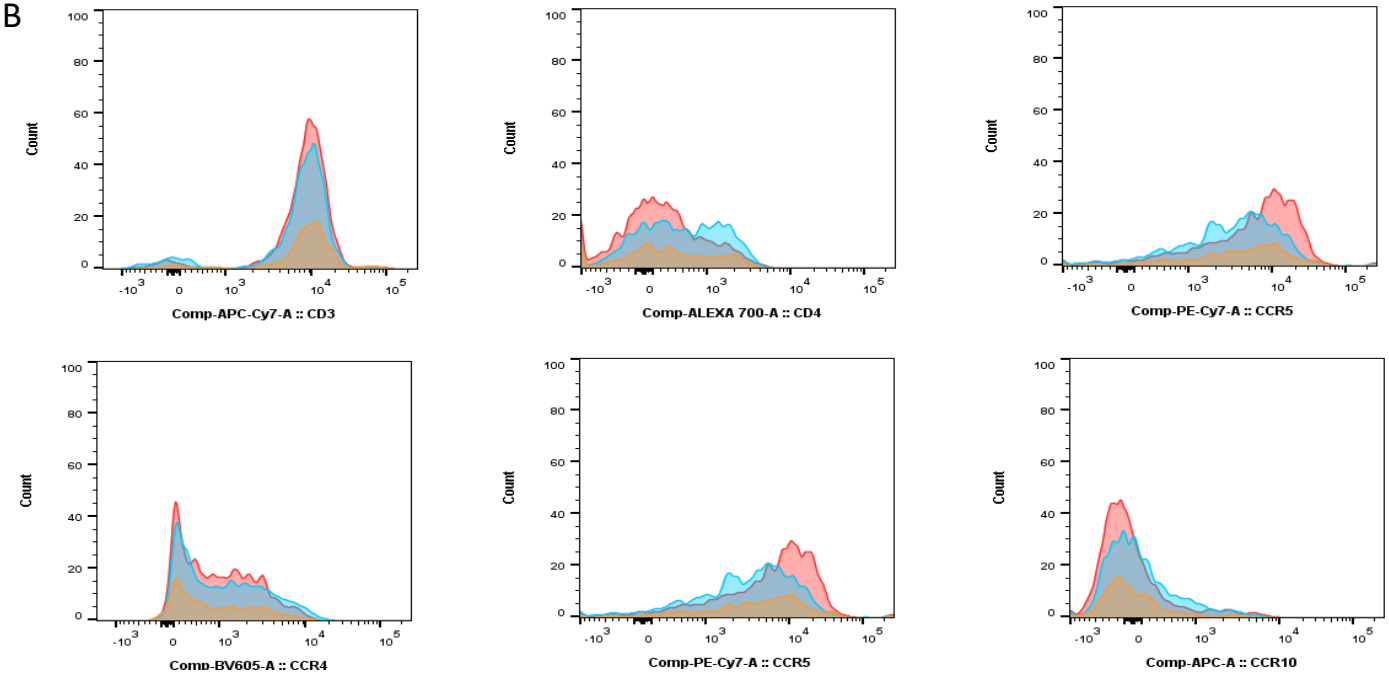

Sample Name	Subset Name	Count
Whole tissue with CCL27	CD45+	737
Whole tissue with TNF	CD45+	1838
Whole tissue unstimulated	CD45+	2056

Figure 4.7: Representative histograms for different markers in whole tissue migrated foreskin tissues from the inner and outer foreskin. A) Histograms of different markers in the inner foreskin migrated cells. B) Histograms of different markers in the outer foreskin migrated cells.

Figures 4.8 and 4.9 show plots of the MFI for different markers of whole tissue migrated cells of 4 foreskin samples in the inner and outer foreskin respectively. The differences in MFI were statistically non-significant across all conditions for cells migrating from either the inner or outer foreskin. In the inner foreskin, the median MFI of CD3 in the unstimulated samples was 10497 (IQR: 9560-10923) compared to TNFα exposed samples (10341, IQR: 8923-11603, *P*=0.875) and CCL27 treated samples (10451, IQR:9220-10648, *p*=0.375). Median MFI of CD4 in the unstimulated samples was 1177 (IQR: 641.80-2302) compared to TNFα exposed samples (1338, IQR: 713.30-2016, *P*=0.875) and CCL27 treated samples (1197, IQR:521.80-2372, *p*=0.875). Median MFI of CCR5 in the unstimulated samples was 7523 (IQR: 4679-11257) compared to TNFα exposed samples (7064, IQR: 4536-9330, *P*=0.625) and CCL27 treated samples (7539, IQR:5845-10300, *p*>0.999). Median MFI of CCR4 in the unstimulated samples was 1693 (IQR: 772.30-2228) compared to TNFα exposed samples (1451, IQR: 583.30-2269, *P*=0.250) and CCL27 treated samples (1540, IQR:625-2337, *p*=0.875). Median MFI of CCR6 in the unstimulated samples was 3017 (IQR: 1387-3211) compared to TNFα exposed samples (2372, IQR: 921.3-3145, *P*=0.250) and CCL27 treated samples (2630, IQR:1276-2710, *p*=0.125). Median MFI of CCR10 in the unstimulated samples was 521 (IQR: 481-845) compared to TNFα exposed samples (755, IQR: 566-760, *P*=0.750) and CCL27 treated tissues (360, IQR:212-854, *p*=0.500).

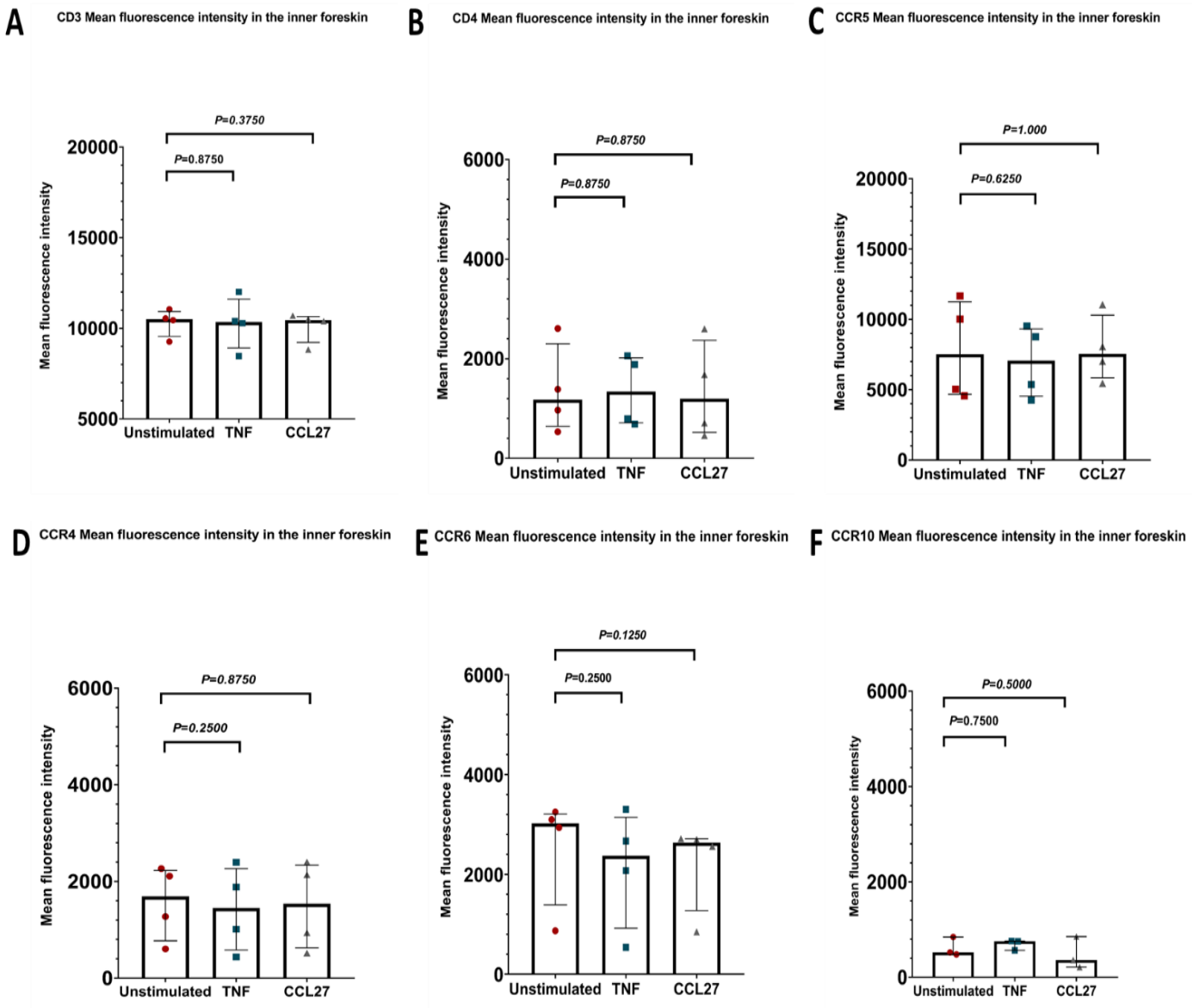

Figure 4.8: Mean fluorescence intensity of different markers in whole tissue migrated foreskin tissues from the inner foreskin (n=4 for each condition).

Similarly for the outer foreskin, no significant differences were observed for MFI for all the markers measured among the treatment conditions. In the outer foreskin, the median MFI of CD3 in the unstimulated samples was 10646 (IQR: 8824-11071) compared to TNFα exposed samples (9861, IQR: 9353-11195, *P*=0.500) and CCL27 treated samples (11985, IQR:8092-12846, *p*=0.375). Median MFI of CD4 in the unstimulated samples was 1104 (IQR: 622-1888) compared to TNFα exposed samples (1029, IQR: 534-1786, *P*=0.500) and CCL27 treated samples (1213, IQR:675.3-4240, *p*=0.625). Median MFI of CCR5 in the unstimulated samples was 9245 (IQR: 4236-11203) compared to TNFα exposed samples (7785, IQR: 7071-8589, *P*=0.250) and CCL27 treated samples (8941, IQR:5695-14325, *p*=0.625). Median MFI of CCR4 in the unstimulated samples was 1487 (IQR: 1047-2051) compared to TNFα exposed samples (1974, IQR: 917-1984, *P*=0.750) and CCL27 treated samples (1437, IQR:1046-1766, *p*=0.625). Median MFI of CCR6 in the unstimulated samples was 2421 (IQR: 1700-3157)

compared to TNFα exposed samples (2475, IQR: 1860-2851, *P*=0.250) and CCL27 treated samples (3243, IQR:2600-4986, *p*=0.125). Median MFI of CCR10 in the unstimulated samples was 528 (IQR: 79.85-895.80) compared to TNFα exposed samples (496, IQR: 409-1533, *P*=0.750) and CCL27 treated samples (745.5, IQR:350.50-971, *p*=0.250).

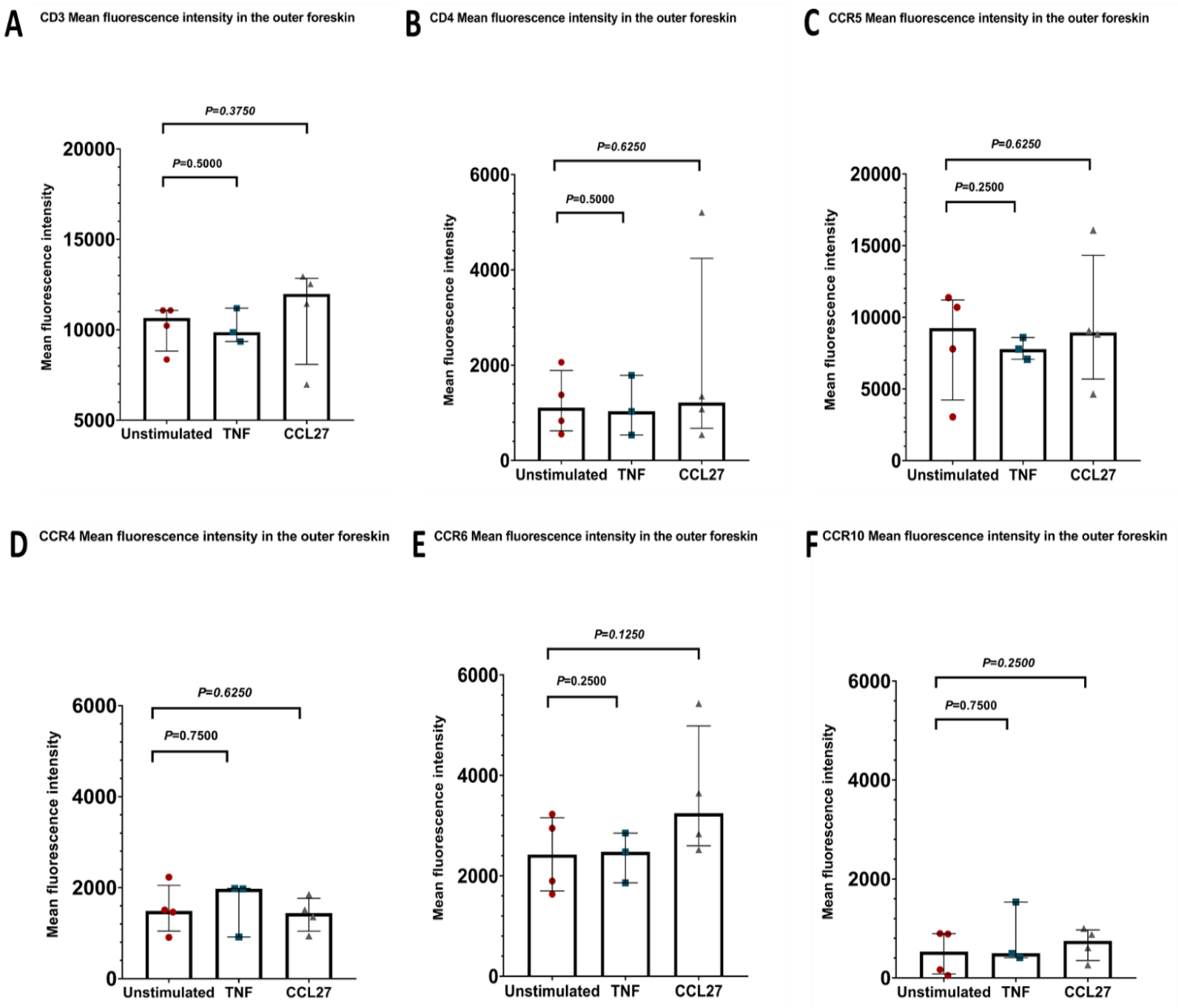

Figure 4.9: Box plots for Mean fluorescence intensity of different markers in whole tissue migrated foreskin tissues from the outer foreskin (n=4 for each condition).

4.4.3 Spontaneous migration after chemokine and Dispase exposure

In the second part of the previous experiment and after cells were migrated from whole foreskin tissues under the influence of chemokines, the tissues were exposed to Dispase enzyme to enable separation of epidermis and dermis of the foreskin samples. The aim of this experiment was to quantify proportions of Th17 and Th22 cells in both the epidermis and dermis of the foreskin tissues in the chemokine exposed tissues compared to the unstimulated controls.

Cells stained and acquired in this experiment showed decreased numbers of CD45+ cells in the lymphocyte population, normally expressing CD45, along with CCR4 and CCR6. These changes were consistent across the 4 samples used and all tested conditions of the experiment (unstimulated, TNFα and CCL27) in epidermis and dermis tissues. Figure 4.10 shows representative flow plots of the differences the CD45+ cells along with CCR4+CCR6+ populations. The decrease in these markers was hypothesized to occur due to either the exposure to chemokines, Dispase and the prolonged exposure to cell culture media (cells were acquired after 48 hours of being treated with chemokines, 18 hours of Dispase treatment and 48 hours of migration after Dispase).

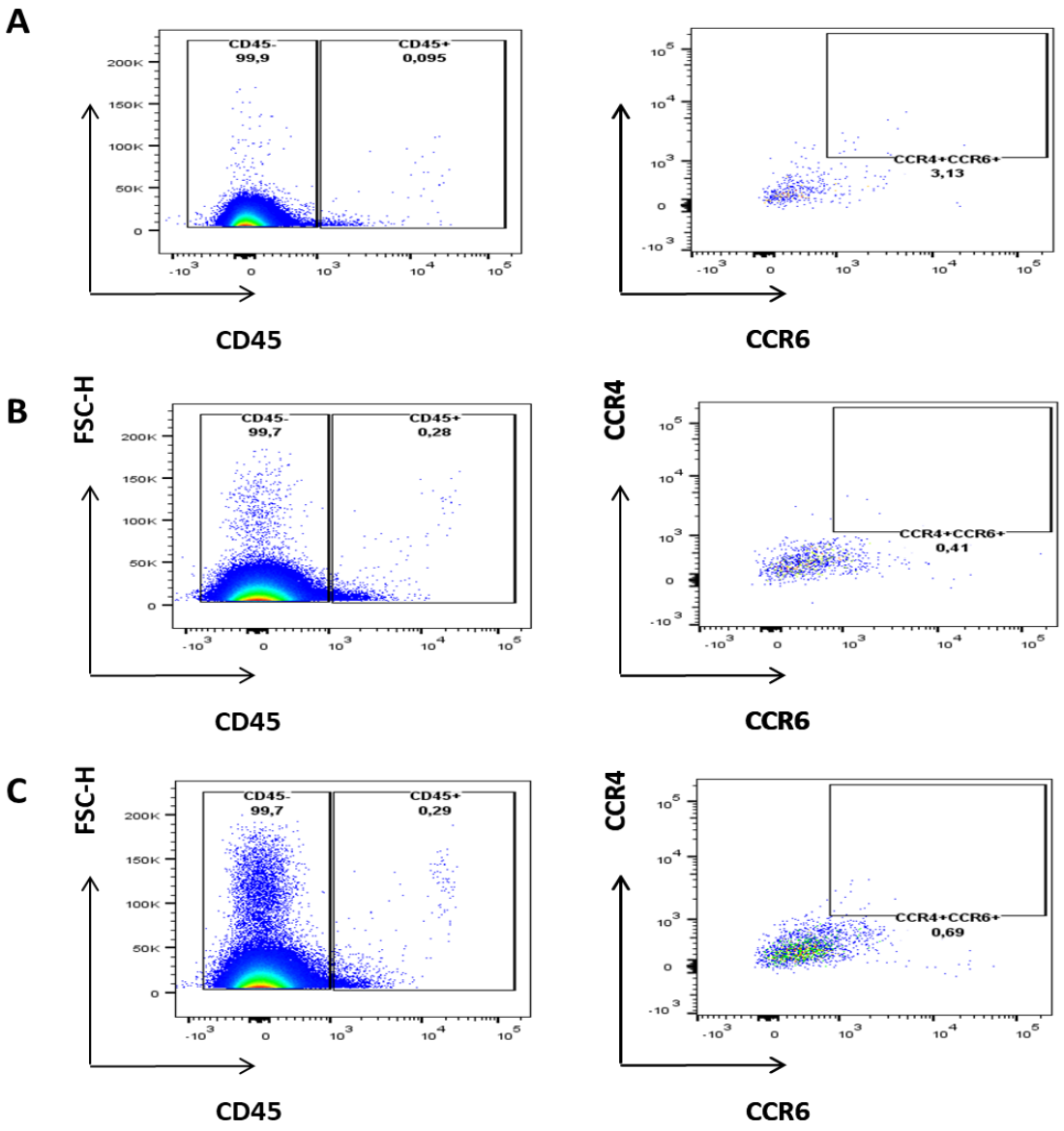

Figure 4.10: Representative flow plots showing the populations of CD45, CCR4+CCR6+ cells in the Dermis of inner foreskin. A) CD45+, CCR4+CCR6+ populations in the unstimulated control. B) CD45+, CCR4+CCR6+ populations in the TNFα exposed tissue. C) CD45+, CCR4+CCR6+ populations in the CCL27 exposed tissue.

Figure 4.11 shows a significant decrease in CD45+ expression in all 4 samples across all conditions in both inner and outer foreskin between the cells migrated and acquired directly after chemokine exposure for 48 hours and the cells of the epidermis and dermis that were acquired at the later point (after 48 hours exposure to chemokines, 18 hours of Dispase treatment and 48 hours of migration after Dispase) showing almost complete loss of the CD45 marker. Median frequency of CD45+ cells was 13,20% (IQR: 7.65-19.30) compared to 0.10% (IQR: 0.04-0.15, p<0.0001) in Dispase treated epidermis cells and 0,19% (IQR:0.12-0.48, p<0.0001) in Dispase treated dermis cells.

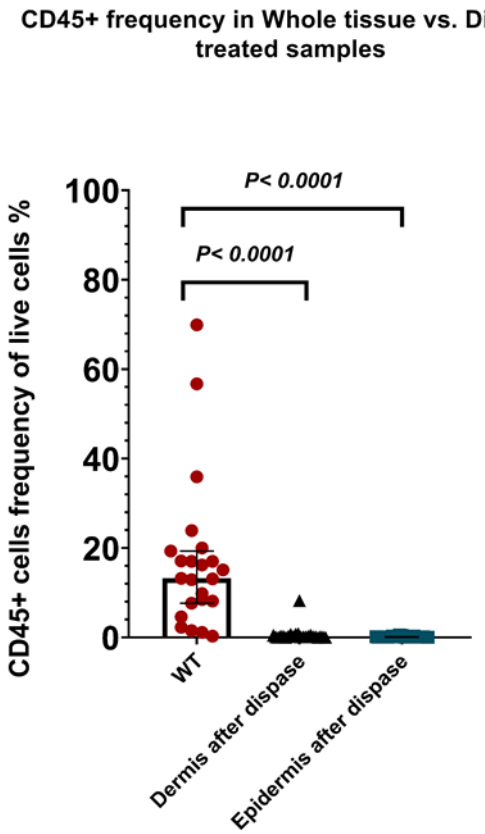

Figure 4.11: Mann-Whitney test of CD45+ frequency in whole tissue migrated samples vs. samples exposed to migration after Dispase (n=23 for each condition).

4.4.4 Effect of Dispase and time on markers in the foreskin tissue

To understand the impact of Dispase and prolonged *in vitro* cell culturing time on the integrity of the foreskin tissue and whether these conditions contributed to the loss of marker expression, we conducted the last experiment where we exposed 2 foreskin samples (inner and outer foreskin pooled) to two conditions (controls in HBSS for 18 hours of in Dispase for 18 hours) in three different time points (24 hours, 48 hours and 96 hours of migration in RPMI). Samples treated with HBSS or Dispase for 18 hours were only harvested for the first time after 24 hours of resting in culture media because it was reported to allow cleaved markers to recover (215).

There was a change in the gating strategy for this experiment where CCR4 and CCR6 were gated from CD45 directly to view the overall expression of these markers (Figure 4.12). Figure 4.13 shows representative plots of difference in CD45+ cell proportions in whole tissue controls and Dispase treated tissues in three time points while Figure 4.14 shows representative plots of difference in CCR4+ and CCR6+ cell proportions in Whole tissue controls and Dispase treated tissues in three time points. Table 4.3 shows the mean number of events acquired of CD45+, CCR4+ and CCR6+ cells in the samples; the large standard deviation indicates large variation between the number of cells in each sample.

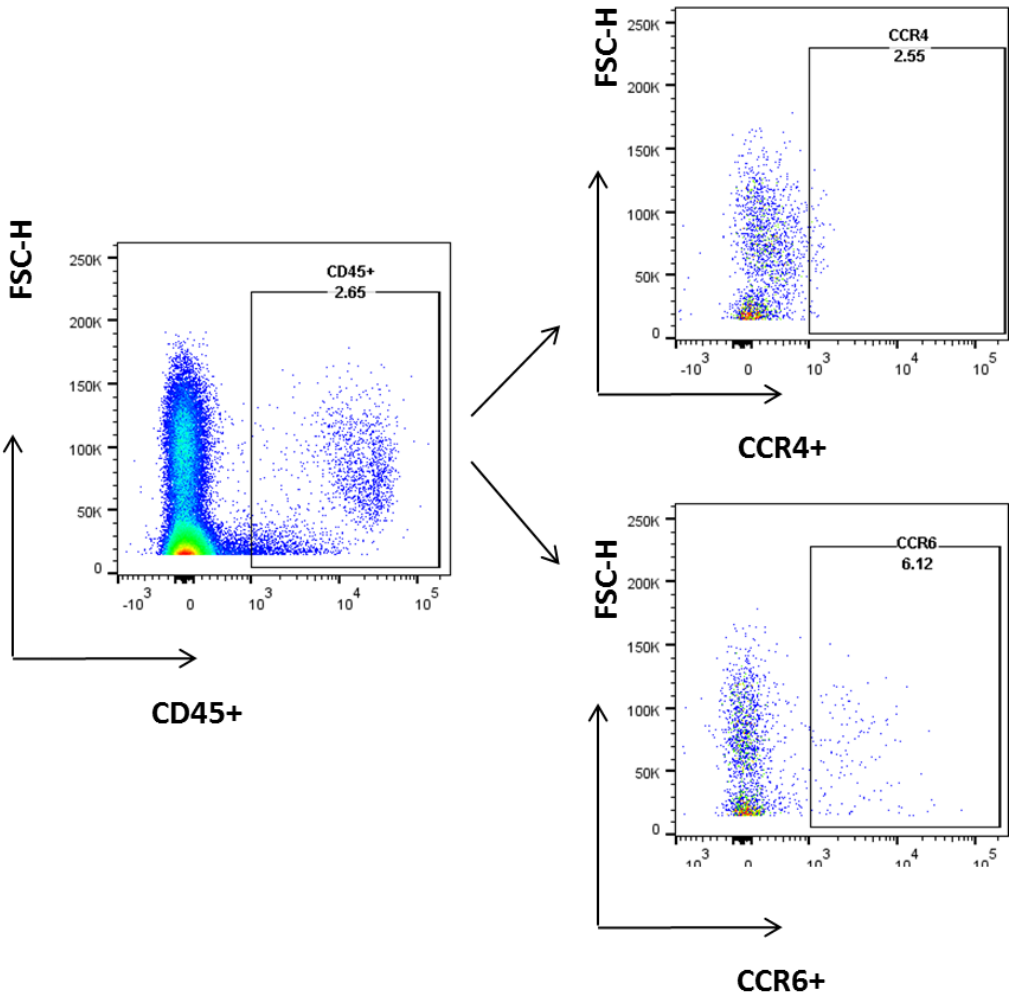

Figure 4.12: Change in gating strategy.

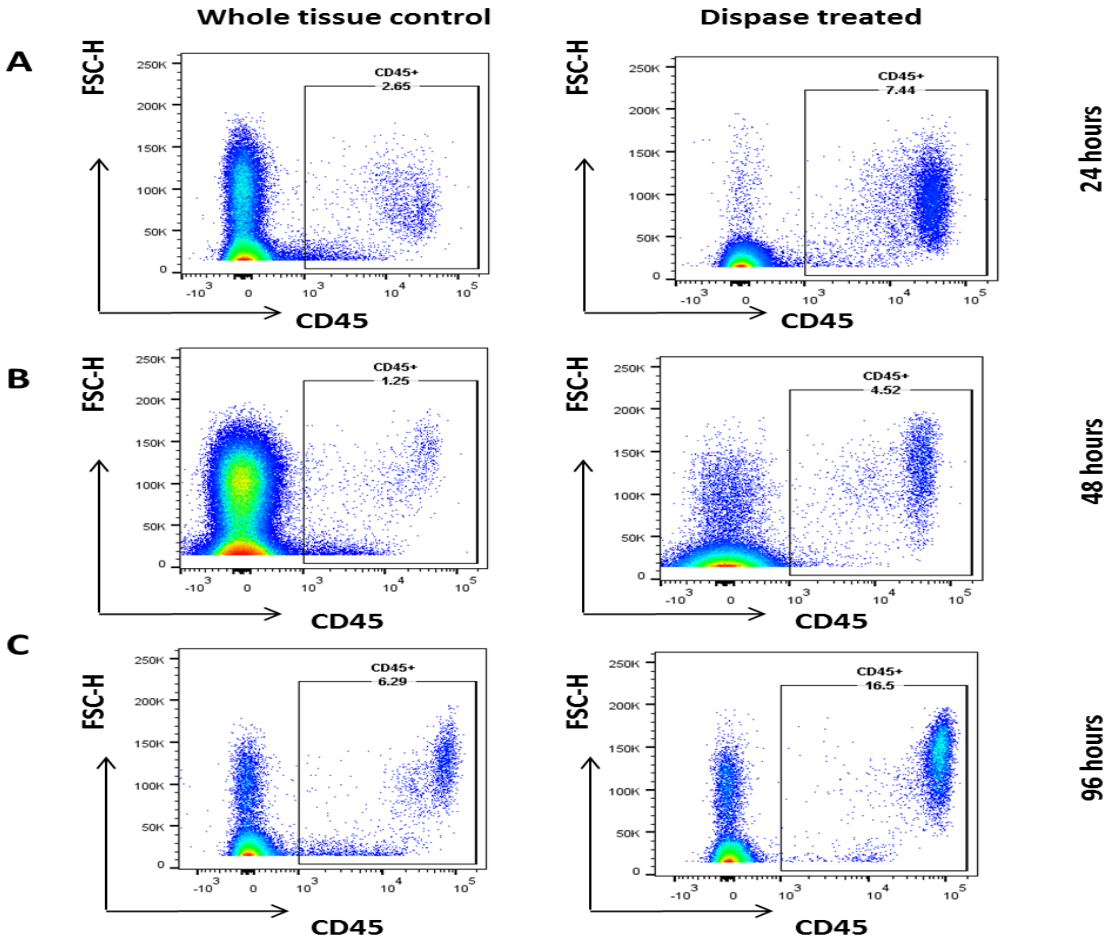

Figure 4.13 Representative flow plots of difference in CD45+ expression in Whole tissue controls and Dispase treated tissues in three time points. A) CD45+ expression in Whole tissue controls and Dispase treated tissues after 24 hours. B) CD45+ expression in Whole tissue controls and Dispase treated tissues after 48 hours. C) CD45+ expression in Whole tissue controls and Dispase treated tissues after 96 hours.

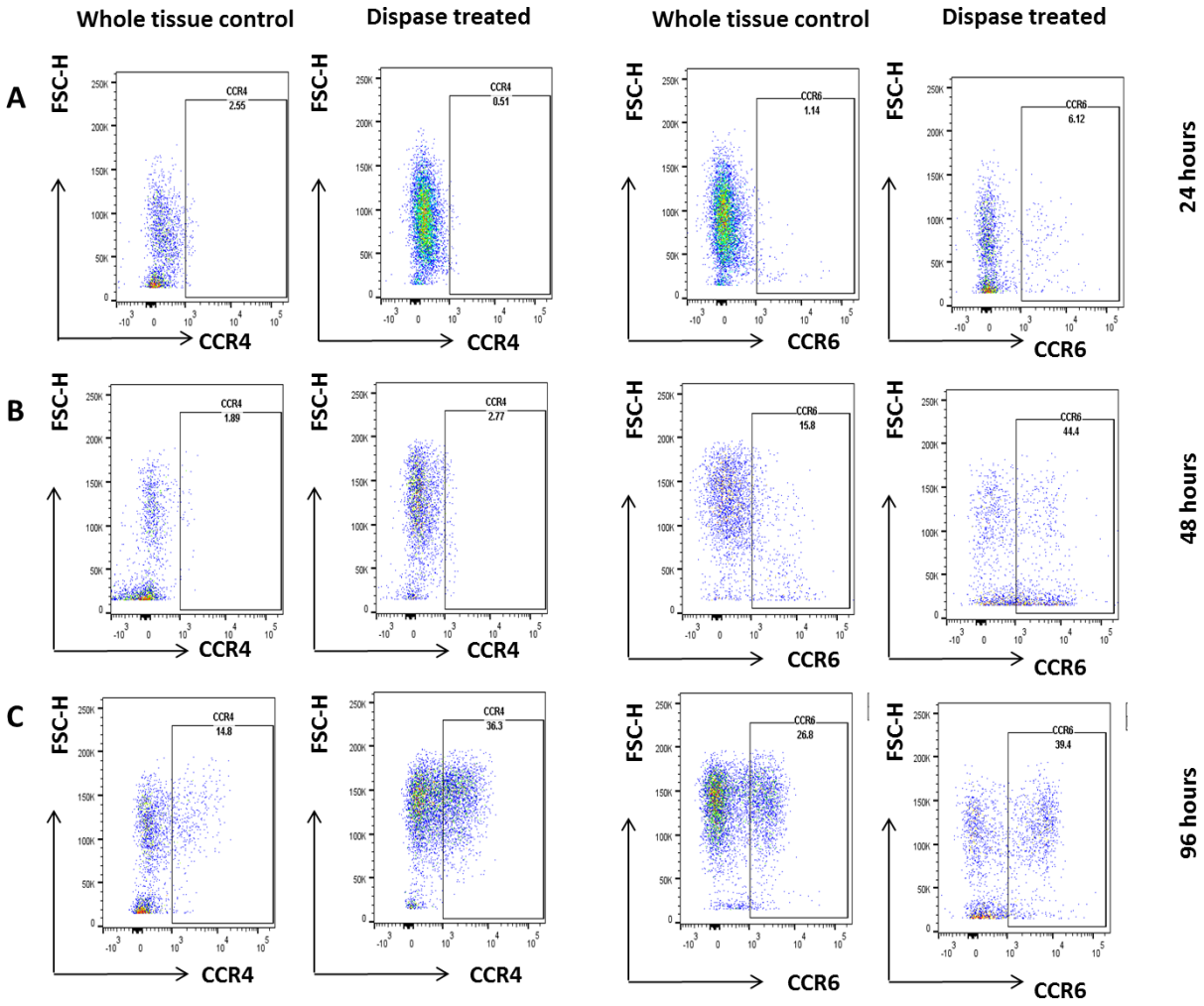

Figure 4.14: Representative flow plots of difference in CCR4+ and CCR6+ cell proportions in Whole tissue controls and Dispase treated tissues in three time points. A) CCR4+ and CCR6+ cell proportions in Whole tissue controls and Dispase treated tissues after 24 hours. B) CCR4+ and CCR6+ cell proportions in Whole tissue controls and Dispase treated tissues after 48 hours. C) CCR4+ and CCR6+ cell proportions in Whole tissue controls and Dispase treated tissues after 96 hours.

Table 4.3: Number of events of CD45+, CCR4+ and CCR6+ cells in 2 pooled (inner and outer foreskin samples) in whole tissue controls and Dispase treated samples.

Number of events / Population		24 hours		48 hours		96 hours	
		WT controls	Dispase treated	WT controls	Dispase treated	WT controls	Dispase treated
CD45+	1st sample	4938	9026	261	1208	2174	195
	2nd sample	2076	9026	1799	2712	2441	5786
CCR4+	1st sample	512	234	31	39	469	53
	2nd sample	53	36	34	75	362	2100
CCR6+	1st sample	1377	100	193	253	1406	64
	2nd sample	127	80	798	428	962	1548

Figure 4.15 shows the differences in the frequencies of lymphocytes expressing CD45, CCR4 and CCR6 in three different time point after 18 hours of exposure to either HBSS in whole tissue control samples or Dispase treated samples. The median frequency of CD45+ lymphocytes in whole tissue controls was low (4.07%, IQR: 2.65-5.49) compared to Dispase treated samples (9.62%, 7.44-11.80) at 24 hours (Figure 4.15a). The percentage of CD45 in whole tissue samples became even lower after 48 hours with a frequency of 0.75% (IQR:0.25-1.25) in whole tissue controls compared to 3.35% (IQR:2.17-4.52). After 96 hours, results are conflicted between the two samples tested (median frequency is 7.69%, IQR: 6.29-9.09 in whole tissue controls compared to 8.70%, IQR: 0.91-16.50). From that, it is not possible to see a specific trend regarding a negative impact of Dispase treatment or time on CD45 marker.

However, Dispase treated samples were seen to have considerably lower frequencies of CCR4+ cells compared to the whole tissue controls after 24 hours and 48 hours (Figure 4.15b). Median frequency of CCR6+ cells was 6.48% (IQR:2.55-10.40) in whole tissue samples compared to 1.32% (IQR:0.05-2.59) in Dispase treated samples after 24 hours. It showed a median frequency of 6.89% (IQR:1.89-11.90) in whole tissue samples compared to 3% (IQR: 2.77-3.23) in Dispase treated samples after 48 hours. This seems to change after 96 hours where CCR4+ cells seem to have a median frequency 18.20% (IQR: 14.80-21.60) in whole tissue controls compared to 31.75% (IQR: 27.20-36.30) in Dispase treated samples.

Dispase treated samples appear to have lower frequencies of CCR6+ cells compared to whole tissue samples in all the three time points (Figure 4.15c). Dispase treated samples were seen to have considerably lower frequencies of CCR6+ cells compared to the whole tissue controls after 24 hours with a median frequency of 17.01% (IQR:6.12-27.90) in whole

tissue samples compared to 1.12% (IQR:1.11-1.14) in Dispase treated samples, a median frequency of 59.15% (IQR: 44.40-73.90) in whole tissue samples compared to 18.35% (15.80-20.90) in Dispase treated samples after 48 hours. CCR6+ cells in whole tissue control samples had a mean frequency of 52.05% (IQR:39.4-64.70) compared to 29.80% (IQR:26.80-32.80) in Dispase treated samples after 96 hours. Figure 4.15d shows significant decrease in the median frequencies of CCR6+ cells in Dispase treated samples across all time points compared to the whole tissue control samples (41.90%, IQR: 22.46-67 in whole tissue control compared to 18.35%, IQR:1.13-28.30; *p*=0.030).

It is worth noting that this experiment was conducted on 2 donors only. Hence, statistical analysis should be interpreted with caution.

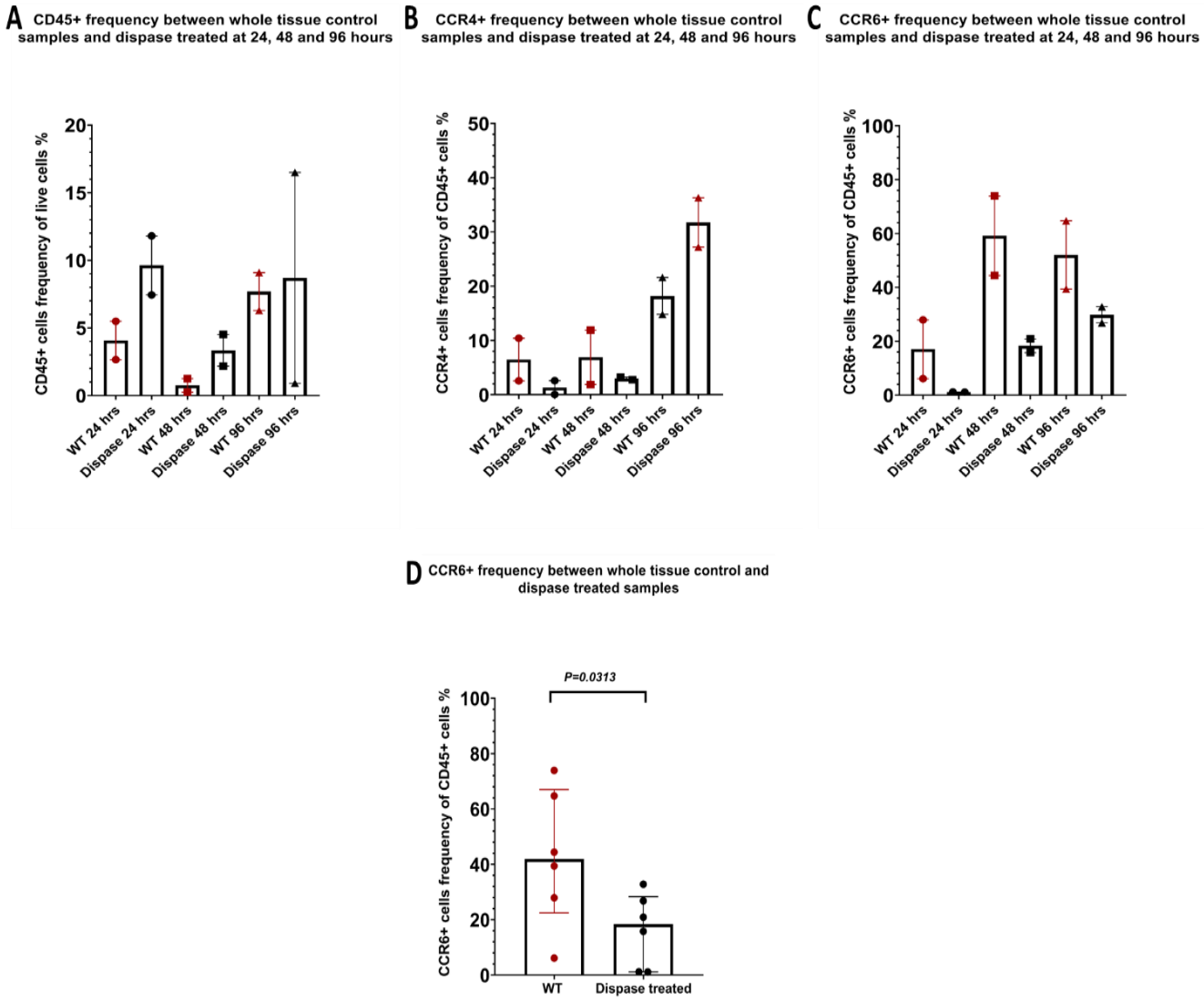

Figure 4.15: Bar graphs showing CD45+, CCR4+ and CCR6+ Frequency in Whole tissue controls and Dispase treated tissues after 24, 48 and 96 hours. A) CD45+ Frequency in Whole tissue controls and Dispase treated tissues in the three time points (n=2 for each condition). B) CCR4+ Frequency in Whole tissue controls and Dispase treated tissues in the three time points (n=2 for each condition). C) CCR6+ Frequency in Whole tissue controls and Dispase treated tissues in the three time points (n=2 for each condition). D) CCR6+ Frequency in Whole tissue controls and Dispase treated tissues with all-time points pooled together (n=6 for each condition).

4.5 Discussion

In Chapter 3, we observed a significant impact of TNFα and CCL27 on proportions of CD3+CD4+ T cells in the epithelium of the inner foreskin tissue, but not the outer. However, one limitation was the need to characterize the T cell subsets that were recruited in the inner foreskin tissue under the influence of TNFα and CCL27. Immunofluorescence imaging allowed only 4 markers to be explored. Hence, we chose flow cytometry to complement our work. We wished to explore Th17 and Th22 cells in the foreskin tissue. Th17 are a T cell subset that is abundant in the foreskin tissue compared to blood and was observed to be highly susceptible to HIV *in vitro* and preferentially depleted *in vivo* (12–14,95). Furthermore, it was observed to be two fold higher in density in the inner foreskin tissue compared to the outer foreskin (121). Th22 cells are also highly susceptible to HIV and expresses CCR10 which is the chemokine receptor for CCL27. This chapter aimed at reproducing these results using multi-parameter flow cytometry to measure the impact of TNFα and CCL27 on specific Th17 and Th22 cell populations and marker expression in both the epidermis and dermis of the foreskin tissue. We stimulated the foreskin tissue and then used two different methods to liberate the cells: spontaneous migration from whole tissue sections and digestion with Dispase then spontaneously migrating cells from separate epidermal sheets and dermal tissue. The experiments were aiming at using multi-parameter flow cytometry in observing the impact on a cellular level and marker expression in both epidermis and dermis tissues of the inner and outer foreskin. It also aimed at validating that CCL27 caused recruitment of CD4+ T cells in the inner foreskin tissue, and that our results were not caused by a modulation of marker expression in the foreskin tissue due to chemokine exposure. However, optimizing the best experimental design that allows that had many limitations. The use of digesting enzymes such as Dispase and Liberase along with long *in vitro* culturing time might have resulted in less expression of certain markers on the foreskin cells and lower cell yields which resulted in limitations and affected the results. The lower cell yield did not allow viewing the changes occurring on cellular levels in the foreskin tissue whether on a cell number or Mean fluorescence intensity under the exposure to TNFα and CCL27 (section 4.3). The experiments required more optimization to provide higher cell yield that allows investigating impact of TNFα and CCL27 on cell frequencies and marker expression.

No significant difference was viewed in the number of Th17 or Th22 cells in cells spontaneously migrating from whole foreskin tissues under the influence of TNFα or CCL27 compared to the untreated tissues (section 4.4.1). There was also no significant change in the Mean fluorescence intensity of each marker of cells from whole tissues exposed to the chemokines compared to the untreated tissues (section 4.4.2). Even though there is limited data in the experiment conducted, we view that marker expression did not undergo any significant changes due to chemokine exposure. Therefore, linking this with chapter 3, we view that chemokines caused the recruitment of the CD3+CD4+ increase in numbers of cells. This showed that the chemokines might not have an impact on the number or expression of different T cell subsets that spontaneously migrate out of the foreskin tissue and their effect was on recruitment of the cells to the epithelium of the inner foreskin which was viewed in chapter 3 using immunofluorescence imaging. However, low sample size used in the experiment (4 samples) and the low cell yield across the experiments was a major limitation.

After exposing the tissues to the chemokines then Dispase then allowing them to spontaneously migrate into the R10 media, spontaneously migrated cells after exposure to chemokines and Dispase had a prominent decrease in the number of CD45+, CCR4+ and CCR6+ cells compared to the whole tissue samples from the same donors (section 4.5). This needed further investigation to understand what incited the change in the cells. We hypothesized that it could be due to one or both the following reasons: enzymes (Dispase) and/or prolonged experimental conditions. We inspected the effect of Dispase treatment on the foreskin derived cells in 2 foreskin samples and viewed that Dispase had a negative effect on CCR4 and CCR6 markers even after resting the cells for 24 hours before staining. There was a significant decrease in the number of CCR6 cells in Dispase treated cells compared to the control samples. That impact was not reversible after 96 hours of culturing in R10 media. In CCR4, there was also a trend showing decrease in the number of cells in Dispase treated tissue compared to control samples. However, the decrease was reversible after 96 hours of culturing. Meanwhile, there was no significant difference in CD45 levels between Dispase treated samples compared to controls. This might indicate that the depletion of CD45 marker occurring after exposure to chemokines, Dispase and then culturing might be due to other mechanisms. Literature has discussed the effect of Dispase on marker expression and mentioned that Dispase decreased lymphocytes and macrophages cell surface marker expression including CD45, CD69, CD3, CD4, CD11C and CD14 (215,216). However, CD3, CD4 and CD45 had no changes under lower levels of Dispase (0.8 U/ml) while CD4 was only affected by high concentrations of Dispase (50 U/ml) and cells regained marker expression of the other affected markers after culturing for 24 hours (215). Other publications mentioned CD4 being affected in blood, foreskin tissue and mice skin by exposure to Dispase (95,217) However, CCR4 and CCR6 were not discussed in literature. Our results indicate the need to explore the effect of Dispase on T cells marker to view the impact it has as well as the reversibility of that effect on them after resting. The low sample size and low cell yield have also been a limitation to this experiment. The experiments in this chapter, though carefully designed, had affected the foreskin cells greatly; foreskin cells might have been affected by enzyme exposure and long *in vitro* culturing time after 84 hours of chemokine exposure which might have caused cell death and that resulted in low cell yield and further on caused CD45, CCR4 and CCR6 marker loss.

Another plausible mechanism in CD45 marker loss was the impact of TNFα exposure on immune activation and proliferation of naïve T cells and apoptosis to highly activated effector T cells. This might explain the decreased number of T cells in the TNFα exposed foreskin tissues (218–220). However, it does not explain the same impact occurring in both CCL27 treated tissues and controls cultured in R10 only. In summary, we showed the different results from different experiment design to show the impact of TNFα and CCL27 on frequencies of T cells in the foreskin tissue. We also showed a significant decrease in number of CCR6+ cells in Dispase treated samples compared to whole tissue controls and observed a decrease in CCR4+ cells. These results suggest that despite the optimization of the experiments design, flow cytometry had many limitations in measuring the recruitment of T

cells in the foreskin tissue. It suggests that immunofluorescence imaging is the most optimal method to measure recruitment of T cells in the foreskin tissue.

Chapter 5: Discussion and conclusion

This dissertation sheds light on the association between a chemokine (CCL27), putatively secreted by keratinocytes in the foreskin tissue, and the recruitment of CD4+ T cells to the epithelium of the inner foreskin. We also compared two different methods for counting cells using immunofluorescence (IF) imaging and flow cytometry. These findings support our findings included in our publication demonstrating the impact of CCL27 on increased density of CD4+ T cells in the inner but not the outer foreskin (91).

Male medical circumcision (MMC) has been proven to decrease HIV-1 acquisition by 52-64% (35,36,126) and that is why it has been rolled out by WHO and UNAIDS as a method for HIV prevention (33,34). However, a better understanding of HIV transmission and acquisition in men is still required. MMC involves the surgical removal of more than 95% of the foreskin tissue that is rich in HIV target cells including T cells, LCs and macrophages. This is postulated to be one of the plausible mechanisms responsible for the observed impact of MMC in decreasing HIV acquisition (8,9,90). The foreskin tissue was observed to play an essential role in HIV acquisition specially the inner foreskin, which has been observed by many studies to have higher susceptibility to HIV infection compared to the outer foreskin (25,90,119,120,194). Furthermore, It was observed that the foreskin tissue caused dysbiosis in the skin microbiome compromising skin's barrier integrity and increasing susceptibility to HIV infection through enrichment of bacteria correlated with secretion of proinflammatory chemokines (27–29,31,32). MMC also provides protection against STIs such as HPV and HSV-2 which also contributes in the decrease of HIV acquisition (51,52,161). Other mechanisms that were discussed as potential factors in the susceptibility of the foreskin tissue were the large surface area (26) and the thinner keratinization in the inner foreskin tissue compared to the outer foreskin tissue (27,91,92,94,221,222). HIV target cells inhabiting the foreskin tissue include CD4+ T cell subsets which express the markers CD4 and CCR5, considered pivotal for productive HIV infection, along with a range of proinflammatory chemokines and cytokines such as IL-17, IL-22, TNFα and IFNγ (8,89,95). Other penile sites including the urethra have also been proposed as targets for infection, which explains the approximate 40% incomplete protection of MMC against HIV infection (102,198).

In a recent publication, it was shown that there was a notable difference in the expression levels of chemokine genes in the inner and outer foreskin tissues. Significant upregulation of

CCL27, CXCL12, TLR4 and CCL28 genes was noticed in the inner foreskin compared to the outer foreskin (91); CCL27 was approximately 7-fold more elevated in the inner foreskin compared to the outer foreskin tissue (91). This was associated with another observation that the inner foreskin tissue contained a higher proportion of CD4+CCR5+ T cells, known to be HIV target cells, compared to the outer foreskin (77,78,91,223). We hypothesized that CCL27 protein pronounced expression mediated the recruitment of CD4+ T cells in the epithelium of the inner foreskin tissue and that CCL27 exogenous exposure will have an impact on the increase in the number of CD3+CD4+ T cells in the epithelium of the foreskin tissue. In chapter 3 of this dissertation, we viewed the changes occurring on a tissue level in the foreskin under the influence of exogenous exposure to CCL27 using IF imaging and showed that exogenous exposure to CCL27 resulted in a significant rise in the densities of CD3+CD4+ T cells in the epithelium of the inner foreskin tissue while it caused no significant difference in the CD3+CD4+ T cells in the epithelium of the outer foreskin. This is a key finding in identifying the higher susceptibility of potential HIV infection of the inner foreskin compared to the outer foreskin. Our results also showed that in the untreated foreskin tissues, the median density of CD3+CD4+ T cells in the epithelium of the inner foreskin tissue was higher compared to the outer foreskin tissue. This suggests that the difference in the inflammatory environment and differences in chemokine production between the inner and outer foreskin tissues might cause recruitment of CD4+ T cells in the epithelium of the inner foreskin compared to the outer.

CCL27 expression in skin induces homing of memory T cells and also Langerhans cells that express the ligand for CCL27, CCR10 (191,192). Recruitment of LCs and T cells is essential for an efficient HIV entry since HIV forms viral synapses that infects Langerhans-T cells conjugates (25). That provided clues of the decrease in HIV acquisition in men who undergo MMC due to the removal of the foreskin tissue rich in LCs and T cells. A separate study also highlighted that CCL27 high expression was involved in the movement of CD4+CCR10+ T cells in the skin of individuals with inflamed skin diseases (224). This implies that CCR10 has a role in controlling effector T cells migration under inflammatory conditions (224,225). Furthermore, CCL27 was strongly expressed in the adult epidermal cells in the basal Keratinocytes and the stratum corneum (226). This might be an indication that the inner foreskin tissue's production and secretion of high CCL27 concentrations result in an influx of

CD4+ T cells in the inner foreskin, forming an environment that is possibly more prone to both STIs and HIV infection.

Notably, CCR10 is the marker prominently expressed by most Th22 cells. Th22 cells have been identified as a newly discovered HIV target cell due to their expression of CD4 and CCR5 along with pro inflammatory cytokines IL-22 and TNFα (121,190,227,228). It is suggested that the cells that were observed to be recruited in the epithelium of the inner foreskin tissue under the influence of CCL27 might be Th22 which have been identified as HIV target cells (191,227). This is consistent with data showing that CCR10 was mainly expressed on circulating skin homing CD4+ T cells while circulating CD8+ T cells had minor levels of CCR10 (224). The interaction between CCL27 and CCR10 promotes migration of skin homing T cells of the memory type (195,201,224). However, from our experiments, we were unable to confirm that the cells recruited in the epithelium of the inner foreskin were Th22 cells and therefore further investigations are required to test this hypothesis. It is plausible that other unexplored mechanisms are involved, probably in a synergistic manner with CCL27, in the recruitment of different CD4+ T cells subsets and that other inflammatory cytokines and chemokines in the inner foreskin are related to the higher susceptibility to HIV infection (31,91,121).

Chemokines in the foreskin tissue were reported to have a pivotal role in the inflammation of foreskin tissue and increase in HIV acquisition. In 60% of coronal sulcus swabs of males undergoing circumcision, IL-8 was detected. In 25% of swabs, Monokine Induced by γ-interferon (MIG) was detected (31). Other cytokines (IL-1a, MCP-1, RANTES, GM-CSF and MIP3α) were detected in 10% of participants. This prevalence of cytokines was not related to sexual behavior or demographics but was connected to STI symptomatic infections (31). IL-8 levels were noticed to significantly decrease after MMC compared to the control group that didn't undergo circumcision. Furthermore, the seroconversion rates increased when more than one of the cytokines were detected in the coronal sulcus swabs in the control group (31). IL-8 and MIG were specifically correlated with higher HIV acquisition in males. Circumcision was reported to decrease IL-8 levels significantly which would decrease HIV acquisition. IL-8 and MIG are pro-inflammatory cytokines with a function of recruitment of immune cells to inflamed tissues (31). This is consistent with our results regarding the impact of CCL27 on the recruitment of CD4+ T cells in the epithelium of the inner foreskin tissue. It highlights that other chemokines and cytokines are also involved in the process of

CD4+ T cell recruitment that might increases HIV susceptibility and that the presence of CCL27 could enhance the effect of these chemokines and/or cytokines.

Although MMC was reported to decrease the rate of HIV acquisition by 60%, there still remains other target sites in the male genital tract that facilitate HIV infection including the glans penis and the urethra (102,198). All penile regions (penis glans, urethra and fossa) were also seen to be able to produce pro-inflammatory and anti-inflammatory cytokines such as IL-17 and IL-22 and other important intermediaries in the infection process (108). Multiple cytokines were found in the urethra, fossa and glans of the penis (108). IFN-γ-secreting cells, CD4+ cells expressing both IL-4 and IL-5 were detected in the three tissues and to a lesser extent TNFα secreting cells and IL-2 secreting cells (108). In the other penile tissues (glans penis, fossa and urethra), proportions of IL-17 and IL-22 were considerably lower than in the inner or the outer foreskin tissue (108). Urethra, fossa and glans have a wide range of cytokines including CCL28, RANTES and IL-13 which are very predominant in the urethra and TRAIL, MCP-1 and CCL25 in intermediate concentrations and IL-4, MIP-3α, MCP-4 and Etoaxin in low levels (121). In fossa and glans IL-13, IL-4, MIP-3α, CCL25 and TRAIL were detected at concentrations equivalent to the urethra while CCL28 and RANTES were significantly lower than that detected in the urethra (121).

Limitations of our findings were that CCR5, CCR10 markers staining along with the CD3 and CD4 was required to further characterize the CD4+ T cells recruited in the epidermis of the inner foreskin under the influence of CCL27. It also might have been beneficial to stain for Langerhans cells markers to understand the impact of CCL27 on LCs which are essential in the infection process due to their HIV susceptibility and formation of viral synapses. Another limitation was the small sample size compared in the outer foreskin tissue. This affected the ability to have a conclusive finding regarding the impact of CCL27 on the outer foreskin tissue.

We also explored different methods of counting cells in Chapter 3. We compared two different methods of counting dually labeled cells: manual method of counting cells perceived as dually labeled (CD3+ and CD4+) on the Softworx software and analyzing the results using IDL (Interactive Data Language) and a semi-automated counting using ImageJ and PIPSQUEAK AI to automatically detect the single labeled cells in both FITC and CY5 channels and then merge them to detect and count the dually labeled cells. We created correlation plots and difference plots to view the alignment and differences between the

two methods of counting. From these results, we could determine that at some instances the manual counting was overestimating cell numbers compared to the semi-automated counting while in others it was underestimating cell numbers. Despite the differences between the two counting, there was no conclusive way to highlight which method was less biased and more reliable in counting the double labeled cells in the foreskin tissue. One limitation is that both methods of counting required visual inspection by two or more people to decrease subjectivity of the comparison. Both methods included manual verification of the cell numbers which can lead to bias. To minimize bias, the samples conditions were blinded to the personnel preforming the counting. Altogether, we suggest that one method is used consistently in the counting to decrease discrepancies across experiments. Finally, we have shown a trend of CD4+CD3- cells increasing in the epithelium of the foreskin tissue under the impact of TNFα and CCL27, albeit insignificant. The CD4+CD3- cells might possibly be Langerhans cells or macrophages which reside in the foreskin tissue and also have a role in HIV infection (127,195).

In chapter 4, we used flow cytometry to optimize experiments to measure the impact of TNFα and CCL27 on T cell subsets including Th17 and Th22 to compliment the imaging data. Limitations to using flow cytometry to characterize these cells under the influence of TNFα and CCL27 were numerous including the use of enzymes that affected the cells viability and yield, hence the low number of events acquired. Another limitation was prolonged *in vitro* culturing time and addition of chemokines that might have caused the marker expression in the foreskin tissue to significantly decrease or promote apoptosis. Future experiments would require further optimization of experiment optimal culturing time to improve cell yields to allow for conclusive results. We also explored the impact of TNFα and CCL27 on cells spontaneously migrating from whole foreskin tissue samples (no digestive enzymes were used). There was no significant difference in the density or mean fluorescence intensity of markers in cells spontaneously migrating from whole foreskin tissues between unstimulated cells and TNFα and CCL27 exposed cells. This indicates that the chemokines might not have an impact on either subset of cells spontaneously migrating from the foreskin tissue or the markers that were used to enumerate the cells. We also observed the effect of Dispase treatment on CCR4 and CCR6 markers in the foreskin tissue and how they are affected by Dispase even after resting of cells. There was a trend in CCR4 being affected by Dispase treatment while CCR6 had a significant change that was not reversible compared to the

control samples. Dispase was previously reported to affect lymphocytes and macrophages cell surface markers although no study has reported the impact of Dispase on CCR4 and CCR6 expression and detection (216,217). The small sample size analysed in this experiment was a limitation in having conclusive results regarding how Dispase affected marker expression. We suggest more exhaustive optimization to determine the effect of digestive enzymes on T cells and myeloid cells markers.

In conclusion, this dissertation shows that exogenous exposure of inner foreskin tissue to CCL27 significantly increased the number of CD3+CD4+ T cells in the epithelium compared to untreated tissues. while the outer foreskin had no significant changes in the number of CD3+CD4+ T cells in the epithelium. Furthermore, we evaluated the differences between manual and semi-automated counting of cells in the foreskin tissue. Finally, we attempted to understand the effect of Dispase and prolonged experiments on the number and marker expression of T cells. Overall, this dissertation highlights that the higher expression of CCL27 in the inner foreskin tissue contributes to the higher number of HIV target cells that are in proximity to the outermost layer of the tissue. Ultimately this provides mechanistic insight into the protective mechanism of MMC.

References:

1. Morris BJ, Wamai RG, Henebeng EB, Tobian AAR, Klausner JD, Banerjee J, et al. Estimation of country-specific and global prevalence of male circumcision. Popul Health Metr. 2016;14:4.
2. UNAIDS. Male circumcision: global trends and determinants of prevalence, safety and acceptability. 2007;
3. David A. Bolnick, Martin Koyle AY. Surgical Guide to Circumcision. 2012.
4. Aggleton P. Roundtable: "Just a Snip"?: A Social History of Male Circumcision. Reprod Health Matters. 2007;15(29):15–21.
5. Dunsmuir WD, Gordon EM. The history of circumcision. BJU Int Suppl. 1999;83(S1):1–12.
6. Brown MS, Brown CA. Circumcision decision: Prominence of social concerns. Pediatrics. 1987;80(2):215–9.
7. Westercamp N, Bailey RC. Acceptability of male circumcision for prevention of HIV/AIDS in sub-Saharan Africa: A review. AIDS Behav. 2007;4(11):e7687.
8. Johnson KE, Sherman ME, Ssempiija V, Tobian AAR, Zenilman JM, Duggan MA, et al. Foreskin inflammation is associated with HIV and herpes simplex virus type-2 infections in Rakai, Uganda. Aids. 2009;23(14):1807–15.
9. Hussain LA, Lehner T. Comparative investigation of Langerhans' cells and potential receptors for HIV in oral, genitourinary and rectal epithelia. Immunology. 1995;85(3):475–84.
10. Blauvelt A, Asada H, Saville MW, Klaus-Kovtun V, Altman DJ, Yarchoan R, et al. Productive infection of dendritic cells by HIV-1 and their ability to capture virus are mediated through separate pathways. J Clin Invest. 1997 Oct 15;100(8):2043–53.
11. Zaitseva M, Blauvelt A, Lee S, Lapham CK, Klaus-Kovtun V, Mostowski H, et al. Expression and function of CCR5 and CXCR4 on human Langerhans cells and macrophages: Implications for HIV primary infection. Nat Med. 1997 Dec;3(12):1369–75.
12. Alvarez Y, Tuen M, Shen G, Nawaz F, Arthos J, Wolff MJ, et al. Preferential HIV Infection of CCR6+ Th17 Cells Is Associated with Higher Levels of Virus Receptor Expression and Lack of CCR5 Ligands. J Virol. 2013;87(19):10843–54.
13. El Hed A, Khaitan A, Kozhaya L, Manel N, Daskalakis D, Borkowsky W, et al. Susceptibility of Human Th17 Cells to Human Immunodeficiency Virus and Their Perturbation during Infection. J Infect Dis. 2010;201(6):843–54.
14. Gosselin A, Monteiro P, Chomont N, Diaz-Griffero F, Said EA, Fonseca S, et al. Peripheral Blood CCR4 + CCR6 + and CXCR3 + CCR6 + CD4 + T Cells Are Highly Permissive to HIV-1 Infection. J Immunol. 2010;184(3):1604–16.
15. Wein AJ, Kavoussi LR, Novick AC, Partin AW, Peters C a. Campbell-Walsh Urology 10th Edition. Campbell-Walsh Urology. 2012.
16. Waller DP, Nikurs AR. Review of the Physiology and Biochemistry of the Male Reproductive Tract. Int J Toxicol. 1986;5(4):209–23.

17. Creasy DM, Chapin RE. Male Reproductive System. In: Fundamentals of Toxicologic Pathology: Third Edition. 2018.

18. Sam P, LaGrange CA. Anatomy, Abdomen and Pelvis, Penis. 2018.

19. Prodger JL, Kaul R. The biology of how circumcision reduces HIV susceptibility: Broader implications for the prevention field. AIDS Res Ther. 2017;14(1):1–5.

20. Dinh MH, Anderson MR, McRaven MD, Cianci GC, McCoombe SG, Kelley ZL, et al. Visualization of HIV-1 Interactions with Penile and Foreskin Epithelia: Clues for Female-to-Male HIV Transmission. PLoS Pathog. 2015;11(3):1–20.

21. Penile Anatomy-Detailed: Image Details - NCI Visuals Online [Internet]. 2017. Available from: https://visualsonline.cancer.gov/details.cfm?imageid=11321

22. Jayathunge PH., McBride WJ., MacLaren D, Kaldor J, Vallely A, Turville S. Male Circumcision and HIV Transmission; What Do We Know? Open AIDS J. 2014;8(1):31–44.

23. Fahrbach KM, Barry SM, Anderson MR, Hope TJ. Enhanced cellular responses and environmental sampling within inner foreskin explants: Implications for the foreskin's role in HIV transmission. Mucosal Immunol. 2010;3:410–418.

24. Patterson BK, Landay A, Siegel JN, Flener Z, Pessis D, Chaviano A, et al. Susceptibility to human immunodeficiency virus-1 infection of human foreskin and cervical tissue grown in explant culture. Am J Pathol. 2002;161(3):867–73.

25. Ganor Y, Zhou Z, Tudor D, Schmitt A, Vacher-Lavenu MC, Gibault L, et al. Within 1 h, HIV-1 uses viral synapses to enter efficiently the inner, but not outer, foreskin mucosa and engages Langerhans-T cell conjugates. Mucosal Immunol. 2010;3(5):506–22.

26. Kigozi G, Wawer M, Ssettuba A, Kagaayi J, Nalugoda F, Watya S, et al. Foreskin surface area and HIV acquisition in Rakai, Uganda (size matters). AIDS. 2009;23(16):2209–13.

27. Dinh MH, McRaven MD, Kelley ZL, Penugonda S, Hope TJ. Keratinization of the adult male foreskin and implications for male circumcision. AIDS. 2010;24(6):899–906.

28. Price LB, Liu CM, Johnson KE, Aziz M, Lau MK, Bowers J, et al. The effects of circumcision on the penis microbiome. PLoS One. 2010;5(1):e8422.

29. Nelson DE, Dong Q, van der Pol B, Toh E, Fan B, Katz BP, et al. Bacterial communities of the coronal sulcus and distal urethra of adolescent males. PLoS One. 2012;7(5):e36298.

30. Liu CM, Prodger JL, Tobian AAR, Abraham AG, Kigozi G, Hungate BA, et al. Penile anaerobic dysbiosis as a risk factor for HIV infection. MBio. 2017;8(4):1–10.

31. Prodger JL, Gray RH, Shannon B, Shahabi K, Kong X, Grabowski K, et al. Chemokine Levels in the Penile Coronal Sulcus Correlate with HIV-1 Acquisition and Are Reduced by Male Circumcision in Rakai, Uganda. PLoS Pathog. 2016;12(11):1–21.

32. Liu CM, Hungate BA, Tobian AAR, Serwadda D, Ravel J, Lester R, et al. Male circumcision significantly reduces prevalence and load of genital anaerobic bacteria. MBio. 2013;4(2):e00076.

33. UNAIDS. Safe, voluntary, informed male circumcision and comprehensive HIV prevention: guidance for decision-makers on human rights, ethical and legal

considerations. 2009. p. 1–40.

34. WHO, UNAIDS. New Data on Male Circumcision and HIV Prevention : Policy and Programme Implications. WHO Press. 2007;1–10.

35. Auvert B, Taljaard D, Lagarde E, Sobngwi-Tambekou J, Sitta R, Puren A. Randomized, controlled intervention trial of male circumcision for reduction of HIV infection risk: The ANRS 1265 trial. PLoS Med. 2005;2(11):e298.

36. Gray RH, Kigozi G, Serwadda D, Makumbi F, Watya S, Nalugoda F, et al. Male circumcision for HIV prevention in men in Rakai, Uganda: a randomised trial. Lancet. 2007;369(9562):657–66.

37. Bailey RC, Moses S, Parker CB, Agot K, Maclean I, Krieger JN, et al. Male circumcision for HIV prevention in young men in Kisumu, Kenya: a randomised controlled trial. Lancet. 2007;369(9562):643–56.

38. WHO. VOLUNTARY MEDICAL MALE CIRCUMCISION FOR HIV PREVENTION Men making a difference for HIV prevention. 2018. p. 1–2.

39. UNAIDS. Voluntary medical male circumcision: Remarkable progress in the scale-up of volontary medical male circumcision as a HIV prevention intervention in 15 eastern and southern African countries. 2019.

40. Wawer MJ, Makumbi F, Kigozi G, Serwadda D, Watya S, Nalugoda F, et al. Circumcision in HIV-infected men and its effect on HIV transmission to female partners in Rakai, Uganda: a randomised controlled trial. Lancet. 2009;374(9685):229–237.

41. Tobian AAR, Adamu T, Reed JB, Kiggundu V, Yazdi Y, Njeuhmeli E. Voluntary medical male circumcision in resource-constrained settings. Nat Rev Urol. 2015;12:661–670.

42. Silverman EK. Anthropology and circumcision. Annu Rev Anthropol. 2004;33:419–45.

43. Drain PK, Halperin DT, Hughes JP, Klausner JD, Bailey RC. Male circumcision, religion, and infectious diseases: An ecologic analysis of 118 developing countries. BMC Infect Dis. 2006;6:172.

44. Wilcken A, Keil T, Dick B. Traditional male circumcision in eastern and southern Africa: A systematic review of prevalence and complications. Bull World Health Organ. 2010;88(12):907–914.

45. Douglas M, Maluleke TX. Traditional Male Circumcision: Ways to Prevent Deaths Due to Dehydration. Am J Mens Health. 2018;12(3):584–593.

46. Vincent L. Cutting tradition: The political regulation of traditional circumcision rites in South Africa's liberal democratic order. J South Afr Stud. 2008;34(1):77–91.

47. World Health Organization. Male Circumcision Policy , Practices and Services in the Eastern Cape Province of South Africa Case Study. 2008. p. 1–45.

48. Peltzer K, Nqeketo A, Petros G, Kanta X. Traditional circumcision during manhood initiation rituals in the Eastern Cape, South Africa: A pre-post intervention evaluation. BMC Public Health. 2008;8:64.

49. Bailey RC, Egesah O, Rosenberg S. Male circumcision for HIV prevention: A prospective study of complications in clinical and traditional settings in Bungoma, Kenya. Bull

World Health Organ. 2008;86(9):669–77.

50. Johnson KE, Redd AD, Quinn TC, Collinson-Streng AN, Cornish T, Kong X, et al. Effects of HIV-1 and herpes simplex virus type 2 infection on lymphocyte and dendritic cell density in adult foreskins from Rakai, Uganda. J Infect Dis. 2011;203(5):602–9.

51. Tobian AAR, Serwadda D, Quinn TC, Kigozi G, Gravitt PE, Laeyendecker O, et al. Male circumcision for the prevention of HSV-2 and HPV infections and syphilis. N Engl J Med. 2009;360:1298–309.

52. Gray RH, Serwadda D, Kong X, Makumbi F, Kigozi G, Gravitt PE, et al. Male Circumcision Decreases Acquisition and Increases Clearance of High-Risk Human Papillomavirus in HIV-Negative Men: A Randomized Trial in Rakai, Uganda. J Infect Dis. 2010;201(10):1455–62.

53. Joelle ST, Taljaard D, Lissouba P, Zarca K, Puren A, Lagarde E, et al. Effect of HSV-2 serostatus on acquisition of HIV by young men: Results of a longitudinal study in orange farm, South Africa. J Infect Dis. 2009 Apr 1;199(7):958–64.

54. Gray RH, Kigozi G, Serwadda D, Makumbi F, Nalugoda F, Watya S, et al. The effects of male circumcision on female partners' genital tract symptoms and vaginal infections in a randomized trial in Rakai, Uganda. Am J Obstet Gynecol. 2009;200(1):42.e1-7.

55. Wawer MJ, Tobian AA, Kigozi G, Kong X, Gravitt PE, Serwadda D, et al. Effect of circumcision of HIV-negative men on transmission of human papillomavirus to HIV-negative women: A randomised trial in Rakai, Uganda. Lancet. 2011;377(9761):209–18.

56. Castellsagué X, Bosch FX, Muñoz N, Meijer CJLM, Shah K V., de Sanjosé S, et al. Male Circumcision, Penile Human Papillomavirus Infection, and Cervical Cancer in Female Partners. N Engl J Med. 2002 Apr 11;346(15):1105–12.

57. Sobngwi-Tambekou J, Taljaard D, Nieuwoudt M, Lissouba P, Puren A, Auvert B. Male circumcision and Neisseria gonorrhoeae, Chlamydia trachomatis and Trichomonas vaginalis: Observations after a randomised controlled trial for HIV prevention. Sex Transm Infect. 2009;85(2):116–120.

58. Auvert B, Sobngwi-Tambekou J, Cutler E, Nieuwoudt M, Lissouba P, Puren A, et al. Effect of male circumcision on the prevalence of high-risk human papillomavirus in young men: Results of a randomized controlled trial conducted in orange farm, South Africa. J Infect Dis. 2009;199(1):14–9.

59. Mehta SD, Gaydos C, MacLean I, Odoyo-June E, Moses S, Agunda L, et al. The effect of medical male circumcision on urogenital mycoplasma genitalium among men in Kisumu, Kenya. Sex Transm Dis. 2012 Apr;39(4):276–80.

60. Tobian AAR, Gaydos C, Gray RH, Kigozi G, Serwadda D, Quinn N, et al. Male circumcision and mycoplasma genitalium infection in female partners: A randomised trial in rakai, uganda. Sex Transm Infect. 2014;90(2):150–4.

61. Gray RH, Serwadda D, Tobian AAR, Chen MZ, Makumbi F, Suntoke T, et al. Effects of genital ulcer disease and herpes simplex virus type 2 on the efficacy of male circumcision for HIV prevention: Analyses from the Rakai trials. PLoS Med. 2009 Nov;6(11):e1000187.

62. Marx JL. Strong new candidate for AIDS agent. Science (80-). 1984 May 4;224(4648):475–7.

63. Case K. Nomenclature: Human immunodeficiency virus. Ann Intern Med. 1986;105(1):133.

64. UNAIDS. Global HIV & AIDS statistics — Fact sheet | UNAIDS [Internet]. UNAIDS 2021 epidemiological estimates. 2021. Available from: https://www.unaids.org/en/resources/fact-sheet

65. UNAIDS 2019. Joint United Nations Programme on HIV/AIDS (UNAIDS). 2019.

66. UNAIDS 2017. Program HIV/AIDS. 2017;1–248.

67. UNAIDS 90-90-90. to help end the AIDS epidemic. 2017.

68. UNAIDS data 2020 | UNAIDS [Internet]. 2020. Available from: https://www.unaids.org/en/resources/documents/2020/unaids-data

69. UNAIDS. Global Aids Strategy 2021 – 2026 End Inequalities . End Aids . 2021;160.

70. Vermund SH. Global HIV epidemiology: A guide for strategies in prevention and care. Curr HIV/AIDS Rep. 2014;11(2):93–8.

71. Woods S. 2004 Report on the Global AIDS Epidemic. Vol. 291, Book. 2004. 31 p.

72. Boily MC, Baggaley RF, Wang L, Masse B, White RG, Hayes RJ, et al. Heterosexual risk of HIV-1 infection per sexual act: systematic review and meta-analysis of observational studies. Lancet Infect Dis. 2009;9(2):118–29.

73. Ramjee G, Daniels B. Women and HIV in Sub-Saharan Africa. AIDS Res Ther. 2013 Dec 13;10(1):1–9.

74. Quinn TC, Wawer MJ, Sewankambo N, Serwadda D, Li C, Wabwire-Mangen F, et al. Viral load and heterosexual transmission of human immunodeficiency virus type 1. N Engl J Med. 2000;17(10):901–10.

75. Fideli ÜS, Allen SA, Musonda R, Trask S, Hahn BH, Weiss H, et al. Virologic and immunologic determinants of heterosexual transmission of human immunodeficiency virus type 1 in Africa. AIDS Res Hum Retroviruses. 2001;17(10):901–10.

76. Seitz R. Human Immunodeficiency Virus (HIV). Transfus Med Hemotherapy. 2016;43(3):203–22.

77. Feng Y, Broder CC, Kennedy PE, Berger EA. HIV-1 entry cofactor: Functional cDNA cloning of a seven-transmembrane, G protein-coupled receptor. Science (80-). 1996;272(5263):872–7.

78. Dean M, Carrington M, Winkler C, Huttley GA, Smith MW, Allikmets R, et al. Genetic restriction of HIV-1 infection and progression to AIDS by a deletion allele of the CKR5 structural gene. Science (80-). 1996;273(5283):1856–62.

79. Bleul CC, Farzan M, Choe H, Parolin C, Clark-Lewis I, Sodroski J, et al. The lymphocyte chemoattractant SDF-1 is a ligand for LESTR/fusin and blocks HIV-1 entry. Nature. 1996;382(6594):829–33.

80. Berger EA, Murphy PM, Farber JM. Chemokine receptors as HIV-1 coreceptors: Roles in viral entry, tropism, and disease. Annu Rev Immunol. 1999 Nov 28;17:657–700.

81. Poveda E, Briz V, Quiñones-Mateu M, Soriano V. HIV tropism: Diagnostic tools and implications for disease progression and treatment with entry inhibitors. AIDS. 2006 Jun;20(10):1359–67.

82. Assessing chemokine co-receptor usage in HIV : Current Opinion in Infectious Diseases. 2005;18(1):9–15.

83. Berger EA, Doms RW, Fenyo EM, Korber BTM, Littman DR, Moore JP, et al. A new classification for HIV-1. Nature. 1998 Jan 15;391:240.

84. He J, Chen Y, Farzan M, Choe H, Ohagen A, Gartner S, et al. CCR3 and CCR5 are co-receptors for HIV-1 infection of microglia. Nature. 1997 Feb 13;385(6617):645–7.

85. Archin NM, Sung JM, Garrido C, Soriano-Sarabia N, Margolis DM. Eradicating HIV-1 infection: Seeking to clear a persistent pathogen. Nat Rev Microbiol. 2014;12(11):750–64.

86. Stein BS, Gowda SD, Lifson JD, Penhallow RC, Bensch KG, Engleman EG. pH-independent HIV entry into CD4-positive T cells via virus envelope fusion to the plasma membrane. Cell. 1987;49(5):659–68.

87. Sousa R, Chung YJ, Rose JP, Wang BC. Crystal structure of bacteriophage T7 RNA polymerase at 3.3 Å resolution. Nature. 1993;364(6438):593–9.

88. Herrera-Carrillo E, Berkhout B. Bone marrow gene therapy for HIV/AIDS. Viruses. 2015 Jul 17;7(7):3910–36.

89. Hirbod T, Bailey RC, Agot K, Moses S, Ndinya-Achola J, Murugu R, et al. Abundant expression of HIV target cells and C-type lectin receptors in the foreskin tissue of young Kenyan men. Am J Pathol. 2010;176(6):2798–2805.

90. Dinh MH, Fahrbach KM, Hope TJ. The Role of the Foreskin in Male Circumcision: An Evidence-Based Review. Am J Reprod Immunol. 2011;65(3):279–83.

91. Gray CM, O'Hagan KL, Lorenzo-Redondo R, Olivier AJ, Amu S, Chigorimbo-Murefu N, et al. Impact of chemokine C–C ligand 27, foreskin anatomy and sexually transmitted infections on HIV-1 target cell availability in adolescent South African males. Mucosal Immunol. 2019;13(1):118–27.

92. McCoombe SG, Short R V. Potential HIV-1 target cells in the human penis. AIDS. 2006;20(11):1491–500.

93. Fischetti L, Barry SM, Hope TJ, Shattock RJ. HIV-1 infection of human penile explant tissue and protection by candidate microbicides. AIDS. 2009;23(3):319–28.

94. Qin Q, Zheng XY, Wang YY, Shen HF, Sun F, Ding W. Langerhans' cell density and degree of keratinization in foreskins of Chinese preschool boys and adults. Int Urol Nephrol. 2009;41(4):747–53.

95. Prodger JL, Gray R, Kigozi G, Nalugoda F, Galiwango R, Hirbod T, et al. Foreskin T-cell subsets differ substantially from blood with respect to HIV co-receptor expression, inflammatory profile, and memory status. Mucosal Immunol. 2012;5(2):121–8.

96. De Jong MAWP, De Witte L, Oudhoff MJ, Gringhuis SI, Gallay P, Geijtenbeek TBH. TNF-α and TLR agonists increase susceptibility to HIV-1 transmission by human Langerhans cells ex vivo. J Clin Invest. 2008;118(10):3440–52.

97. Fahrbach KM, Barry SM, Ayehunie S, Lamore S, Klausner M, Hope TJ. Activated CD34-Derived Langerhans Cells Mediate Transinfection with Human Immunodeficiency Virus. J Virol. 2007;81(13):6858–68.

98. Ding J, Rapista A, Teleshova N, Mosoyan G, Jarvis GA, Klotman ME, et al. Neisseria gonorrhoeae Enhances HIV-1 Infection of Primary Resting CD4 + T Cells through TLR2 Activation. J Immunol. 2010 Mar 15;184(6):2814–24.

99. Holstein AF, Davidoff MS, Breucker H, Countouris N, Orlandini G. Different epithelia in the distal human male urethra. Cell Tissue Res. 1991 Apr;264(1):23–32.

100. Pudney J, Anderson DJ. Immunobiology of the human penile urethra. Am J Pathol. 1995;147(1):155–65.

101. Pudney J, Anderson D. Innate and acquired immunity in the human penile urethra. J Reprod Immunol. 2011 Mar;88(2):219–27.

102. Ganor Y, Zhou Z, Bodo J, Tudor D, Leibowitch J, Mathez D, et al. The adult penile urethra is a novel entry site for HIV-1 that preferentially targets resident urethral macrophages. Mucosal Immunol. 2013;6(4):776–86.

103. Shigehara K, Sasagawa T, Kawaguchi S, Kobori Y, Nakashima T, Shimamura M, et al. Prevalence of human papillomavirus infection in the urinary tract of men with urethritis. Int J Urol. 2010;17(6):563–8.

104. Srugo I, Steinberg J, Madeb R, Gershtein R, Elias I, Tal J, et al. Agents of non-gonococcal urethritis in males attending an Israeli clinic for sexually transmitted diseases. Isr Med Assoc J. 2003;5(1):24–7.

105. Bradshaw CS, Tabrizi SN, Read TRH, Garland SM, Hopkins CA, Moss LM, et al. Etiologies of nongonococcal urethritis: Bacteria, viruses, and the association with orogenital exposure. J Infect Dis. 2006 Feb 1;193(3):336–45.

106. Wagenlehner FME, Weidner W, Naber KG. Chlamydial infections in urology. World J Urol. 2006 Feb 19;24(1):4–12.

107. Ganor Y, Zhou Z, Bodo J, Tudor D, Leibowitch J, Mathez D, et al. The adult penile urethra is a novel entry site for HIV-1 that preferentially targets resident urethral macrophages. Mucosal Immunol. 2013 Jul 28;6(4):776–86.

108. Sennepin A, Real F, Duvivier M, Ganor Y, Henry S, Damotte D, et al. The human penis is a genuine immunological effector site. Front Immunol. 2017;8:1732.

109. Luckheeram RV, Zhou R, Verma AD, Xia B. CD4 +T cells: Differentiation and functions. Clin Dev Immunol. 2012;2012:925135.

110. Janeway CA Jr Walport M, et al. TP. Principles of innate and adaptive immunity - Immunobiology - NCBI Bookshelf. In: New York: Garland Science. Garland Science; 2001. p. 1–9.

111. Morris BJ, Wamai RJ. Biological basis for the protective effect conferred by male circumcision against HIV infection. Int J STD AIDS. 2012;23(3):153–9.

112. Deng HK, Liu R, Ellmeier W, Choe S, Unutmaz D, Burkhart M, et al. Identification of a major co-receptor for primary isolates of HIV-1. Nature. 1996;381(6584):661–6.

113. Dragic T, Litwin V, Allaway GP, Martin SR, Huang Y, Nagashima KA, et al. HIV-1 entry

into CD4+ cells is mediated by the chemokine receptor CC-CKR-5. Nature. 1996;381(6584):667–73.

114. Rottman JB, Ganley KP, Williams K, Wu L, Mackay CR, Ringler DJ. Cellular localization of the chemokine receptor CCR5: Correlation to cellular targets of HIV-1 infection. Am J Pathol. 1997 Nov;151(5):1341–51.

115. Struyf S, Menten P, Lenaerts JP, Put W, D'Haese A, De Clercq E, et al. Diverging binding capacities of natural LD78β isoforms of macrophage inflammatory protein-1α to the CC chemokine receptors 1, 3 and 5 affect their anti-HIV-1 activity and chemotactic potencies for neutrophils and eosinophils. Eur J Immunol. 2001;31(7):2170–8.

116. Miyakawa T, Obaru K, Maeda K, Harada S, Mitsuya H. Identification of amino acid residues critical for LD78β a variant of human macrophage inflammatory protein-1α, binding to CCR5 and inhibition of R5 human immunodeficiency virus type 1 replication. J Biol Chem. 2002 Feb 15;277(7):4649–55.

117. Contento RL, Molon B, Boularan C, Pozzan T, Manes S, Marullo S, et al. CXCR4-CCR5: A couple modulating T cell functions. Proc Natl Acad Sci U S A. 2008 Jul 22;105(29):10101–6.

118. Castellino F, Huang AY, Altan-Bonnet G, Stoll S, Scheinecker C, Germain RN. Chemokines enhance immunity by guiding naive CD8+ T cells to sites of CD4+ T cell-dendritic cell interaction. Nature. 2006 Apr 13;440:890–5.

119. Lemos MP, Lama JR, Karuna ST, Fong Y, Montano SM, Ganoza C, et al. The inner foreskin of healthy males at risk of HIV infection harbors epithelial CD4+ CCR5+ cells and has features of an inflamed epidermal barrier. PLoS One. 2014;9(9):e108954.

120. Liu A, Yang Y, Liu L, Meng Z, Li L, Qiu C, et al. Differential compartmentalization of HIV-targeting immune cells in inner and outer foreskin tissue. PLoS One. 2014;9(1):e85176.

121. Galiwango RM, Yegorov S, Joag V, Prodger J, Shahabi K, Huibner S, et al. Characterization of CD4+ T cell subsets and HIV susceptibility in the inner and outer foreskin of Ugandan men. Am J Reprod Immunol. 2019;82(1):1–10.

122. Merad M, Sathe P, Helft J, Miller J, Mortha A. The Dendritic Cell Lineage: Ontogeny and Function of Dendritic Cells and Their Subsets in the Steady State and the Inflamed Setting. Annu Rev Immunol. 2013;31:563–604.

123. Birbeck MS, Breathnach AS, Everall JD. An Electron Microscope Study of Basal Melanocytes and High-Level Clear Cells (Langerhans Cells) in Vitiligo**From the Chester Beatty Research Institute, Royal Cancer Hospital, London, S.W. 3, and the Departments of Anatomy, and Dermatology, St. Mary's Hos. J Invest Dermatol. 1961 Jul 1;37(1):51–64.

124. Valladeau J, Ravel O, Dezutter-Dambuyant C, Moore K, Kleijmeer M, Liu Y, et al. Langerin, a novel C-type lectin specific to langerhans cells, is an endocytic receptor that induces the formation of Birbeck granules. Immunity. 2000 Jan 1;12(1):71–81.

125. Fithian E, Kung P, Goldstein G, Rubenfeld M, Fenoglio C, Edelson R. Reactivity of Langerhans cells with hybridoma antibody. Proc Natl Acad Sci U S A. 1981;78(4):2541–4.

126. Donoval BA, Landay AL, Moses S, Agot K, Ndinya-Achola JO, Nyagaya EA, et al. HIV-1 target cells in foreskin of African men with varying histories of sexually transmitted infections. Am J Clin Pathol. 2006;125(3):386–91.

127. Flacher V, Bouschbacher M, Verronèse E, Massacrier C, Sisirak V, Berthier-Vergnes O, et al. Human Langerhans Cells Express a Specific TLR Profile and Differentially Respond to Viruses and Gram-Positive Bacteria. J Immunol. 2006 Dec 1;177(11):7959–67.

128. Banchereau J, Briere F, Caux C, Davoust J, Lebecque S, Liu YJ, et al. Immunobiology of dendritic cells. Annu Rev Immunol. 2000 Nov 28;18:767–811.

129. Sallusto F, Lanzavecchia A. Understanding dendritic cell and T-lymphocyte traffic through the analysis of chemokine receptor expression. Immunol Rev. 2000 Oct 1;177(1):134–40.

130. De Witte L, Nabatov A, Pion M, Fluitsma D, De Jong MAWP, De Gruijl T, et al. Langerin is a natural barrier to HIV-1 transmission by Langerhans cells. Nat Med. 2007;13(1):367–71.

131. Turville SG, Cameron PU, Handley A, Lin G, Pöhlmann S, Doms RW, et al. Diversity of receptors binding HIV on dendritic cell subsets. Nat Immunol. 2002 Sep 23;3(10):975–83.

132. Pivarcsi A, Nagy I, Koreck A, Kis K, Kenderessy-Szabo A, Szell M, et al. Microbial compounds induce the expression of pro-inflammatory cytokines, chemokines and human β-defensin-2 in vaginal epithelial cells. Microbes Infect. 2005 Jul 1;7(9–10):1117–27.

133. Ogawa Y, Kawamura T, Kimura T, Ito M, Blauvelt A, Shimada S. Gram-positive bacteria enhance HIV-1 susceptibility in Langerhans cells, but not in dendritic cells, via Toll-like receptor activation. Blood. 2009;113(21):5157–66.

134. Lynch GW, Slaytor EK, Elliott FD, Saurajen A, Turville SG, Sloane AJ, et al. CD4 is expressed by epidermal Langerhans' cells predominantly as covalent dimers. Exp Dermatol. 2003 Oct;12(5):700–11.

135. De Jong MAWP, Geijtenbeek TBH. Human immunodeficiency virus-1 acquisition in genital mucosa: Langerhans cells as key-players. J Intern Med. 2009;265(1):18–28.

136. Murphy K, Weaver C. Janeway 'S immunobiology 9th Edition. Garland Science : Taylor & Francis group. 2017.

137. Julius M. Cruse REL and HW. MOLECULES, CELLS, AND TISSUES OF IMMUNITY. In: Immunology Guidebook. 2004. p. 1–15.

138. Gorry PR, Francella N, Lewin SR, Collman RG. HIV-1 envelope-receptor interactions required for macrophage infection and implications for current HIV-1 cure strategies. J Leukoc Biol. 2014;95(1):71–81.

139. Stein M, Keshav S, Harris N, Gordon S. Interleukin 4 potently enhances murine macrophage mannose receptor activity: A marker of alternative immunologic macrophage activation. J Exp Med. 1992 Jul 1;176(1):287–92.

140. Stout RD, Suttles J. T cell signaling of macrophage function in inflammatory disease. Front Biosci. 1997;2:197–206.

141. Stout RD, Suttles J. Functional plasticity of macrophages: reversible adaptation to changing microenvironments. J Leukoc Biol. 2004 Sep;76(3):509–13.

142. Sutterwala FS, Noel GJ, Salgame P, Mosser DM. Reversal of proinflammatory responses by ligating the macrophage Fcγ receptor type I. J Exp Med. 1998 Jul 6;188(1):217–22.

143. Martinez FO, Gordon S. The M1 and M2 paradigm of macrophage activation: Time for reassessment. F1000Prime Rep. 2014 Mar 3;6:13.

144. Nathan CF, Murray HW, Wlebe IE, Rubin BY. Identification of interferon-γ, as the lymphokine that activates human macrophage oxidative metabolism and antimicrobial activity. J Exp Med. 1983 Sep 1;158(3):670–89.

145. Mosser DM, Edwards JP. Exploring the full spectrum of macrophage activation. Nat Rev Immunol. 2008 Dec;8(12):958–69.

146. MacMicking J, Xie QW, Nathan C. Nitric oxide and macrophage function. Annu Rev Immunol. 1997 Nov 28;15(1):323–50.

147. Abramson SL, Gallin JI. IL-4 inhibits superoxide production by human mononuclear phagocytes. J Immunol. 1990;144(2):625–30.

148. Doyle AG, Herbein G, Montaner LJ, Minty AJ, Caput D, Ferrara P, et al. Interleukin-13 alters the activation state of murine macrophages in vitro: Comparison with interleukin-4 and interferon-γ. Eur J Immunol. 1994 Jun 1;24(6):1441–5.

149. Krzyszczyk P, Schloss R, Palmer A, Berthiaume F. The role of macrophages in acute and chronic wound healing and interventions to promote pro-wound healing phenotypes. Front Physiol. 2018 May 1;9:419.

150. Strassmann G, Patil-Koota V, Finkelman F, Fong M, Kambayashi T. Evidence for the involvement of interleukin 10 in the differential deactivation of murine peritoneal macrophages by prostaglandin E2. J Exp Med. 1994 Dec 1;180(6):2365–70.

151. Erwig LP, Henson PM. Immunological consequences of apoptotic cell phagocytosis. Am J Pathol. 2007;171(1):2–8.

152. Becker Y. The Changes in the T helper 1 (Th1) and T helper 2 (Th2) Cytokine Balance during HIV-1 Infection are Indicative of an Allergic Response to Viral Proteins that may be Reversed by Th2 Cytokine Inhibitors and Immune Response Modifiers - A Review and Hypothes. Virus Genes. 2004 Jan;28(1):5–18.

153. Li Y, Kang G, Duan L, Lu W, Katze MG, Lewis MG, et al. SIV infection of lung macrophages. PLoS One. 2015 May 1;10(5):e0125500.

154. Groot F, Welsch S, Sattentau QJ. Efficient HIV-1 transmission from macrophages to T cells across transient virological synapses. Blood. 2008 May 1;111(9):4660–3.

155. Ganor Y, Real F, Sennepin A, Dutertre CA, Prevedel L, Xu L, et al. HIV-1 reservoirs in urethral macrophages of patients under suppressive antiretroviral therapy. Nat Microbiol. 2019 Apr 1;4(4):633–44.

156. Castellano P, Prevedel L, Eugenin EA. HIV-infected macrophages and microglia that survive acute infection become viral reservoirs by a mechanism involving Bim. Sci Rep. 2017 Dec 1;7(1).

157. Swingler S, Mann AM, Zhou J, Swingler C, Stevenson M. Apoptotic killing of HIV-1-infected macrophages is subverted by the viral envelope glycoprotein. PLoS Pathog. 2007 Sep;3(9):1281–90.

158. Clayton KL, Collins DR, Lengieza J, Ghebremichael M, Dotiwala F, Lieberman J, et al. Resistance of HIV-infected macrophages to CD8 + T lymphocyte-mediated killing drives activation of the immune system article. Nat Immunol. 2018 May 1;19(5):475–86.

159. Rasaiyaah J, Tan CP, Fletcher AJ, Price AJ, Blondeau C, Hilditch L, et al. HIV-1 evades innate immune recognition through specific cofactor recruitment. Nature. 2013;503(7476):402–5.

160. Lim EY, Jackson SE, Wills MR. The CD4+ T Cell Response to Human Cytomegalovirus in Healthy and Immunocompromised People. Front Cell Infect Microbiol. 2020 May 19;10:202.

161. Prodger JL, Gray R, Kigozi G, Nalugoda F, Galiwango R, Nehemiah K, et al. Impact of asymptomatic Herpes simplex virus-2 infection on T cell phenotype and function in the foreskin. AIDS. 2012 Jun 19;26(10):1319–22.

162. Mosmann TR, Coffman RL. TH1 and TH2 cells: Different patterns of lymphokine secretion lead to different functional properties. Annu Rev Immunol. 1989;7:145–73.

163. Orlova-Fink N, Chowdhury FZ, Sun X, Harrington S, Rosenberg ES, Yu XG, et al. Preferential susceptibility of Th9 and Th2 CD4 + T cells to X4-tropic HIV-1 infection. AIDS. 2017 Oct 23;31(16):2211–5.

164. Kaplan MH. Th9 cells: Differentiation and disease. Immunol Rev. 2013 Mar;252(1):104–15.

165. Walker JA, McKenzie ANJ. TH2 cell development and function. Nat Rev Immunol. 2018 Oct 30;18(2):121–33.

166. Kolls J, Sandquist I. Update on regulation and effector functions of Th17 cells. Vol. 7, F1000Research. Faculty of 1000 Ltd; 2018. p. 205.

167. Langrish CL, Chen Y, Blumenschein WM, Mattson J, Basham B, Sedgwick JD, et al. IL-23 drives a pathogenic T cell population that induces autoimmune inflammation. J Exp Med. 2005 Jan 17;201(2):233–40.

168. Bettelli E, Carrier Y, Gao W, Korn T, Strom TB, Oukka M, et al. Reciprocal developmental pathways for the generation of pathogenic effector TH17 and regulatory T cells. Nature. 2006;441:235–8.

169. Mangan PR, Harrington LE, O'Quinn DB, Helms WS, Bullard DC, Elson CO, et al. Transforming growth factor-β induces development of the T H17 lineage. Nature. 2006;441:231–234.

170. Veldhoen M, Hocking RJ, Atkins CJ, Locksley RM, Stockinger B. TGFβ in the context of an inflammatory cytokine milieu supports de novo differentiation of IL-17-producing T cells. Immunity. 2006;24(2):179–89.

171. Awasthi A, Kuchroo VK. Th17 cells: From precursors to players in inflammation and infection. Int Immunol. 2009;21(5):489–98.

172. Huang W, Na L, Fidel PL, Schwarzenberger P. Requirement of interleukin-17A for systemic anti-Candida albicans host defense in mice. J Infect Dis. 2004 Aug 1;190(3):624–31.

173. Ye P, Garvey PB, Zhang P, Nelson S, Bagby G, Summer WR, et al. Interleukin-17 and lung host defense against klebsiella pneumoniae infection. Am J Respir Cell Mol Biol. 2001 Dec 14;25(3):335–40.

174. Happel KI, Dubin PJ, Zheng M, Ghilardi N, Lockhart C, Quinton LJ, et al. Divergent roles of IL-23 and IL-12 in host defense against Klebsiella pneumoniae. J Exp Med. 2005 Sep 19;202(6):761–9.

175. Khader SA, Bell GK, Pearl JE, Fountain JJ, Rangel-Moreno J, Cilley GE, et al. IL-23 and IL-17 in the establishment of protective pulmonary CD4+ T cell responses after vaccination and during Mycobacterium tuberculosis challenge. Nat Immunol. 2007 Mar 11;8(4):369–77.

176. Pelletier M, Maggi L, Micheletti A, Lazzeri E, Tamassia N, Costantini C, et al. Evidence for a cross-talk between human neutrophils and Th17 cells. Blood. 2010 Jan 14;115(2):335–43.

177. Yu JJ, Ruddy MJ, Wong GC, Sfintescu C, Baker PJ, Smith JB, et al. An essential role for IL-17 in preventing pathogen-initiated bone destruction: Recruitment of neutrophils to inflamed bone requires IL-17 receptor-dependent signals. Blood. 2007 May 1;109(9):3794–802.

178. Stieh DJ, Matias E, Xu H, Fought AJ, Blanchard JL, Marx PA, et al. Th17 Cells Are Preferentially Infected Very Early after Vaginal Transmission of SIV in Macaques. Cell Host Microbe. 2016;19(4):529–40.

179. Sempere JM, Soriano V, Benito JM. T regulatory cells and HIV infection. AIDS Rev. 2007;9:734.

180. Maloy KJ, Powrie F. Regulatory T cells in the control of immune pathology. Nat Immunol. 2001;2(9):816–22.

181. Itoh M, Takahashi T, Sakaguchi N, Kuniyasu Y, Shimizu J, Otsuka F, et al. Thymus and autoimmunity: production of CD25+CD4+ naturally anergic and suppressive T cells as a key function of the thymus in maintaining immunologic self-tolerance. J Immunol. 1999;162(9):5317–26.

182. Shevach EM. CD4+CD25+ suppressor T cells: More questions than answers. Nat Rev Immunol. 2002;2(6):389–400.

183. Oswald-Richter K, Grill SM, Shariat N, Leelawong M, Sundrud MS, Haas DW, et al. HIV infection of naturally occurring and genetically reprogrammed human regulatory T-cells. PLoS Biol. 2004;2(7):0955–66.

184. Moreno-Fernandez ME, Zapata W, Blackard JT, Franchini G, Chougnet CA. Human Regulatory T Cells Are Targets for Human Immunodeficiency Virus (HIV) Infection, and Their Susceptibility Differs Depending on the HIV Type 1 Strain. J Virol. 2009;83(24):12925–33.

185. Sousa AE, Carneiro J, Meier-Schellersheim M, Grossman Z, Victorino RMM. CD4 T Cell Depletion Is Linked Directly to Immune Activation in the Pathogenesis of HIV-1 and

HIV-2 but Only Indirectly to the Viral Load. J Immunol. 2002 Sep 15;169(6):3400–6.

186. Moreno-Fernandez ME, Joedicke JJ, Chougnet CA. Regulatory T cells diminish HIV infection in dendritic cells - conventional CD4+ T cell clusters. Front Immunol. 2014;5(5):199.

187. Tran TA, de Goër de Herve MG, Hendel-Chavez H, Dembele B, Le Névot E, Abbed K, et al. Resting regulatory CD4 T cells: A site of HIV persistence in patients on long-term effective antiretroviral therapy. PLoS One. 2008 Oct 1;3(10):e3305.

188. Rocco J, Mellors JW, Macatangay BJ. Regulatory T cells: the ultimate HIV reservoir? J Virus Erad. 2018 Oct;4(4):209–14.

189. Duhen T, Geiger R, Jarrossay D, Lanzavecchia A, Sallusto F. Production of interleukin 22 but not interleukin 17 by a subset of human skin-homing memory T cells. Nat Immunol. 2009;10(8):857–63.

190. Trifari S, Kaplan CD, Tran EH, Crellin NK, Spits H. Identification of a human helper T cell population that has abundant production of interleukin 22 and is distinct from TH-17, TH1 and TH2 cells. Nat Immunol. 2009;10(8):864–71.

191. Kim CJ, Nazli A, Rojas OL, Chege D, Alidina Z, Huibner S, et al. A role for mucosal IL-22 production and Th22 cells in HIV-associated mucosal immunopathogenesis. Mucosal Immunol. 2012;5(6):670–80.

192. Homey B, Wang W, Soto H, Buchanan ME, Wiesenborn A, Catron D, et al. Cutting Edge: The Orphan Chemokine Receptor G Protein-Coupled Receptor-2 (GPR-2, CCR10) Binds the Skin-Associated Chemokine CCL27 (CTACK/ALP/ILC). J Immunol. 2000;146(7):3465–70.

193. Boniface K, Bernard F-X, Garcia M, Gurney AL, Lecron J-C, Morel F. IL-22 Inhibits Epidermal Differentiation and Induces Proinflammatory Gene Expression and Migration of Human Keratinocytes. J Immunol. 2005 Mar 15;174(6):3695–702.

194. Zhou Z, Barry de Longchamps N, Schmitt A, Zerbib M, Vacher-Lavenu MC, Bomsel M, et al. HIV-1 efficient entry in inner foreskin is mediated by elevated CCL5/RANTES that recruits T cells and fuels conjugate formation with Langerhans cells. PLoS Pathog. 2011;7(6):e1002100.

195. Morales J, Homey B, Vicari AP, Hudak S, Oldham E, Hedrick J, et al. CTACK, a skin-associated chemokine that preferentially attracts skin-homing memory T cells. Proc Natl Acad Sci U S A. 1999;96(25):14470–14475.

196. Vestergaard C, Johansen C, Otkjaer K, Deleuran M, Iversen L. Tumor necrosis factor-α-induced CTACK/CCL27 (cutaneous T-cell-attracting chemokine) production in keratinocytes is controlled by nuclear factor κB. Cytokine. 2005 Jan 21;29(2):49–55.

197. Yang XW, Jiang HX, Lei R, Lu WS, Tan SH, Qin SY. Recruitment and significance of Th22 cells and Th17 cells in malignant ascites. Oncol Lett. 2018;16(4):5389–97.

198. Anderson D, Politch JA, Pudney J. HIV Infection and Immune Defense of the Penis. Am J Reprod Immunol. 2011;65(3):220–9.

199. Politch JA, Tucker L, Bowman FP, Anderson DJ. Concentrations and significance of cytokines and other immunologic factors in semen of healthy fertile men. Hum

Reprod. 2007 Nov 1;22(11):2928–35.

200. Cameron PU, Saleh S, Sallmann G, Solomon A, Wightman F, Evans VA, et al. Establishment of HIV-1 latency in resting CD4+ T cells depends on chemokine-induced changes in the actin cytoskeleton. Proc Natl Acad Sci U S A. 2010;107(39):16934–9.

201. Karnezis T, Farnsworth RH, Harris NC, Williams SP, Caesar C, Byrne DJ, et al. CCL27/CCL28-CCR10 chemokine signaling mediates migration of lymphatic endothelial cells. Cancer Res. 2019 Apr 1;79(7):1558–72.

202. Deshmane SL, Kremlev S, Amini S, Sawaya BE. Monocyte chemoattractant protein-1 (MCP-1): An overview. J Interf Cytokine Res. 2009 Jun 1;29(6):313–25.

203. Luther SA, Cyster JG. Chemokines as regulators of T cell differentiation. Nat Immunol. 2001 Feb;2(2):102–7.

204. Anderson DJ, Pudney J. Human Male Genital Tract Immunity. In: Mucosal Immunology: Fourth Edition. 2015. p. 2125–40.

205. Ghiran IC. Introduction to fluorescence microscopy. In: Methods in molecular biology (Clifton, NJ). 2011. p. 93–136.

206. Jameson DM, Croney JC, Moens PDJ. Fluorescence: Basic concepts, practical aspects, and some anecdotes. Methods Enzymol. 2003;360:1–43.

207. Jalali M, Saldanha FYL, Jalali M. Basic Science Methods for Clinical Researchers. Basic Science Methods for Clinical Researchers. 2017. 1–355 p.

208. Flynn J, Gorry P. Flow Cytometry Analysis to Identify Human CD4+ T Cell Subsets. In: Methods in Molecular Biology. 2019. p. 15–25.

209. Davila ML, Xiong N. The role of CCL27 in the establishment, maintenance, and homeostasis of skin-resident CCR10+ lymphocytes. J Immunol. 2020 May 1;204(1):157.5.

210. Schneider CA, Rasband WS, Eliceiri KW. NIH Image to ImageJ: 25 years of image analysis. Nat Methods. 2012;9(7):671–675.

211. Altman DG, Bland JM. Measurement in Medicine: The Analysis of Method Comparison Studies. Stat. 1983;32(3):307–17.

212. Giavarina D. Understanding Bland Altman analysis. Biochem Medica. 2015;25(2):141–151.

213. Prodger JL, Hirbod T, Gray R, Kigozi G, Nalugoda F, Galiwango R, et al. HIV infection in uncircumcised men is associated with altered CD8 T-cell function but normal CD4 T-cell numbers in the foreskin. J Infect Dis. 2014;209(8):1185–94.

214. Ganor Y, Zhou Z, Tudor D, Schmitt A, Vacher-Lavenu MC, Gibault L, et al. Within 1 h, HIV-1 uses viral synapses to enter efficiently the inner, but not outer, foreskin mucosa and engages Langerhans-T cell conjugates. Mucosal Immunol. 2010 Sep;3(5):506–22.

215. Autengruber A, Gereke M, Hansen G, Hennig C, Bruder D. Impact of enzymatic tissue disintegration on the level of surface molecule expression and immune cell function. Eur J Microbiol Immunol. 2012;2(2):112–20.

216. Ford AL, Foulcher E, Goodsall AL, Sedgwick JD. Tissue digestion with dispase

substantially reduces lymphocyte and macrophage cell-surface antigen expression. J Immunol Methods. 1996;194(1):71–5.

217. Li Z, Gothard E, Coles MC, Ambler CA. Quantitative methods for measuring repair rates and innate-immune cell responses in wounded mouse skin. Front Immunol. 2018 Feb 27;9(2):347.

218. Mehta AK, Gracias DT, Croft M. TNF activity and T cells. Cytokine. 2018 Jan 1;101:14–8.

219. Scheurich P, Thoma B, Ucer U, Pfizenmaier K. Immunoregulatory activity of recombinant human tumor necrosis factor (TNF)-alpha: induction of TNF receptors on human T cells and TNF-alpha-mediated enhancement of T cell responses. J Immunol. 1987;138(6):1786–90.

220. Yokota S, Geppert TD, Lipsky PE. Enhancement of antigen- and mitogen-induced human T lymphocyte proliferation by tumor necrosis factor-α. J Immunol. 1988;140(2):531–6.

221. Dinh MH, Hirbod T, Kigozi G, Okocha EA, Cianci GC, Kong X, et al. No difference in keratin thickness between inner and outer foreskins from elective male circumcisions in Rakai, Uganda. PLoS One. 2012;7(7).

222. Ganor Y, Bomsel M. HIV-1 Transmission in the Male Genital Tract. Am J Reprod Immunol. 2011;65(3):284–91.

223. Wilen CB, Tilton JC, Doms RW. HIV cell binding and entry. 2012;2:1–5.

224. Homey B, Alenius H, Müller A, Soto H, Bowman EP, Yuan W, et al. CCL27-CCR10 interactions regulate T cell-mediated skin inflammation. Nat Med. 2002;8(2):157–65.

225. Reiss Y, Proudfoot AE, Power CA, Campbell JJ, Butcher EC. CC chemokine receptor (CCR)4 and the CCR10 ligand cutaneous T cell-attracting chemokine (CTACK) in lymphocyte trafficking to inflamed skin. J Exp Med. 2001 Nov 19;194(10):1541–7.

226. Mildner M, Prior M, Gschwandtner M, Schuster C, Tschachler E, Elbe-Bürger A. Epidermal CCL27 expression is regulated during skin development and keratinocyte differentiation. Vol. 134, Journal of Investigative Dermatology. Nature Publishing Group; 2014. p. 855–8.

227. Eyerich S, Eyerich K, Pennino D, Carbone T, Nasorri F, Pallotta S, et al. Th22 cells represent a distinct human T cell subset involved in epidermal immunity and remodeling. J Clin Invest. 2009;119:3573–3585.

228. Tian T, Yu S, Ma D. Th22 and related cytokines in inflammatory and autoimmune diseases. Vol. 17, Expert Opinion on Therapeutic Targets. Taylor & Francis; 2013. p. 113–25.